Cenozoic paleoceanographic changes of the South Pacific from seismic reflection data

Kumulative Dissertation

zur Erlangung des akademischen Grades eines

Doktors der Naturwissenschaften

Dr. rer. nat.

am Fachbereich Geowissenschaften

der Universität Bremen

vorgelegt von

Michael Horn

Bremen, Januar 2015

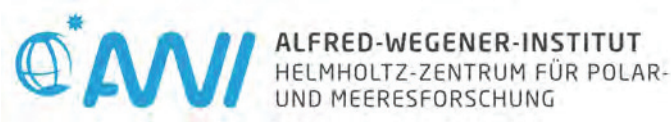

This thesis was conducted within the research division Geophysics at the Alfred Wegener Institute, Helmholtz Centre for Polar and Marine Research (AWI) Bremerhaven between April 2011 and December 2014. This study is part oft the Helmholtz Research Programme **Paces I 3.2** (2009 – 2013) and **II 3.2** (since 2014) "Earth system on tectonic time scales: From greenhouse to icehouse world". The research was funded by the Bundesministerium für Bildung und Forschung under contract number 03G0213A.

Datum des Colloquiums

21.04.2015

Betreuer und Erstgutachter der Dissertation:

Prof. Dr. Wilfried Jokat

Zweitgutachterin

Prof. Dr. Kathrin Huhn

Mitglieder der Prüfungskommission

Prof. Dr. Heiko Pälike
Dr. Hendrik Müller
Herrn Dr. Jannis Kuhlmann
Isabell Sauermilch

Name: Michael Horn
Anschrift: Achtern Höben 35
28279 Bremen

Datum: 05. Januar 2015

ERKLÄRUNG

Hiermit versichere ich, dass ich

1. die Arbeit ohne unerlaubte fremde Hilfe angefertigt habe
2. keine anderen als die von mir angegebenen Quellen und Hilfsmittel benutzt habe
3. die den benutzten Werken wörtlich oder inhaltlich entnommenen Stellen als solche kenntlich gemacht habe

Bremen, den 05.01.2015

_____
Michael Horn

Abstract

The Thermohaline Circulation (THC) in the world oceans is closely coupled with earth climate. With reconstructions of past oceanic conditions and comparisons with past climate conditions this coupling can be better understood. This in turn allows to provide better boundary conditions on ocean-climate coupling for forecasting models. However, the paleoceanographic setup is far from being completely revealed. One of the largest areas of the world oceans poorly surveyed is the South Pacific Ocean. The present ocean currents that transport deep cold water into the South Pacific are the Antarctic Circumpolar Current (ACC) and two northward setting flows directly influenced by the ACC, the Deep Western Boundary Current (DWBC) or western limb close to New Zealand and an eastern limb above the western flank of the East Pacific Rise (EPR). Understanding changes of this current system is important for reconstructions of past climates and the Antarctic Glaciation history. At present the reconstructed paleoceanographic history of the South Pacific is limited to ACC and DWBC at the western margin of the Southwest Pacific Basin and only reveals changes back to the Eocene/Oligocene boundary. This thesis presents new multichannel seismic reflection data surveying two regions at the eastern and western margin in the Southwest Pacific Basin. The objective is the identification and characterization of deep current derived sediment deposits in the South Pacific. The investigation covers the whole Cenozoic and thus provides indications for paleoceanographic changes due to East Antarctic Ice Sheet build-up prior to 34 Ma. Furthermore the study helps to fill a data gap in the open Pacific Ocean between New Zealand and South America and presents the first evidence for paleoceanographic changes in this poorly explored area.

East of New Zealand at the Bounty Trough mouth a sediment drift indicates the onset of a deep cold current originating from the South Pacific Ocean around the Cretaceous/Palaeocene boundary. This current prevailed until the establishment of the ACC around the Eocene/Oligocene boundary. A second sediment drift indicates a current modification due to climate cooling around 44 - 42 Ma occurs contemporaneously with first indications of an East Antarctic Ice Sheet. These results are the first hints on a deep cold current in the South Pacific Ocean before the Opening of the Tasmanian Gateway and thus support the hypotheses that an Antarctic Ice Sheet was present at that time. Since ~19 Ma the history of the ACC has been recorded by the sedimentary deposits at the western flank of the EPR and east of the Bounty Trough mouth. Close to the EPR (45°S) the sedimentary cover suggests a weak bottom current flow allowing deposition that is followed by a bottom current intensification around 9 Ma. The stronger bottom current flow has continued until today. East of New Zealand seismic data and drilling results reveal a current that created a sediment drift between 19.5 Ma and 10 Ma followed by a 5.4 Ma long hiatus in deposition caused by bottom current intensification due to West Antarctic Ice Sheet build-up. Thus, both limbs of bottom current flow into the South Pacific show intensification at the same time that was probably caused by an intensified ACC. Although deposition close to New Zealand starts again around 5 Ma, the flow of the DWBC remained

strong, which is also evident at the eastern limb. A higher sediment load due to upstream erosion of the DWBC caused further deposition. The sediment deposits seen in seismic profiles also suggest that a limb of the DWBC enters the Bounty Trough, which until present was only inferred from erosional structures at the Bounty Trough mouth. A new approach based on spectral analysis of Parasound sub-bottom profiler data was used to further quantify the extent of the DWBC in the Bounty Trough. Under the assumption that the 41 kyr obliquity cycle is related to DWBC changes, mapping of this cyclicity in Parasound data is used to show that the extent of the DWBC into the Bounty Trough is limited to 178.2°E.

Zusammenfassung

Die Thermohaline Zirkulation (THC) in den Weltozeanen ist eng an das Erdklima gekoppelt. Mit Hilfe der Rekonstruktion von paleoozeanischen Bedingungen der Vergangenheit und deren Vergleich mit den Klimabedingungen vergangener Zeit kann diese Art der Kopplung untersucht und besser verstanden werden. Dieses bessere Verständnis kann wiederum dazu genutzt werden, bessere Rahmenbedingungen für Vorhersagemodelle bereitzustellen. Der paleoozeanische Aufbau der Weltozeane ist allerdings momentan nur unzureichend rekonstruiert. Eines der am wenigsten untersuchten Gebiete ist der südpazifische Ozean. Heutzutage sind die wichtigsten Ozeanströmungen, die kaltes Tiefenwasser in den Pazifik transportieren, der Antarktische Zirkumpolarstrom (ACC) sowie zwei vom ACC beeinflusste nach Norden fließende Strömungsarme: Der westliche Arm nahe Neuseeland, auch bekannt als der „Deep Western Boundary Current (DWBC)“ sowie der östliche Arm an der westlichen Flanke des Ost-Pazifischen Rückens (EPR). Das Verständnis dieses Strömungssystems und seine zeitliche Entwicklung sind von entscheidender Bedeutung für die Rekonstruktion der klimatischen Vergangenheit und der Vereisung der Antarktis. Bisher beschränken sich die Rekonstruktion der paleoozeanischen Bedingungen des Südpazifiks auf den DWBC und den ACC am westlichen Rand des südwestpazifischen Beckens nahe Neuseeland und reichen nur bis zur Eozän/Oligozän-Grenze zurück. Diese Arbeit basiert auf neuen seismischen Reflexionsdaten, die am östlichen und westlichen Rand des südwestpazifischen Beckens gesammelt wurden. Ziel dieser Dissertation ist die Identifizierung und Charakterisierung von Sedimentstrukturen, die durch Bodenströmungen generiert wurden. Die so erzielten Informationen decken die Geschichte des gesamten Neozoikums ab und können daher auch die Einflüsse der Entstehung des ostantarktischen Eisschildes vor 34 Millionen Jahren auf den Ozean aufzeigen. Des Weiteren kann diese Studie eine Datenlücke im offenen Pazifischen Ozean zwischen Neuseeland und Südamerika füllen und erste paleoozeanische Bedingungen in einer kaum erkundeten Region der Weltozeane rekonstruieren.
Östlich von Neuseeland am Ausgang des Bounty Trogs kann anhand eines Sedimentdriftes das Einsätzen einer kalten Bodenströmung impliziert werden. Diese stammt aus dem damaligen Südpazifik und war seit dem Beginn des Känozoikum aktiv. Diese Strömung war bis zur Bildung des

ACC um die Eozän/Oligzän-Grenze aktiv. Ein weiterer Sedimentdrift in dieser Region deutet auf eine Modifikation der Strömungsbedingungen durch kälter werdendes Klima um etwa 44 - 42 Millionen Jahre hin. Diese Modifikation tritt etwa zeitgleich mit den ersten Anzeichen für einen ostantarktischen Eisschild auf und ist damit ein erster Hinweis auf eine kalte Tiefenströmung im südpazifischen Ozean vor Öffnung des tasmanischen Seeweges. Dadurch unterstützen die Sedimentdrifte die Theorie, dass die Ostantarktis bereits vor der Öffnung des tasmanischen Seeweges Anzeichen für Vereisung aufweist. Seit etwa 19 Millionen Jahren zeichnen die Sedimentablagerungen östlich des Ausgangs des Bounty Troges und an der westlichen Flanke des EPR die Geschichte des ACCs auf. Nahe dem EPR (45°S) deutet die Bildung einer pelagischen Sedimentdecke auf eine Phase mit schwachen Bodenströmungen hin. Vor etwa 9 Millionen Jahren tritt eine Intensivierung der Bodenströmungen ein, die bis heute anhält. Östlich von Neuseeland zeigen seismische Daten und Bohrlochergebnisse, dass sich ein weiterer Sedimentdrift zwischen 19,5 und 10 Millionen Jahren gebildet hat. Darauf folgt ebenfalls eine Intensivierung der Bodenströmung, die zu einem Hiatus in der Ablagerung von 5 Millionen Jahren führt. Diese Intensivierung wird durch die Klimaabkühlung hervorgerufen, die auch zur Bildung des westantarktischen Eisschildes führte. Daraus folgt, dass beide Strömungsarme durch eine Intensivierung des ACC verstärkt werden. Auch wenn vor 5 Millionen Jahren ein neuer Sedimentdrift östlich von Neuseeland gebildet wird, bleibt die Strömungsgeschwindigkeit des DWBC hoch. Die Ablagerung kann nur gebildet werden durch mehr Sedimentvolumen im Strom des DWBC, das stromaufwärts durch Erosion aufgenommen wird. Die hohe Strömungsgeschwindigkeit von vor 9 Millionen Jahren bis heute deckt sich mit den Interpretationen am EPR. Des Weiteren deutet die Sedimentverteilung am Ausgang des Bounty Troges darauf hin, dass ein Strömungsarm des DWBC in den Bounty Trog hineinverläuft. Dieses Eindringen wurde bisher nur durch Erosionsspuren am Ausgang des Bounty Troges impliziert. Ein neuer Ansatz basierend auf der spektralen Analyse von Parasound Sedimentecholot Daten erlaubt die nähere Untersuchung der Ausdehnung des Arms des DWBC. Unter der Annahme, dass der 41000 Jahre Milankovitch Zyklus auf den Einfluss des DWBC zurückzuführen ist, kann die Kartierung des Auftretens der zugehörigen Frequenz aus den Parasound Daten dazu genutzt werden, die Ausdehnung des DWBC in den Bounty Trog hinein auf westlich von 178,2°E zu beschränken.

Table of Contents

A. List of figures

B. List of tables

C. List of abbreviations

ACC	Antarctic Circumpolar Current
AGC	Automatic Gain Control
ampl	Amplitude
AWI	Alfred Wegener Institute
BS	Bollons Seamount
BT	Bounty Trough
CCD	Carbonate Compensation Depth
CDP	Common Depth Point
CP or CaP	Campbell Plateau
CR	Chatman Rise
DB 1 – DB 4	Drift body 1 (oldest) to drift body 4 (youngest) in Chapter 6
DP	Drake Passage
DSDP	Deep Sea Drilling Program
DWBC	Deep Western Boundary Current
EAC	East Australian Current
ENZOSS	Eastern New Zealand Oceanic Sedimentary System
EPR	East Pacific Rise
EPR-1	older seismic Unit EPR-1 from Chapter 5
EPR-2	younger seismic Unit EPR-2 from Chapter 5
GEBCO	General Bathymetric Chart of the Oceans
GI-Gun	Generator Injector Gun
H	Hunt lines 141 and 143 from Uenzelmann-Neben et al. (2009)
HP	Hikurangi Plateau
IODP	Integrated Ocean Drilling Program
LCDW	Lower Circumpolar Deep Water
LHR	Lord Howe Rise
MeBo	“Meeresboden Bohrgerät” , Drill Rig of the Marum
mbsf	metre below seafloor
NI	North Island of New Zealand
NMO	Normal Moveout
ODP	Ocean Drilling Program
P14	World Ocean Circulation Experiment profile 14 in the South Pacific Ocean

P15	World Ocean Circulation Experiment profile 15 in the South Pacific Ocean
P17A	World Ocean Circulation Experiment profile 17A in the South Pacific Ocean
RV	Research Vessel
SI	South Island of New Zealand
SO	Sonne
SOPATRA	South Pacific Transects
STC	South Tasmanian Current
STR	South Tasmanian Rise
THC	Thermohaline Circulation
TS	Tasman Gateway
TWT	Two Way Traveltime
WOCE	World Ocean Circulation Experiment
Zealandia	New Zealand landmass including adjacent submerged continental crust

1. Introduction

1.1 The Thermohaline Circulation

The Thermohaline Circulation (THC), also known as the great conveyor belt (Houtz et al. 1977), is one of the driving forces of global climate (e.g. Kuhlbrodt et al. 2007; van Aken 2007; Marshall and Speer 2012). The circulation is driven by differences in temperature and salinity creating buoyancy loss or gain. Mechanisms generating these differences are downwelling in polar regions (surface waters cools and sinks to greater depth) and upwelling around the equator and Antarctica (deep water gets warmer and less salty due to mixing) (e.g. Kuhlbrodt et al. 2007; van Aken 2007; Figure 1.1). Two limbs of water mass transport exist between the upwelling and downwelling regions. Cold water is transported from the high latitudes in the deep limb of the THC while warm waters are transported back from the upwelling regions to the high latitudes in the surface limb where waters downwell again (Figure 1.1). The resulting heat transport is one driving factor of the maintenance of the global climate. Climate in turn can change the rate of deep water formation: For example, when temperatures are decreasing in downwelling regions, this results in a stronger flow of deep waters (Figure 1.1; e.g. Kuhlbrodt et al. 2007; van Aken 2007). Thus changes in climate have a direct effect on the THC and vice versa making up a complex system of coupled processes (e.g. Kuhlbrodt et al. 2007; van Aken 2007).

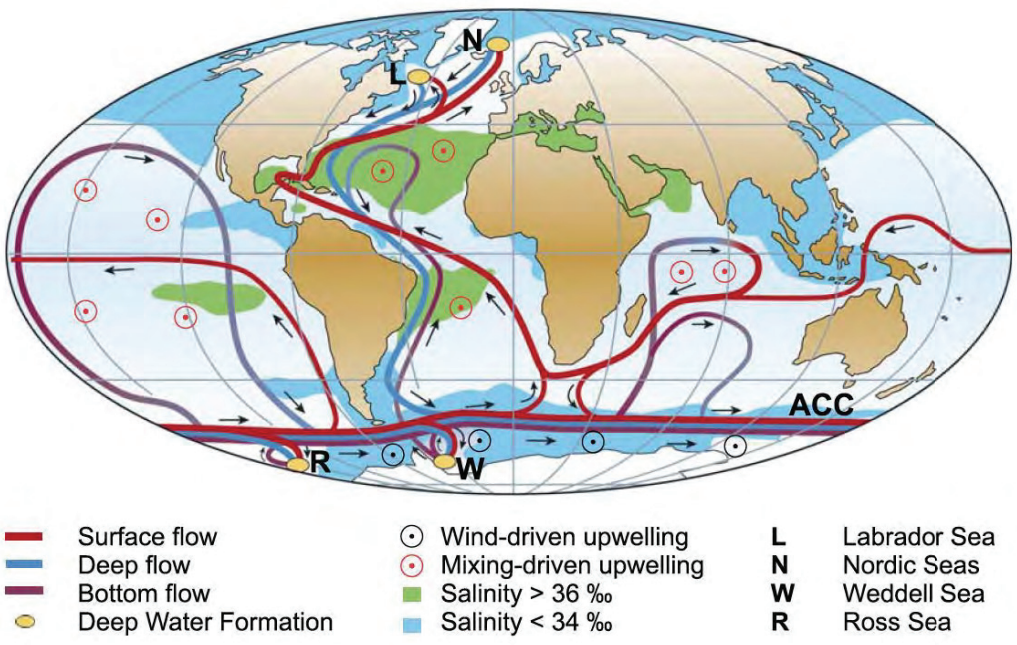

Figure 1.1: Schematic sketch of the Thermohaline Circulation (THC), taken from Kuhlbrodt et al. (2007).

The present locations of ocean currents and physical properties of transported water masses (now referred to as oceanographic setup) are relatively well known, as they can be measured directly. Such experiments where conducted for example by the World Ocean Circulation Experiment (WOCE, Sparrow et al. 2004 - 2006). In contrast, the paleoceanographic setup for former periods of earth history can only be reconstructed by studying geological archives that recorded past hydrographic processes. These reconstructions are needed to provide adequate boundary conditions for climate models that simulate past environmental changes and climate ocean interactions. These paleomodels in turn allow to construct better forecasting models for future changes in global climate (e.g. van Aken 2007) and are of broad interest for both science and politics.

1.2 Reconstructing paleoceanographic conditions

To reconstruct paleoceanographic conditions an archive capable of recording those conditions has to be identified. Evidence for a past oceanographic setup can be found in sedimentary deposits: paleo-currents have left deposits with characteristic sediment compositions and paleoceanographic tracer (e.g. $\delta^{18}O$, $\delta^{13}C$, sortable silt) signatures. In addition, these currents formed characteristic sedimentary structures still visible today (for further details please refer to chapter 3 and Rebesco et al. 2008). To reveal the information stored in sedimentary archives, structures beneath the seafloor have to be imaged and/or sediments have to be sampled by coring. Seismic reflection profiling can be used to generate an image of the sediments beneath the seafloor (Yilmaz 2001). Once the sedimentary record has been imaged it is useful to constrain these findings and assign ages to the identified structures by direct sediment sampling. Deep sediment sampling by scientific drilling has been done for approximately 50 years. Programs such as the Deep Sea Drilling Project (DSDP), the Ocean Drilling Program (ODP), the Integrated Ocean Drilling Program (IODP) and the most recent International Ocean Discovery Project launched multiple expeditions with drill ships to analyse sedimentary archives all over the world. An overview about the history of deep sea drilling and seismic exploration of sedimentary deposits for paleoceanographic reconstructions can be found in Rebesco et al. (2014).

1.3 The South Pacific Ocean

The South Pacific Ocean is the largest sector of the Southern Ocean and includes one of the main drivers of the THC, the Antarctic Circumpolar Current (ACC, Figure 1.1; e.g. Kuhlbrodt et al. 2007; van Aken 2007; Marshall and Speer 2012). However, because of massive erosion caused by the ACC (e.g. Carter et al. 2004a) archives directly inside the core flow are rare in the South Pacific. Sediments documenting millions of years of earth history are missing, for example in the Emerald Basin (Osborn et al. 1983) or at the slope of the Campbell Plateau (Carter et al. 1999a). Deposits below limbs that leave the ACC core flow show less erosion due to lower flow speeds (e.g. Carter and McCave 1994; Carter et al. 1994) but still record changes in the oceanic setup analogue to the ACC as observed close to New Zealand (e.g. Carter and Wilkin 1999; Neil et al. 2004). Two limbs that leave the ACC are

located in the Southwest Pacific Basin. The "western limb", associated with the Pacific Deep Western Boundary Current (DWBC, dusky pink dotted line in Figure 1.2) and an "eastern limb" (dark yellow dotted line in Figure 1.2) leave the ACC towards the Southwest Pacific Basin. Here, these limbs travel north where upwelling takes place and upwelled water masses travel back to polar regions in the upper limb of the THC (Reid 1997). The ACC limbs may have left corresponding footprints in sedimentary deposits. However, especially away from the landmasses of New Zealand and adjacent continental crust for example the Challenger Plateau, the Lord Howe Rise, the Campbell Plateau and Chatham Rise and other continental fragments (now reffered to as Zealandia; Lewis et al. 2012) or South America no information is available on the paleoceanographic setup of these limbs. Figure 1.2 shows the area of interest with the present location of the eastern limb and the DWBC and available drill sites.

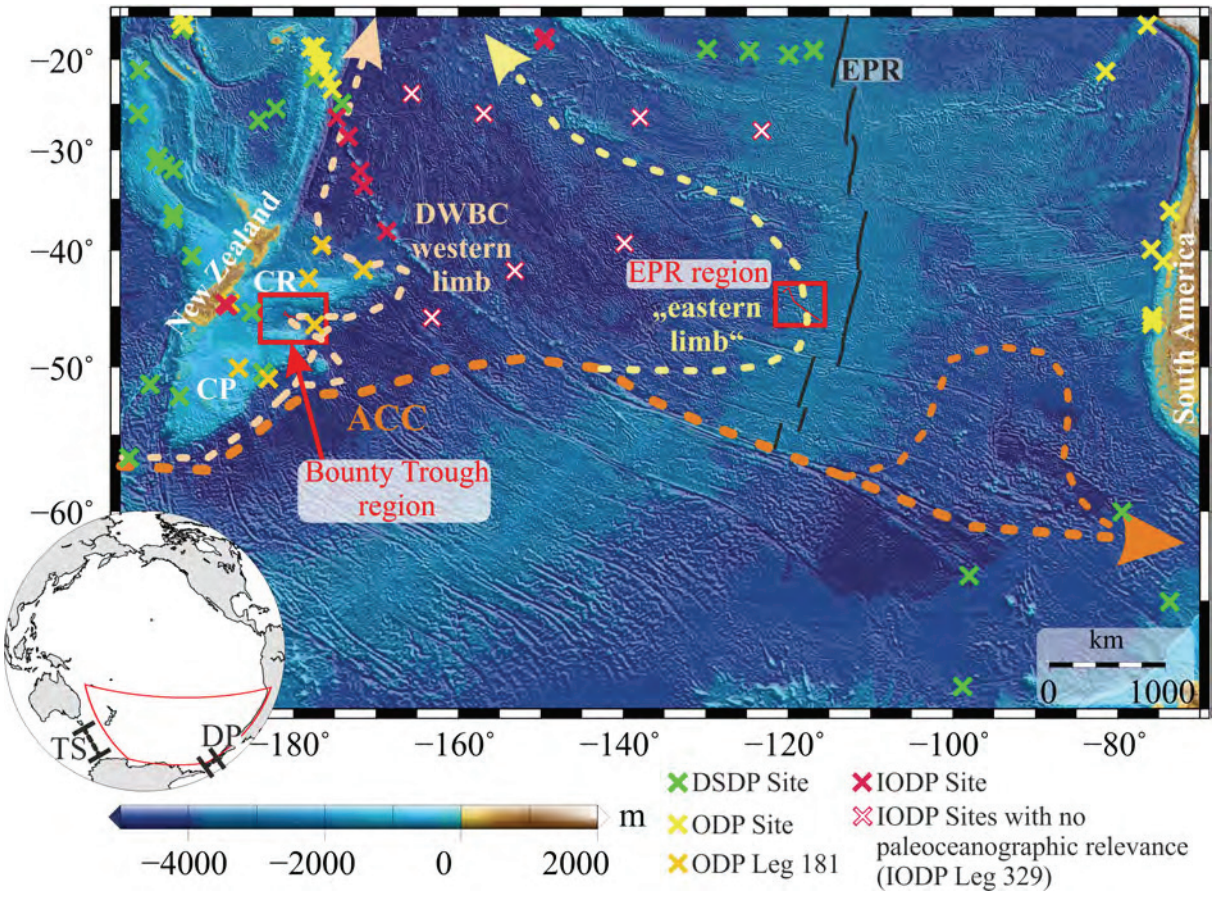

Figure 1.2: Overview of the Southwest Pacific Basin between the Tasmanian Gateway (TS) and the Drake Passage (DP). Bathymetry is taken from the GEBCO_08 grid, (Smith and Sandwell 1997). The two areas of interest (red boxes) are located east of New Zealand and adjusted Campbell Plateau (CP) and Chatham Rise (CR) and west of the East Pacific Rise (EPR). The main deep flows of the Antarctic Circumpolar Current (ACC), the Deep Western Boundary Current (DWBC, western limb) and the eastern limb are marked in dotted lines. Flows are taken from Reid (1997) at depth between 3000 and 3500 metres. Coloured crosses indicate the locations of available borehole locations of the Deep Sea Drilling Project (DSDP, green), the Ocean Drilling Program (ODP, yellow) and the Integrated Ocean Drilling Program (IODP, red). ODP Leg 181 is marked in light orange as it is further used in this dissertation.

Although some IODP drill sites are located in the open ocean of the South Pacific (Figure 1.2 white crosses with red rim) theses drill sites do not provide any useful information about the long term paleoceanographic history of the eastern limb (IODP Leg 329, D'Hondt et al. 2011). Seismic reflection profiling is limited to single channel profiles from the 1960ties and 70ties of the USNS Eltanin. Seismic data of that time cannot resolve current derived structures within the sedimentary column and thus the region remained a white spot in paleoceanographic reconstructions.

Drill cores from ODP Leg 181 around (summarised by Carter et al. (2004a) and Carter et al. (2004b)) provided detailed information on the paleoceanographic setup of the DWBC since the opening of the Tasmanian Gateway (~33.7 Ma; e.g. Stickley et al. 2004). However, information of Eocene and older oceanic currents is sparse and limited to one drill site north of the Chatman Rise, suggesting a warm deep water flow from the central Pacific (Carter et al. 2004b). As Antarctic glaciation began before the Opening of the Tasmanian Gateway information about the paleoceanographic setup before the opening is desirable. In this context the Southwest Pacific Basin can help to answer several open questions of paleoceanography, which have not been addressed yet. At the eastern margin of the Southwest Pacific Basin close to the East Pacific Rise (EPR, Figure 1.2 EPR region), sediment deposits are above the present carbonate compensation depth (CCD). Here, sediments are thick enough to be imaged by seismic reflection data and were able to record changes in the oceanic setup of the eastern limb. The western limb (the DWBC) passes a sediment archive east of the Campbell Plateau and Chatman Rise. Sediments have accumulated since Cretaceous times (Carter et al. 1994) and can thus provide information about the paleoceanographic setup during Eocene and older time periods (Figure 1.2 Bounty Trough region). This allows to find evidence on cold oceanic current before the opening of the Tasmanian Gateway that indicate cold climate conditions hinting on the presence of an East Antarctic Ice Sheet during the Eocene as proposed by ice rafted debris at the Kerguelen Plateau (e.g. Ehrmann and Mackensen 1992; Zachos et al. 1992).

1.4 Agenda

New seismic reflection data collected in 2011 and additional sub-bottom profiler data are the basis of this thesis. This dataset and additional data sources such as results from deep sea cores are further described in chapter 2. Chapter 3 will describe the basics the seismic reflection method and how bottom current structures can be identified and interpreted. Three manuscripts have been prepared for publication in scientific journals and my contributions to these manuscripts are described in Chapter 4. The first manuscript (chapter 5) deals with the eastern limb of the deep inflow of the Pacific Ocean, published in Geo-Marine Letters (Horn and Uenzelmann-Neben 2013). This paper answers the following questions:

1. Does the sedimentary cover at the western flank of the East Pacific Rise look like it was predicted by Ewing and Ewing (1967)?
2. Is there any information about processes that took part in shaping the sedimentary cover?

The second manuscript (Horn and Uenzelmann-Neben, submitted to Marine Geology in 06/2014, revision submitted 10/2014, chapter 6) deals with the sedimentary deposits at the western edge of the Southwest Pacific Basin close to Zealandia. Here I combine the findings of ODP Site 1122 (Carter et al. 1999b) and the former work of Carter et al. (1994) to construct a new seismic stratigraphy for the Outer and Middle Bounty Trough region. This new stratigraphy is then used to answer the following questions:

1. Is there a hint on former occurrence of deep currents before the opening of the Tasmanian Gateway that could confirm cold conditions at Antarctica and potential Antarctic Glaciation?
2. Can the history of the DWBC since the opening of the Tasmanian Gateway (~33.7 Ma) be derived from the sediment deposits?
3. Has the DWBC a limb that enters the Bounty Trough?

The third manuscript (prepared for resubmission to Geophysical Research Letters, chapter 7), further investigates the limb of the DWBC. I adapt a method of Weigelt and Uenzelmann-Neben (2007) to Parasound data in order to:

1. Reveal the presence of Milankovitch cycles within the upper sedimentary column
2. Estimate the regional influence of the DWBC from the spatial occurrence of these Milankovitch cycles

With chapters 5 to 7 I contribute to fill the white spots on the paleoceanographic map of the South Pacific Ocean. In addition, I create a link between both regions that allows me to transfer interpretations of the DWBC to the eastern limb (Chapter 8). Finally I present concluding remarks (chapter 9) and an outlook on future research (Chapter 10).

1.5 References

Carter, L., R. M. Carter, et al. (2004a). "Evolution of the sedimentary system beneath the deep Pacific inflow off eastern New Zealand." Marine Geology **205**(1-4): 9-27. doi:10.1016/s0025-3227(04)00016-7

Carter, L. and I. N. McCave (1994). "Development of sediment drifts approaching an active plate margin under the SW Pacific Deep Western Boundary Current." Paleoceanography **9**(6): 1061-1085. doi:10.1029/94pa01444

Carter, L. and J. Wilkin (1999). "Abyssal circulation around New Zealand - a comparison between observations and a global circulation model." Marine Geology **159**(1–4): 221-239. doi:10.1016/S0025-3227(98)00205-9

Carter, R. M., L. Carter, et al. (1994). "Seismic stratigraphy of the Bounty Trough, south-west Pacific Ocean." Marine and Petroleum Geology **11**(1): 79-93. doi:10.1016/0264-8172(94)90011-6

Carter, R. M., I. N. McCave, et al. (2004b). "1. Leg 181 Synthesis: Fronts, Flows, Drifts, Vocanoes, and the Evolution of the Southwestern Gateway to the Pacific Ocean, Eastern New Zealand". Published in: Proceedings of the Ocean Drilling Programm, Scientific Results. C. Richter. Texas, College Station (Ocean Drilling Program). **181**. doi:10.2973/odp.proc.sr.181.210.2004

Carter, R. M., I. N. McCave, et al. (1999a). "Site 1121: The Campbell "Drift"". Published in: Proceedings of the Ocean Drilling Program, Initial reports:. R. M. Carter, I. N. McCave, C. Richter and L. Carter. Texas, USA, College Station (Ocean Drilling Program). **181:** 1 - 62. doi:10.2973/odp.proc.ir.181.105.2000

Carter, R. M., I. N. McCave, et al. (1999b). "Site 1122: Turbidites with a Contourite Foundation". Published in: Proceedings of the Ocean Drilling Program, Initial reports:. R. M. Carter, I. N.

McCave, C. Richter and L. Carter. Texas, USA, College Station (Ocean Drilling Program). **181:** 1 - 146. doi:10.2973/odp.proc.ir.181.106.2000

D'Hondt, S., F. Inagaki, et al. (2011). "Expedition 329 summary". Published in: Proceedings of the Integrated Ocean Drilling Program. S. D'Hondt, F. Inagaki, C. A. Alvarez Zarikian and a. t. E. Scientists. Tokyo, Integrated Ocean Drilling Program Management International, Inc. **329**. doi:10.2204/iodp.proc.329.101.2011

Ehrmann, W. U. and A. Mackensen (1992). "Sedimentological evidence for the formation of an East Antarctic ice sheet in Eocene/Oligocene time." Palaeogeography, Palaeoclimatology, Palaeoecology **93**(1–2): 85-112. doi:10.1016/0031-0182(92)90185-8

Ewing, J. and M. Ewing (1967). "Sediment Distribution on the Mid-Ocean Ridges with Respect to Spreading of the Sea Floor." Science **156**(3782): 1590 – 1592. doi:10.1126/science.156.3782.1590

Horn, M. and G. Uenzelmann-Neben (2013). "Nonlinear sediment thickness increase on the western East Pacific Rise flank, 45°S." Geo-Marine Letters **33**(5): 381 - 390. doi:10.1007/s00367-013-0335-1

Houtz, R. E., D. E. Hayes, et al. (1977). "Kerguelen Plateau bathymetry, sediment distribution and crustal structure." Marine Geology **25**(1–3): 95-130. doi:10.1016/0025-3227(77)90049-4

Kuhlbrodt, T., A. Griesel, et al. (2007). "On the driving processes of the Atlantic meridional overturning circulation." Reviews of Geophysics **45**(2): RG2001. doi:10.1029/2004rg000166

Lewis, K., S. D. Nodder, et al. (2012, 13.07.2012). "Sea floor geology - Zealandia: the New Zealand continent, Te Ara - the Encyclopedia of New Zealand." from http://www.TeAra.govt.nz/en/sea-floor-geology/page-1

Marshall, J. and K. Speer (2012). "Closure of the meridional overturning circulation through Southern Ocean upwelling." Nature GeoScience **5**(3): 171-180. doi:10.1038/ngeo1391

Neil, H. L., L. Carter, et al. (2004). "Thermal isolation of Campbell Plateau, New Zealand, by the Antarctic Circumpolar Current over the past 130 kyr." Paleoceanography **19**(4): PA4008. doi:10.1029/2003pa000975

Osborn, N. I., P. F. Ciesielski, et al. (1983). "Disconformities and paleoceanography in the southeast Indian Ocean during the past 5.4 million years." Geological Society of America Bulletin **94**(11): 1345-1358. doi:10.1130/0016-7606(1983)94<1345:dapits>2.0.co;2

Rebesco, M., A. Camerlenghi, et al. (2008). "Contourites ". Amsterdam, Elsevier Science.

Rebesco, M., F. J. Hernández-Molina, et al. (2014). "Contourites and associated sediments controlled by deep-water circulation processes: State-of-the-art and future considerations." Marine Geology **352**(0): 111-154. doi:10.1016/j.margeo.2014.03.011

Reid, J. L. (1997). "On the total geostrophic circulation of the pacific ocean: flow patterns, tracers, and transports." Progress In Oceanography **39**(4): 263 – 352. doi:10.1016/S0079-6611(97)00012-8

Smith, W. H. F. and D. T. Sandwell (1997). "Global Sea Floor Topography from Satellite Altimetry and Ship Depth Soundings." Science **277**(5334): 1956 – 1962. doi:10.1126/science.277.5334.1956

Sparrow, M., P. Chapman, et al. (2004 - 2006). The World Ocean Circulation Experiment (WOCE) Hydrographic Atlas Series. M. Sparrow, P. Chapman and J. Gould. Southhampton, U.K., International WOCE Project Office.

Stickley, C. E., H. Brinkhuis, et al. (2004). "Timing and nature of the deepening of the Tasmanian Gateway." Paleoceanography **19**(4): PA4027. doi:10.1029/2004pa001022

van Aken, H. M. (2007). "The Oceanic Thermohaline Circulation: An Introduction". New York, Springer Science and Business Media, LLC.

Weigelt, E. and G. Uenzelmann-Neben (2007). "Orbital forced cyclicity of reflector strength in the seismic records of the Cape Basin." Geophysical Research Letters **34**(1): L01702. doi:10.1029/2006gl028376

Yilmaz, Ö. (2001). "Seismic Data Analysis". Tulsa, Society of Exploration Geophysicists.

Zachos, J. C., J. R. Breza, et al. (1992). "Early Oligocene ice-sheet expansion on Antarctica: Stable isotope and sedimentological evidence from Kerguelen Plateau, southern Indian Ocean." Geology **20**(6): 569-573.

2. Datasets

2.1 Seismic reflection data

Seismic reflection data were collected during R/V Sonne cruise 213/2 (Tiedemann et al. 2012). The cruise targeted the Southwest Pacific Basin for paleoceanographic reconstruction and volcanological studies of the Pacific Plate combined into the Project **So**uth **Pa**cific **Tra**nsects (SOPATRA, Ronge et al. 2013). Besides multiple short cores, the paleoceanographic part included ten multichannel seismic reflection profiles collected in two different survey regions. Each region was covered by five profiles. The locations of these ten profiles are shown in Figure 2.1.

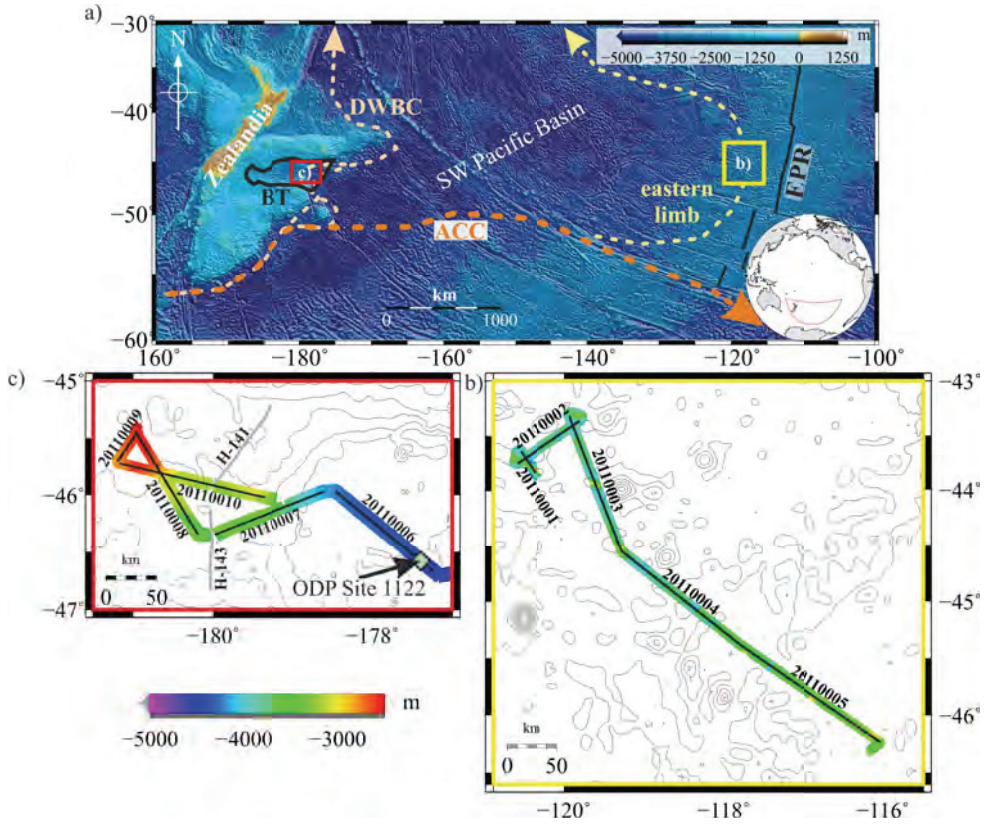

Figure 2.1: **a)** Location of the two survey regions (shown in red and yellow) in the South West (SW) Pacific Basin surveyed during cruise SO 213/2. Dashed lines indicate the main flows of the Deep Western Boundary Current (DWBC, dusky pink) and the eastern limb of the deep inflow (light yellow) as well as the Antarctic Circumpolar Current (ACC, orange line). Solid black lines indicate the locations of the East Pacific Rise (EPR) and of the Bounty Trough area (BT). Bathymetry is taken from the GEBCO_08 grid (Smith and Sandwell 1997); **b)** Layout of the survey area close to the EPR divided into five seismic profiles AWI-20110001 – AWI-20110005 (black); Coloured area represents the swath bathymetry acquired during Sonne cruise 213/2 (Tiedemann et al. 2012) and black contours are taken from GEBO_08 grid (Smith and Sandwell 1997); **c)** Layout of the second survey divided into five seismic profiles AWI-20110006 – AWI-20110010 (black lines) at the eastern end of the Bounty Trough. The light grey profiles represent additional multichannel seismic lines Hunt (H)-141 and Hunt-143 interpreted by Uenzelmann-Neben et al. (2009). The light green diamond indicates the location of Ocean Drilling Program (ODP) Leg 181 Site 1122, the coloured area represents the swath bathymetry acquired during Sonne cruise 213/2 (Tiedemann et al. 2012). The black contours are taken from GEBCO_08 grid (Smith and Sandwell 1997).

Profiles AWI-20110001 to AWI-20110005 are located at the eastern margin of the Southwest Pacific Basin close to the EPR at ~45°S (Figure 2.1a, b) to record sediment structures below the eastern limb of the cold inflow into the Southwest Pacific Basin. Another aim of these five profiles was mapping the sedimentary distribution with respect to the distance from the EPR.

Profiles AWI-20110006 to AWI-20110010 are located at the western margin of the Southwest Pacific Basin where the DWBC turns north and away from the direct influence of the ACC (Figure 2.1 a, c). After leaving the direct influence of the ACC, the DWBC slows down allowing it to deposit its sedimentary load. This has created an archive capable of recording paleoceanographic changes since approximately 80 – 90 Ma. Additionally, profile AWI 20110006 has crossed ODP Leg 181 Site 1122, which allows direct age control from lithological information. Besides this five high-resolution multichannel seismic lines two profiles Hunt-141 and Hunt-143 (grey lines in Figure 2.2c) are available for this region. These profiles have been interpreted by Uenzelmann-Neben et al. (2009).

2.2 Used seismic equipment

During Sonne cruise 213/2, 1134 km of seismic reflection profiles were acquired (Tiedemann et al. 2012). As seismic source, four GI-Guns^{TM} (Generator Injector Gun, total volume 2.4 l) were used, which were towed approximately 20 metres behind the ship. Each GI-Gun^{TM} consists of a generator chamber of 0.7 l and an injector chamber of 1.7 l. The injector chamber was fired 33 ms after the generator chamber to suppress signals caused by the collapse of the bubble. The main frequency of the source is 40 Hz. The seismic signal was recorded with a 3000 metre long Sersel SEAL^{TM} digital streamer plus a lead in cable of 191 metres (distance from ship to first channel). The streamer contains 240 channels with 12.5 metre spacing between each hydrophone. The setup is sketched in Figure 2.2. Seismic signal record length was 9 seconds (10 s for profile AWI-20110001), the shot interval was 10 seconds (12 s for AWI 20110001). The used GI-Guns allow a vertical resolution of approximately 10 metres (please refer also to Chapter 3). For further details please refer to the cruise report (Tiedemann et al. 2012).

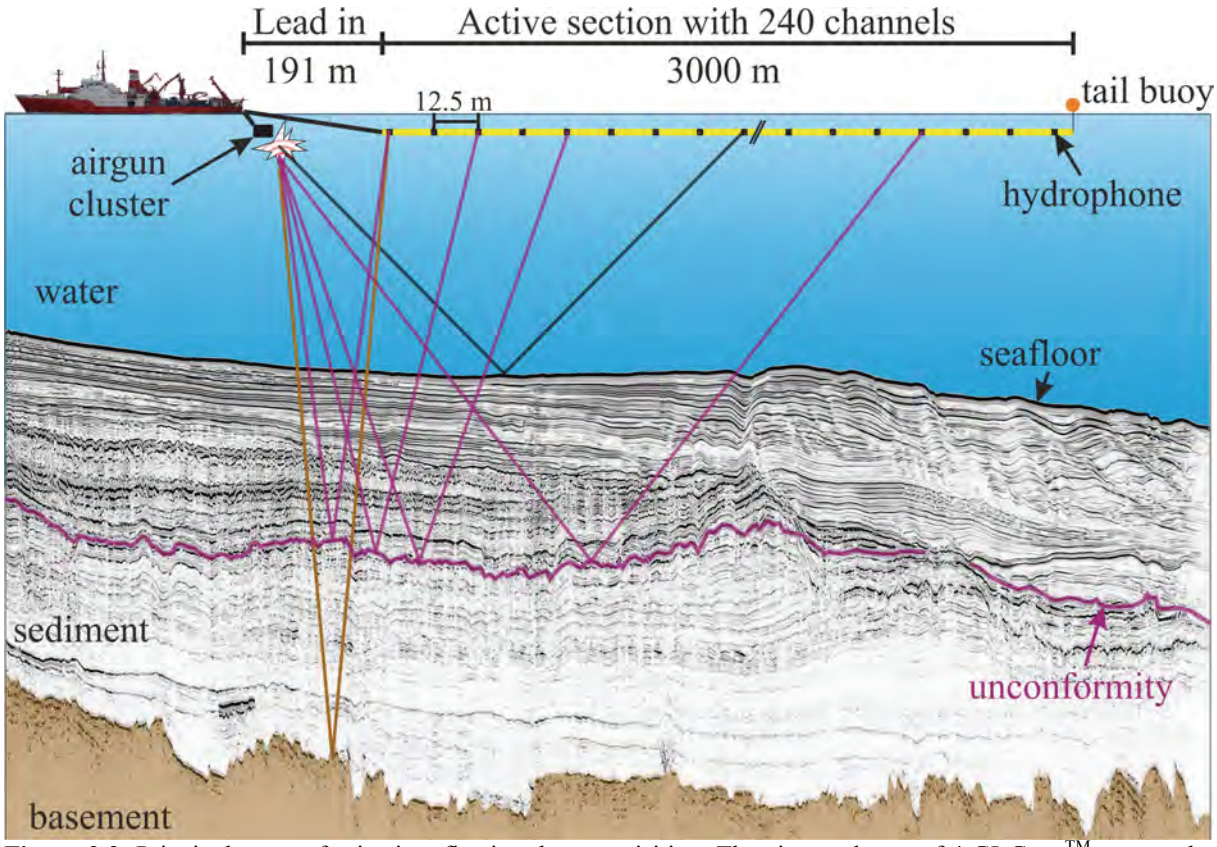

Figure 2.2: Principal setup of seismic reflection data acquisition. The airgun cluster of 4 GI-Guns™ creates the seismic signal. Waves travel through the water and the sediments and are reflected at the boundary between different materials with different impedance values (for example at the purple reflection as indicated by the purple ray path or at the seafloor (black) indicated by the black ray path). The amplitude of the reflected wave is proportional to the difference in impedance (the impedance contrast). The 240 hydrophones in the Sercel SEAL™ streamer (12.5 metre distance between each hydrophone, first hydrophone 191 m behind the ship (lead in)) record the signal. Data are stored on board for further processing.

2.3 Parasound sub-bottom profiler data

RV Sonne is also equipped with a deep-sea parametric sub-bottom profiler, Atlas Parasound P70. The echo sounding pulses are emitted from a transducer array mounted in the ship hull. It is capable of emitting two frequencies between 18 kHz and 33 kHz (Atlas Hydrographic GmbH 2010). The chosen operation mode for cruise SO 213/2 was 18 KHz and 22 KHz. In addition, a parametric low frequency can be created by destructive interference of the two signals. In this case, data with 4 KHz were recorded. The system was constantly operated during the cruise and recorded the three mentioned frequencies (Tiedemann et al. 2012).

The 4 KHz data can be used to analyse the upper sedimentary column in more detail and reveal structures that are on a sub metre scale. In contrast to the 40 Hz seismic reflection profiling, the Parasound data features a higher resolution of ~10 cm (please refer to chapter 3). One drawback in comparison to the seismic reflection data is the low penetration of the signal. It is limited to a maximum of 200 metres (Atlas Hydrographic GmbH 2010). Real penetration is dependent on the material of the strata and compaction and therefore can be less. The typical penetration depth is 35 – 80 metres (40 – 100 ms two way traveltime).

The offered high resolution of the upper sedimentary column of the Bounty Channel levees can be used to study signals created by orbital forcing. Figure 2.3 shows the available Parasound profiles that crossed the Bounty Channel levee. The dataset is extended using older data from Sonne cruise SO 169 gathered in 2003 (Gohl 2003).

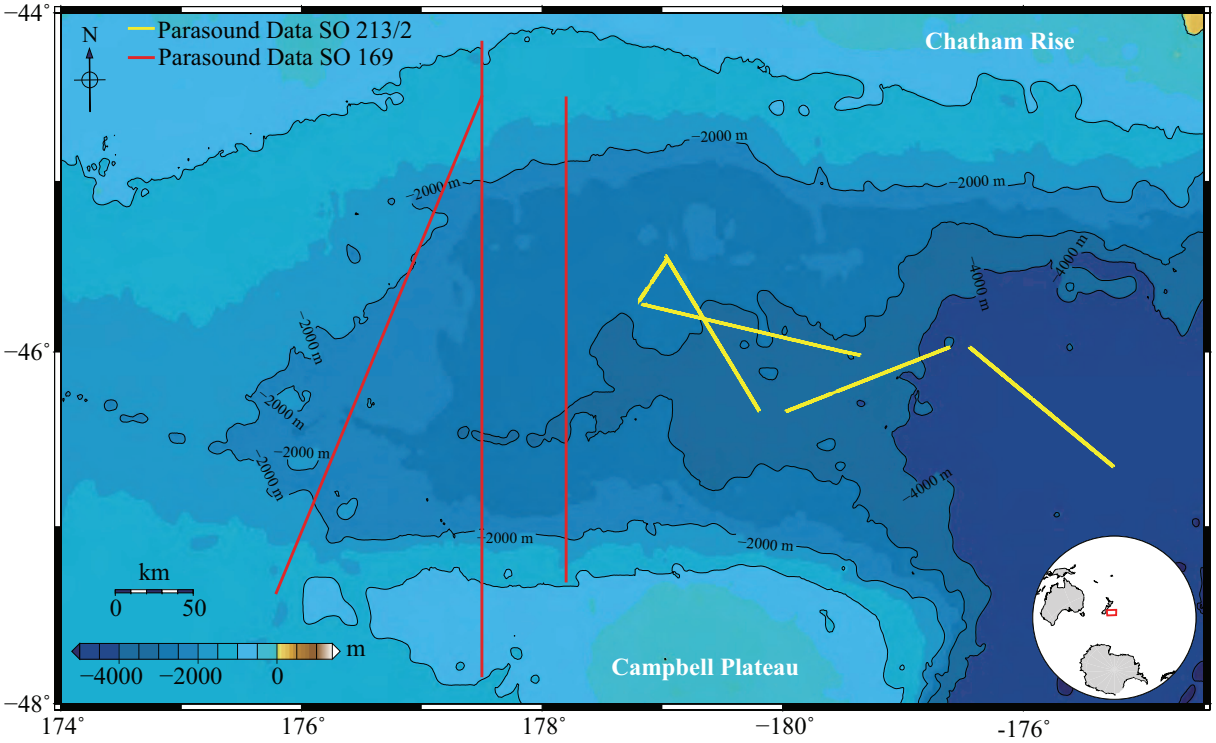

Figure 2.3: Used Parasound sub-bottom profiler data in the Bounty Trough area. Yellow lines indicate the Parasound data available from Sonne (SO) cruise 213/2 (Tiedemann et al. 2012). Red lines indicate Parasound profiles from Sonne cruise 169 (Gohl 2003). Bathymetry data is taken from the GEBGO_08 grid (Smith and Sandwell 1997).

2.4 Used borehole data

The sedimentary archives around Zealandia where explored by multiple drilling campaigns (see Figure 1.2). ODP Leg 181 especially targeted the sedimentary deposits of the DWBC to expand the database on past climate and paleoceanographic conditions in the Southwest Pacific (Carter et al. 1999b; Carter et al. 2004b). Profile AWI-20110006 directly crossed ODP Leg 181 Site 1122 (Figure 2.2c). ODP Site 1122 offers samples for the upper 617.8 metres below seafloor (mbsf). To link lithological and seismic data, a synthetic seismogram from the gathered physical properties is computed (for details please refer to chapter 3).

ODP Site 1122 does not sample the whole sedimentary column. Thus information of oil exploration wells in the Canterbury Basin and Great South Basin has to be used to characterise sediments below 617.8 mbsf. Carter (1988) has published data of five wells allowing a characterisation of the deeper sedimentary column. His lithological interpretations have been transferred to the Bounty Trough via seismic data (Carter et al. 1994; Uenzelmann-Neben et al. 2009). Lines Hunt-141 and Hunt-143 (interpreted by Uenzelmann-Neben et al. 2009) are close to lines AWI-20110007, AWI-20110008 and AWI-20110010 (Figure 2.2c). From here we can transfer the interpretation of the lower sedimentary column to profiles AWI-20110006 to AWI-20110010.

2.5 References

Atlas Hydrographic GmbH (2010). ATLAS PARASOUND Deep-Sea parametric sub-bottom profiler. Bremen, http://www.atlas-elektronik.com/what-we-do/hydrographic-systems/parasound/.

Carter, R. M. (1988). "Post-breakup stratigraphy of the Kaikoura Synthem (Cretaceous-Cenozoic), continental margin, southeastern New Zealand." New Zealand Journal of Geology and Geophysics **31**(4): 405-429. doi:10.1080/00288306.1988.10422141

Carter, R. M., L. Carter, et al. (1994). "Seismic stratigraphy of the Bounty Trough, south-west Pacific Ocean." Marine and Petroleum Geology **11**(1): 79-93. doi:10.1016/0264-8172(94)90011-6

Carter, R. M., I. N. McCave, et al. (2004b). "1. Leg 181 Synthesis: Fronts, Flows, Drifts, Vocanoes, and the Evolution of the Southwestern Gateway to the Pacific Ocean, Eastern New Zealand". Published in: Proceedings of the Ocean Drilling Programm, Scientific Results. C. Richter. Texas, College Station (Ocean Drilling Program). **181**. doi:10.2973/odp.proc.sr.181.210.2004

Carter, R. M., I. N. McCave, et al. (1999b). "Site 1122: Turbidites with a Contourite Foundation". Published in: Proceedings of the Ocean Drilling Program, Initial reports:. R. M. Carter, I. N. McCave, C. Richter and L. Carter. Texas, USA, College Station (Ocean Drilling Program). **181:** 1 - 146. doi:10.2973/odp.proc.ir.181.106.2000

Gohl, K. (2003). Structure and dynamics of a submarine continent: Tectonic-magmatic evolution of the Campbell Plateau (New Zealand) Report of the RV SONNE cruise SO-169, Project CAMP 17 January to 24 February 2003 Reports on Polar and Marine Research. Bremerhaven, Alfred Wegner Institut, Helmholtz Centre for Polar and Marine Reseach, Bremerhaven. **457:** 88. doi:10.2312/BzPM_0457_2003

Ronge, T. A., R. Tiedemann, et al. (2013). SO213 SOPATRA – Fahrtbericht und erste Ergebnisse SONNE Statusseminar. Kiel**:** 24. doi:10013/epic.42135

Smith, W. H. F. and D. T. Sandwell (1997). "Global Sea Floor Topography from Satellite Altimetry and Ship Depth Soundings." Science **277**(5334): 1956 – 1962. doi:10.1126/science.277.5334.1956

Tiedemann, R., J. O'Conner, et al. (2012). Cruise Report SO213: SOPATRA. Bremerhaven, Alfred Wegener Institute, Helmholtz Centre for Polar and Marine Research**:** 111.

Uenzelmann-Neben, G., J. W. G. Grobys, et al. (2009). "Neogene sediment structures in Bounty Trough, eastern New Zealand: Influence of magmatic and oceanic current activity." Geological Society of America Bulletin **121**(1-2): 134-149. doi:10.1130/B26259.1

3. Methods

3.1 Seismic reflection profiling

One way to interpret sedimentary structures is to create an image of the sedimentary deposits below the seafloor. Seismic reflection profiling offers an ideal method for creating sub-bottom images. It is widely used in hydrocarbon exploration and characterisation of sedimentary deposits (e.g. Yilmaz 2001). A seismic wave is emitted from a cluster of airguns that is capable of traveling through the water column and the subsurface. During its way through the different layers, part of the wave energy is reflected at boundaries where the seismic impedance (see below) of the material changes. The rest of the energy travels further down into the subsurface. The wave energy can be reflected at other impedance interfaces until all energy is either reflected or absorbed by the earth. The reflected waves travel back to the sea surface. Here, a chain of hydrophones records the energy of the seismic wave and the time the seismic wave needs for its way down to the sediments and up to the chain of hydrophones. This time is called the two way traveltime (TWT) of the signal. Using multiple hydrophones to record a seismic wave can be used later in the processing to enhance the signal to noise ratio (see next section). An example of such seismic wave propagation is shown in Figure 2.1.

The seismic impedance of geological deposits is defined as the product of density and the P-wave velocity. Thus, a change in either density or in P-wave velocity due to a change in composition, compaction of the rocks or events such as erosional phases alters the seismic impedance. The difference in impedance (now referred to as impedance contrast) between two different materials is proportional to the energy reflected.

To be able to resolve two independent seismic impedance contrasts they have to be separated from each other by one quarter of the wavelength of the seismic source to be detectable as two different objects (Sheriff and Geldart 1982). Sources are characterised by a dominant frequency f. The frequency is directly linked to the wavelength $\boldsymbol{\lambda}$ and the velocity v of the pulse. Thus, the resolution of a seismic wave can be calculated by (equation 1):

$$Resolution = \frac{\boldsymbol{\lambda}}{\mathbf{4}} \text{ and } \boldsymbol{\lambda} = \frac{\mathrm{v}}{\mathrm{f}}$$

$$\rightarrow Resolution = \frac{\mathrm{v}}{4\mathrm{f}} \qquad (1)$$

3.2 Processing of seismic reflection data

Seismic data processing has been carried out using Paradigm software Focus 5.4 and Echos 2011.3. The 240 hydrophones generated 240 traces per shot. These traces have been grouped in 25 metre wide

sub-surface intervals to form common depth point gathers (CDP-sorting, see Yilmaz 2001 for further details). This CDP-sorting also allows a velocity analysis of the seismic waves. These and further processing steps are listed in the flowing bullet points:

- Setting up geometry
- CDP sorting
- Detailed velocity analysis every 50th CDP
- Correction for spherical divergence
- Normal moveout (NMO) correction
- FK-filtering for profiles AWI-20110007, AWI-20110008 and AWI-20110010
- Stacking
- Omega-X migration
- Deconvolution of profiles AWI-20110001 – AWI-20110005 to remove surface ghost (loss of true amplitude)

For display purposes

- Frequency filtering
- Muting of the water column
- Application of Automatic Gain Control (AGC)

Velocity analysis has been carried out every 50th CDP. At steep slopes spacing has been reduced to 10 CDPs to better resolve velocity gradients. Prestack processing has included correction for spherical divergence to account for the loss of seismic wave energy due to spherical expansion. Further, an FK Filter excluding wave number-frequency ranges has been applied to profiles AWI-20110007, AWI-20110008 and AWI-20110010 to reduce noise.

To be able to stack the traces of each CDP the normal moveout (NMO) has been removed from the data using the velocity profile derived by the velocity analysis. The following stacking procedure has enhanced the signal to noise ratio by the square root of the number of ensembles per CDP (Yilmaz 2001). Poststack processing has included migration (omega x migration, based on finite difference approximation for monochromatic waves (Yilmaz 2001)) to collapse diffraction hyperbolas and get a clear seismic image of the strata (Yilmaz 2001). Further, predictive deconvolution using a defined gap length has been applied to profiles AWI-20110001 to AWI-20110005. A gap width of 13 ms has been chosen to suppress the surface ghost.

For display proposes I have applied a frequency filtering (see chapters 5 to 7 for details) and have muted the water column. An automatic gain control (AGC) has been applied to some seismic images. If this is the case, it is indicated in the figure captions.

3.3 Linking borehole data to seismic sections

To link the lithological data of ODP Site 1122 to the seismic reflection data, a conversion of depth to TWT is needed. For this purpose a synthetic seismogram can be used. The values of P-wave velocity of the sediment cores from 390 mbsf and density were measured during drilling of ODP Site 1122 (Carter, McCave et al. 1999). I have used this information and calculated the seismic impedance for the cored sediments. Figure 3.1 sketches the workflow of computing a synthetic seismogram. For further details please refer to Yilmaz (2001).

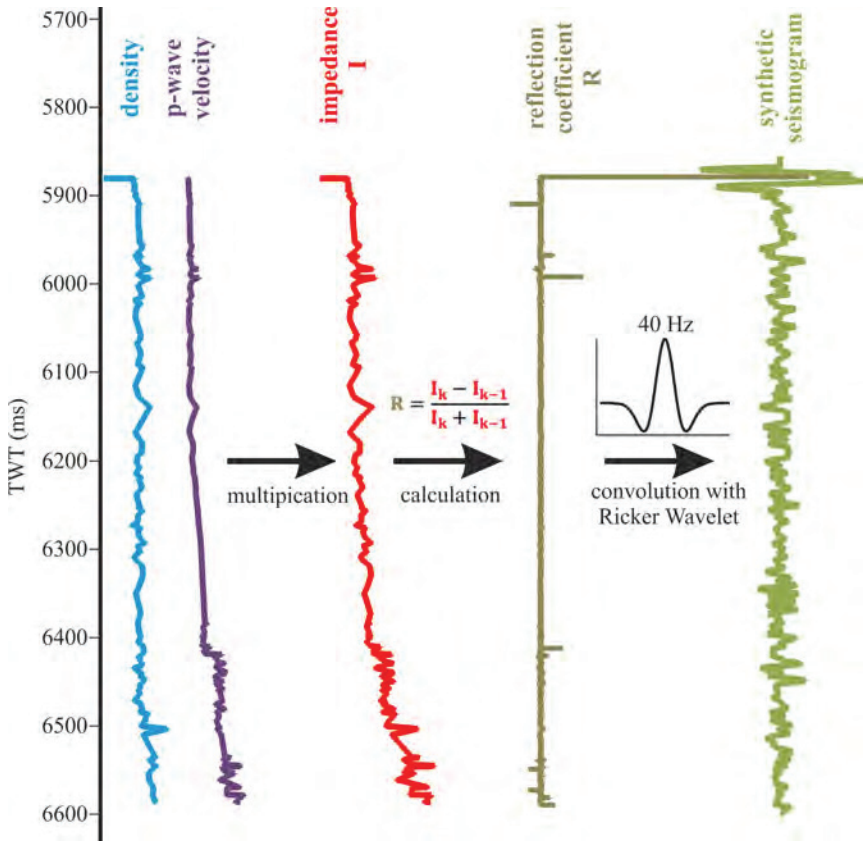

Figure 3.1: Workflow for a computation of the synthetic seismogram: The density (blue curve) and the P-wave velocity (purple curve) from ODP Site 1122 are multiplied to calculate the impedance I (red curve) of the sediments. From the impedance the reflection coefficient R (brown curve) can be calculated using the given formula (Yilmaz 2001). I_k and I_{k-1} represent the impedance value of the k and k-1 layer of the sedimentary column. This reflection coefficient is than convolved with a 40 Hz Ricker wavelet. The result is the synthetic seismogram (light green).

I have chosen a Ricker wavelet for the convolution, a zero phase wavelet defining a single pulse (Ricker 1953) analogue to the seismic source of the GI-Guns. The wavelet amplitude A depends only on the peak frequency f and the time t and is defined as follows (equation 2):

$$A = \left(1 - 2\pi^2 f^2 t^2\right) e^{\pi^2 f^2 t^2} \quad (2)$$

The frequency f of the Ricker wavelet has been adjusted to 40 Hz to mimic the used seismic source (40 Hz is the main frequency of the GI-Guns).

A major problem encountered while computing the synthetic seismogram has been the missing velocities between 0 and 390 mbsf. Here, no velocity data was measured because the sandy deposits of the Bounty Channel where not dense enough for the available velocity measurement tools (Carter et al. 1999b). Below 390 mbsf sediments where compacted enough and measurements were carried out down to 608 mbsf (Carter et al. 1999b). Density was measured every 2 centimetres. Empirical observations have shown that the density is directly linked to the P-wave velocity (e.g. Nafe and Drake 1957; Hamilton 1978) and can be calculated in two steps. First, density $\boldsymbol{\rho_s}$ is converted to the factional porosity **FP** via formula 3 derived by Hamilton (1976):

$$FP = \frac{GD - \rho_s}{GD - \rho_w} \quad (3)$$

$\boldsymbol{\rho_w}$ is density of the water inside the pores of the sediment (set to the density of seawater = $1024 \frac{kg}{m^3}$). The grain density **GD** was measured by the shipboard scientific party (Carter et al. 1999b, their Table 15). The fractional porosity **FP** can now be converted to a P-wave velocity $\mathbf{v_p}$. In this second step I have used the empiric formula 4 derived by Erickson and Jarrard (1998) for normal consolidated sediments. Erickson and Jarrard (1998) further reported that shale also influences the P-wave velocity. Thus they also take into account the shale fraction $\mathbf{v_s}$ of the sediments.

$$v_p = 0.739 + 0.552 * FP + \frac{0.305}{(FP+0.13)^2+0.0725} + 0.61(v_s - 1.123) * (\tanh(40 * (FP - 0.31)) - \operatorname{abs}(\tanh(40 * (FP - 0.31)))) \quad (4)$$

No shale was reported in the ODP Site 1122 drilling report (Carter et al. 1999b). I have assumed that no shale is present and set the value for v_s to zero. This is reasonably as my calculated porosities are well above 0.4 for which the shale ratio does not play a role (see Erickson and Jarrard 1998, their Figure 9). With formulas 3 and 4 the missing velocities have been calculated to calculate the impedance.

With the synthetic seismogram shown in Figure 3.1 I have generated a depth-TWT conversion that I have used to directly compare the recorded traces at the location of ODP Site 1122 with lithological observations of the borehole. The complete interpretation of the synthetic seismogram is shown in chapter 6.

3.4 Revealing bottom current signatures in seismic reflection data

3.4.1 Sediment drifts

To reveal bottom currents in seismic reflection data it is important to know the features currents can create and how those features can be identified. Important features are sediment drift bodies. This generic term (first used by Hollister 1967) describes various forms of bottom current depositional structures, which hint on bottom current direction, evolution of the bottom current, its core flow position and its speed (e.g. Faugères et al. 1999; Stow et al. 2002; Rebesco et al. 2014). Presently

drifts are subdivided into five classes that allow further conclusions on the drift building current: (1) Sheeted drifts, (2) Mounded elongated drifts, (3) Channel-related drifts, (4) Confined drifts and (5) Infill drifts. Additionally drifts can be of mixed composition, which means that other processes such as mass transport or high hemi-/pelagic sediment input modified the drift appearance (Michels et al. 2002). For the area of interest, the Southwest Pacific Basin, the most relevant drift is the mounded elongated drift. An example of a mounded drift structure and how a current creates such drift is given in Figure 3.2.

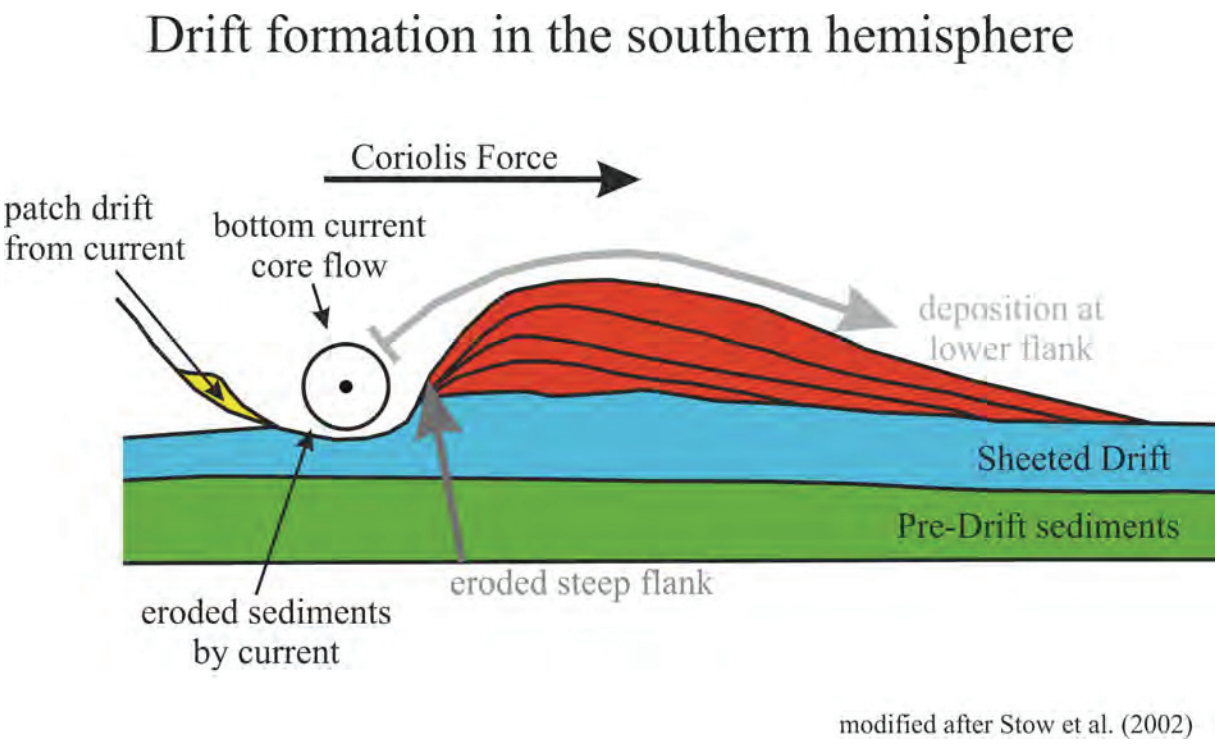

Figure 3.2: Example of a mounded drift deposited on a sheeted drift in the southern hemisphere (Coriolis force deflects currents in flow direction to the left). The creating bottom current flows out of the paper plane. The current's sediment load is deposited on the left flank of the flow where current speeds are slower than in the core flow. The core flow itself still erodes sediments and creates a steep flank on one side of the drift while on the lower flanks sediment accumulates. This creates the characteristic shape of an elongated mounded drift. Drift crest migration and the steep flank indicate the side on which the current is flowing and Coriolis force allows to decipher the direction of the current.

Elongated mounded drifts are further divided into three different subtypes. The information given by Faugères and Stow (2008) are summarised in the list below and in Figure 3.3.

1. Plastered Drift: These drifts can be found at gentle slopes and hint on weak bottom current activity. Drift bodies general exhibit a lateral migration of the drift axis
   Examples: Gardar Drift and Bjorn Drift in the north Atlantic Ocean

2. Separated Drift: Separated drifts are elongated parallel to the slope they are deposited on. They are normally found on steeper slopes than Plastered Drifts. Currents building up these drifts leave a well visible moat inside the sediments. Additionally these currents have a higher speed. Deposition is normally displaced laterally where current speeds are slower (in the Southern Hemisphere to the left due to Coriolis force)

Examples: Faro Drift at the Gulf of Cadiz

3. Detached Drift: Detached drifts from at the base of a for example a continental margin where the margin's trend changes or where bottom and surface currents interact. Their general migration direction is downslope.

Examples: Eirik Drift south of Greenland and Blake Bahama Drift east of the US coast

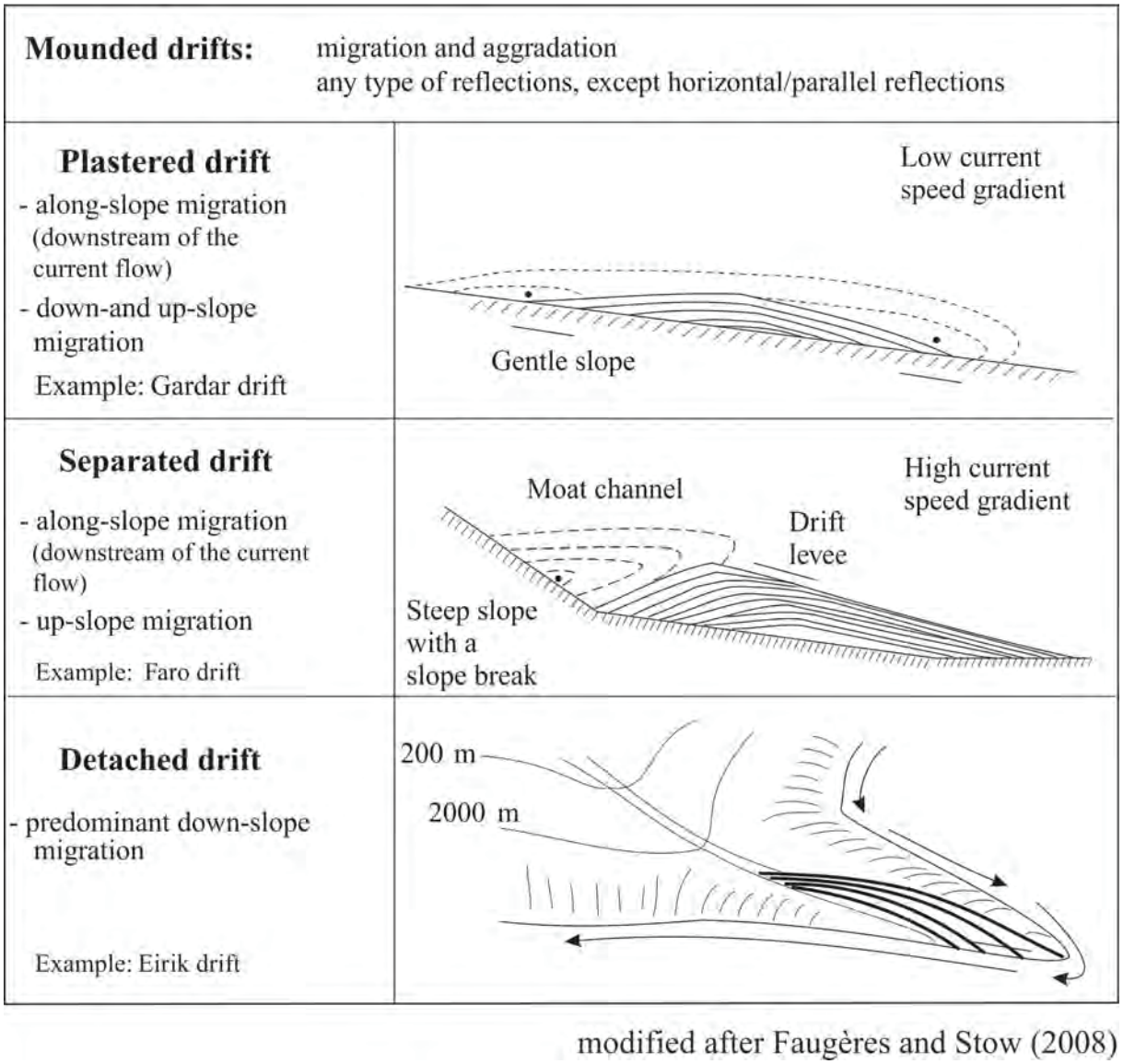

Figure 3.3: Examples for the three different mounded drift types

3.4.2 Other prominent reflection patterns

Besides the drift bodies described above, various other processes can leave a footprint observable in seismic reflection data. The following three processes have been identified in chapters 5 to 7. They cause an identifiable reflection pattern, commonly hint on an active or ancient bottom current or turbidity flow.

(1) Erosional surfaces are prominent features in a seismic image. The surface itself is often marked by a strong amplitude reflection. The reflection pattern above this reflection normally differs from the pattern below (Stow et al. 2002). Additionally reflections of the seismostratigraphic unit below the erosional surface may truncate against the erosional surface. This typically means that the erosion took place after the now truncated reflections have formed. An example for reflections truncation is shown in Figure 3.4. The upper reflections (marked in yellow) truncate against the seafloor reflection. This hints on erosion under a presently active current or at least at a current that was active until recent years.

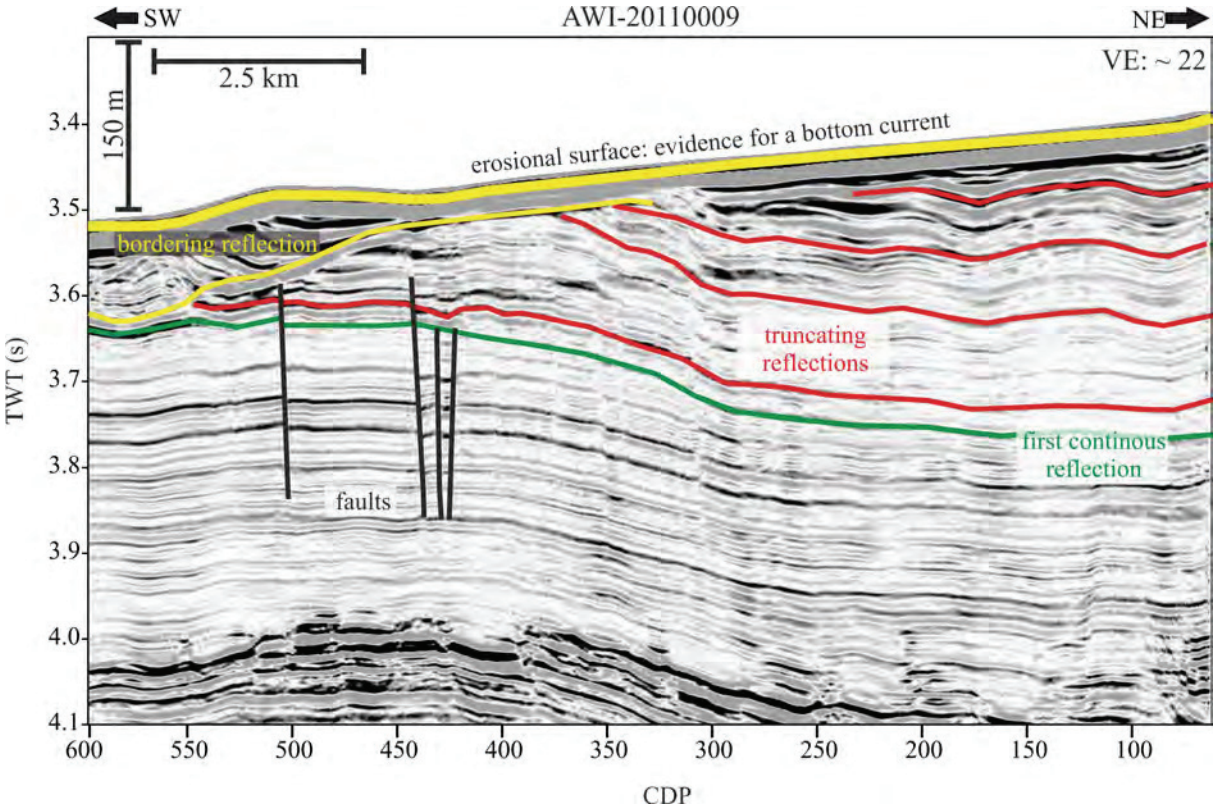

Figure 3.4: An example for truncating reflections in the Bounty Trough region on profile AWI-20110009. The yellow marked reflections represent erosional surfaces that have been created by bottom currents. The red reflections truncate against these erosional surfaces. Since the green reflection is the first reflection that can be traced continuously below the erosional surface this indicates that the erosion has to be younger than this green reflection. As the erosional surface is the seafloor the erosive current began influencing the area after the creation of the green reflection and has prevailed until recent times.

(2) Sediment waves can be recognised in seismic data. Reflections from sediment waves generally show a wavy reflection pattern (Figure 3.5). Sediment waves are typically found perpendicular to the forming bottom current or turbidity flow and migrate in opposite direction (upstream) to the bottom

current in the case of fine grained sediment waves (Wynn and Masson 2008). For down current migrating sediment waves, the sediment waves are made up of coarser grained material (material predominantly of sand size (Wynn and Masson 2008)). Sediment waves are commonly part of sediment drift's lower flanks or can be found in levee deposits of turbidity currents. A prominent example of sediment waves is shown in Figure 3.5. Here sediments of the left levee of the Bounty Channel show a sinuous shape like reflection pattern, which indicates that the sediment waves are of turbiditic origin.

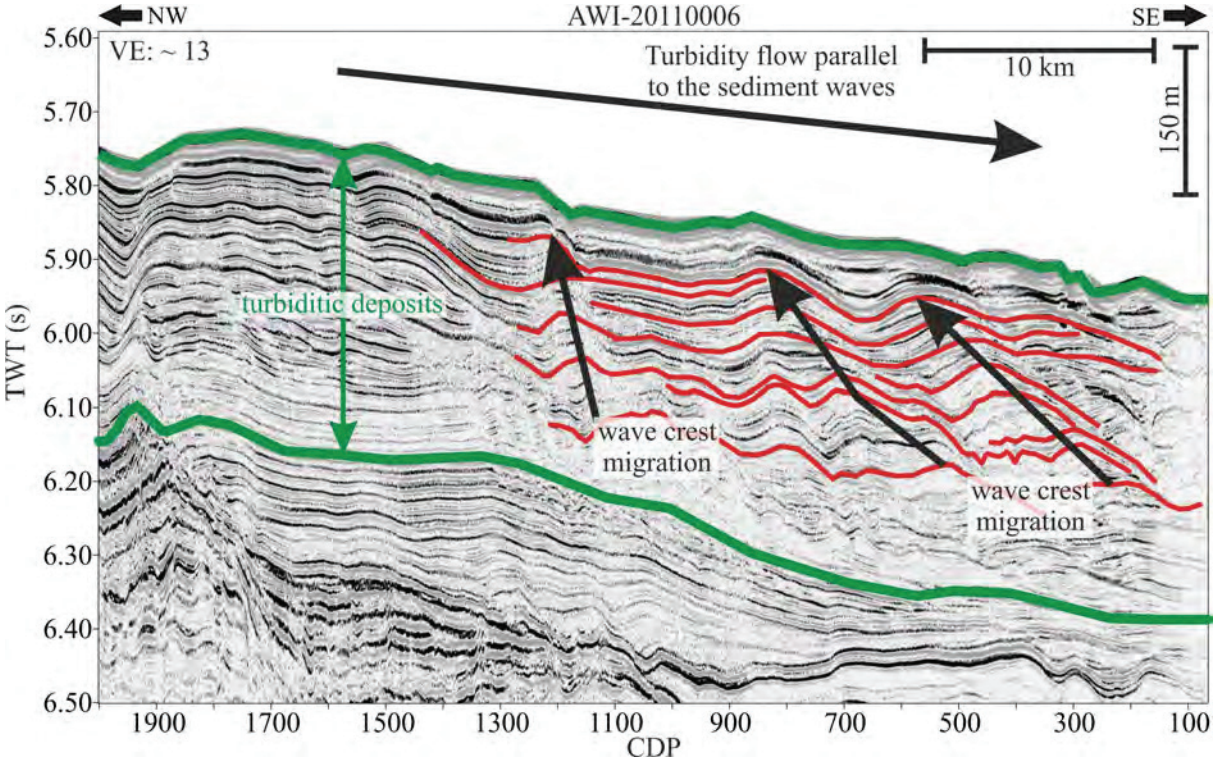

Figure 3.5: Sediment waves generated by a turbidity current (black arrow above sediments, deposits are located between two thick green lines). Sediment waves (marked in red) show a wavy reflection pattern and a migration direction from to the northwest (see arrows). This is approximately upstream to the turbidity flow direction. An upstream migration of sediment waves hints on fine grained sediments (Wynn and Masson 2008). This fits to the sediment composition of fine sand and silt, drilled by ODP Site 1122 (Carter et al. 1999b).

(3) Obstacles within the core flow of a bottom current take an active influence on this current. If a current flow passes an obstacle like a seamount it is forced to flow around this obstacle. The flow is not distributed equally around the seamount. Above the seamount, the current creates two different eddies that cause upwelling on one side of the flow and down welling on the other side of the flow. The eddy influences the bottom current that passes the seamount in two ways. On one side the current is decelerated due to cyclonic down welling, on the other side the current is accelerated due to anticyclonic upwelling (Hernández-Molina et al. 2006). This "seamount-effect" (first observed by Davis and Laughton (1972) and summarised by Hernández-Molina et al. (2006)) is caused by the Coriolis force favouring stronger flow on one side of the obstacle. For the southern hemisphere the right flow (looking down-current) shows an enhanced flow (left for the northern hemisphere). The enhanced flow ("accelerated core" in Figure 3.6) either shows enhanced scouring or less deposition

while the lowered intensity flow ("decelerated core" in Figure 3.6) features less scouring or enhanced deposition (Hernández-Molina et al. 2006). Thus, different depositional patterns on both sides of a seamount indicate a bottom current flow and its direction. Figure 3.6 shows a schematic sketch of the seamount effect and a corresponding seismic image.

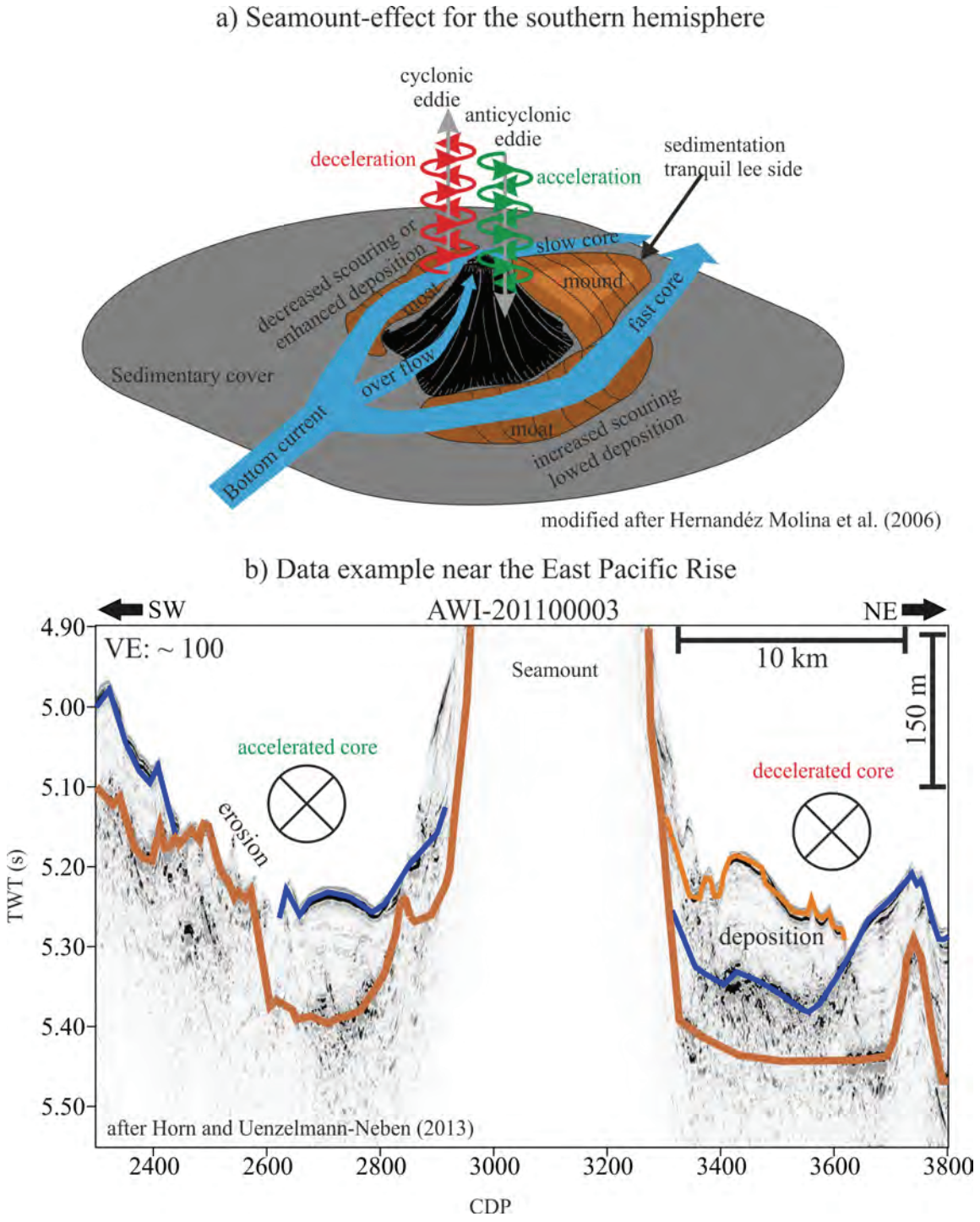

Figure 3.6: Seamount effect after Hernández-Molina et al. (2006). **a)** Schematic overview. A deep current approaching an obstacle is forced to split into two cores. Above the obstacle the deep current creates two eddies, one at each side of the obstacle. These two eddies rotate in different directions; one eddy (green) rotates in the flow direction of one core flow, accelerating it. The other eddy (red) rotates in opposite direction to the flow of the deep current, decelerating it. These acceleration and deceleration affects the sedimentary deposits beside the obstacle. **b)** An example of as seismic image at a seamount, found close to the East Pacific Rise (see Figure 1.2). The decelerated core deposits additional sediment (below orange reflection, CDP 3350 - 3600) while the accelerated core has eroded sediments (CDP 2500 – 2650) exposing the oceanic crust.

3.5 References

Carter, R. M., I. N. McCave, et al. (1999b). "Site 1122: Turbidites with a Contourite Foundation". Published in: Proceedings of the Ocean Drilling Program, Initial reports:. R. M. Carter, I. N. McCave, C. Richter and L. Carter. Texas, USA, College Station (Ocean Drilling Program). **181:** 1 - 146. doi:10.2973/odp.proc.ir.181.106.2000

Davis, A. S. and A. S. Laughton (1972). "Sedimentary Processes in the North Atlantic". Published in: Initial Reports of Deep Sea Drilling Project. L. A. S., W. A. Berggren, R. N. Bensonet al. Washington, D.C., U.S. Government Printing Office. **12:** 905-934. doi:10.2973/dsdp.proc.12.111.1972

Erickson, S. N. and R. D. Jarrard (1998). "Velocity-porosity relationships for water-saturated siliciclastic sediments." Journal of Geophysical Research: Solid Earth **103**(B12): 30385-30406. doi:10.1029/98jb02128

Faugères, J. C. and D. A. V. Stow (2008). "Chapter 14 Contourite Drifts: Nature, Evolution and Controls". Published in: Developments in Sedimentology. M. Rebesco and A. Camerlenghi. Amsterdam, Elsevier Science**:** 257 – 288. doi:10.1016/S0070-4571(08)10014-0

Faugères, J. C., D. A. V. Stow, et al. (1999). "Seismic features diagnostic of contourite drifts." Marine Geology **162**(1): 1-38. doi:10.1016/s0025-3227(99)00068-7

Hamilton, E. L. (1976). "Variations of density and porosity with depth in deep-sea sediments." Journal of Sedimentary Research **46**(2): 280-300. doi:10.1306/212f6f3c-2b24-11d7-8648000102c1865d

Hamilton, E. L. (1978). "Sound velocity–density relations in sea‐floor sediments and rocks." The Journal of the Acoustical Society of America **63**(2): 366-377. doi:10.1121/1.381747

Hernández-Molina, F. J., R. D. Larter, et al. (2006). "Miocene reversal of bottom water flow along the Pacific Margin of the Antarctic Peninsula: Stratigraphic evidence from a contourite sedimentary tail." Marine Geology **228**(1 – 4): 93 – 116. doi:10.1016/j.margeo.2005.12.010

Hollister, C. D. (1967). "Sediment distribution and deep circulation in the western North Atlantic". Published in: Studies in Physical Oceanography. A. L. Gordon. New York, Gorodon and Breach Science Publishers. **2:** 37 - 66.

Michels, K. H., G. Kuhn, et al. (2002). "The southern Weddell Sea: Combined contourite - turbidite sedimentation at the southeastern margin of the Weddell Gyre". Published in: Deep-water contourite systems: Modern drifts and ancient series, seismic and sedimentary characteristics. D. A. V. Stow, C. J. Pudsey, J. A. Howe, J.-C. Faugeres and A. R. Viana. London, Geological Society **22:** 305-323.

Nafe, J. E. and C. L. Drake (1957). "Variation with depth in shallow and deep water marine sediments of porosity, density and velocity of compressional and shear waves." Geophysics **22**(3): 523-552. doi:10.1190/1.1438386

Rebesco, M., F. J. Hernández-Molina, et al. (2014). "Contourites and associated sediments controlled by deep-water circulation processes: State-of-the-art and future considerations." Marine Geology **352**(0): 111-154. doi:10.1016/j.margeo.2014.03.011

Ricker, N. (1953). "The form and laws of Propagation of seismic wavelets." Geophysics **18**(1): 10-40. doi:doi:10.1190/1.1437843

Sheriff, R. E. and L. P. Geldart (1982). "4.3.2 Resolution". Published in: Exploration seismology Volume I: History, theory and data acquisition. Cambridge, Cambridge University Press. **1:** 117 - 122.

Stow, D. A. V., J.-C. Faugères, et al. (2002). "Bottom currents, contourites and deep-sea sediment drifts: current state-of-the-art". Published in: Deep-water contourite systems: Modern drifts and ancient series. D. A. V. Stow, C. J. Pudsey, J. A. Howe, J.-C. Faugères and A. R. Viana. London, Geological Society of London. **22:** 7 - 20. doi:10.1144/GSL.MEM.2002.022.01.02

Wynn, R. B. and D. G. Masson (2008). "Chapter 15 Sediment waves and bedforms". Published in: Contourites. M. Rebesco and A. Camerlenghi. Amsterdam, Elsevier Science**:** 289 - 300. doi:10.1016/S0070-4571(08)00215-X

Yilmaz, Ö. (2001). "Seismic Data Analysis". Tulsa, Society of Exploration Geophysicists.

4. Contribution to paleoceanographic reconstructions in the South Pacific Ocean

In this chapter I briefly present the three manuscripts published or submitted to scientific journals. I have highlighted my contributions to the manuscripts below. Data and methods used have been presented in the previous chapters 2 and 3. If not these methods will be explained in the manuscripts.

4.1 Nonlinear sediment thickness increase on the western East Pacific Rise flank, 45°S

Horn, M., and G. Uenzelmann-Neben (2013), Nonlinear sediment thickness increase on the western East Pacific Rise flank, 45°S, published in *Geo-Marine Letters*, Issue 33(5), pages 381 - 390.
Doi: 10.1007/s00367-013-0335-1

This publication analyses the sedimentary deposits close to the EPR. We have revised the present old model of Ewing and Ewing (1967) on sediment distribution with respect to the distance to the mid ocean ridge. We further have found causes for the observed discrepancies from the model. These indications are based on footprints of bottom currents and the areal distribution of two different sedimentary units.
The publication uses the five high-resolution seismic reflection profiles AWI-20110001 to AWI-20110005. I have processed the five profiles as presented in chapter 3. I further have defined the two different seismic units, identified footprints and computed the age model for the underlying crust based on magnetic anomaly data of Maus et al. (2009) and the corresponding ages of anomalies (Molnar et al. 1975). I also prepared all illustrations used in the publication. Dr. Gabriele Uenzelmann-Neben was the supervising leader of the seismic reflection profiling during Sonne 213/2 and has provided helpful comments during processing for enhancement of the seismic image. She also has contributed helpful comments and discussion of different text elements and has provided further help with the identification of footprints in seismic data.

4.2 The Deep Western Boundary Current at the Bounty Trough, east of New Zealand: Indications for its activity already before the opening of the Tasmanian Gateway

Horn, M. and G. Uenzelmann-Neben (submitted 2014), The Deep Western Boundary Current at the Bounty Trough, east of New Zealand: Indications for its activity already before the opening of the Tasmanian Gateway, submitted to Marine Geology in June 2014, revised version with moderate revisions submitted in October 2014

This manuscript targets the sedimentary deposits inside Bounty Trough region at the eastern New Zealand Continental Margin. Here, huge sediment piles have accumulated due to a terrigenous sediment supply that has been deposited under the influence of the Pacific DWBC. Thus these sediments may reveal changes in oceanic conditions that are directly linked to the ACC. Based on two former seismostratigraphic concepts of Carter et al. (1994) and Carter et al. (1999b) (defined with data from ODP Site 1122) we have compiled a new stratigraphic concept that includes the findings of ODP Site 1122 into the concept of Carter et al. (1994). With this tool we have found the first indication of a deep cold flow in the Bounty Trough area and are now able to report the complete history of deep flow at the eastern New Zealand continental margin since the early Palaeocene.
This publication is based on the five high-resolution seismic reflection profiles AWI-20110006 to AWI-20110010. I have processed these profiles as described in chapter 3 and have prepared the corresponding visualisations. Further, I have computed a synthetic seismogram to link the findings of ODP Site 1122 (Carter et al. 1999b) to the seismic profiles. The definition of the seismic stratigraphy and the identification of structures in the seismic data have been done by myself. Dr. Gabriele Uenzelmann-Neben contributed to the manuscript as head of seismic reflection profiling during cruise Sonne 213/2 and with her interpretation of the seismic profiles Hunt-141 and Hunt-143. Further, she contributed with helpful discussions to my interpretations and revised the manuscript.

4.3 The spatial extent of the Deep Western Boundary Current into the Bounty Trough: New evidence from Parasound Sub-Bottom Profiling

Horn, M. and G. Uenzelmann-Neben (2014), The spatial extent of the Deep Western Boundary Current into the Bounty Trough: New evidence from Parasound Sub-Bottom Profiling, prepared for resubmission to Geophysical Research Letters

This manuscript also targets the upper sedimentary column of the last 800 kyrs of the Bounty Trough area. I have compiled the available Parasound sub-bottom profiler data to analyse the upper sedimentary column. With a method adapted from Weigelt and Uenzelmann-Neben (2007) I have converted the TWT of the sub-bottom profiler data into age. With this age I have been able to analyse the seismic amplitude of periodic signals using Fourier transformation. This analysis has been used to quantify the spatial extent of a limb of the DWBC into the Bounty Trough.

The idea of using different Milankovitch cycles to map the extent of the DWBC into the Bounty Trough has been derived by myself. I have done the analysis of the Parasound sub bottom profiler data including data extraction, preparation and analysis. I further have prepared the data visualisation and interpretation. Dr. Gabriele Uenzelmann-Neben contributed to this Manuscript with helpful discussions and a revision of the Manuscript.

4.4 References

Carter, R. M., L. Carter, et al. (1994). "Seismic stratigraphy of the Bounty Trough, south-west Pacific Ocean." Marine and Petroleum Geology **11**(1): 79-93. doi:10.1016/0264-8172(94)90011-6

Carter, R. M., I. N. McCave, et al. (1999b). "Site 1122: Turbidites with a Contourite Foundation". Published in: Proceedings of the Ocean Drilling Program, Initial reports:. R. M. Carter, I. N. McCave, C. Richter and L. Carter. Texas, USA, College Station (Ocean Drilling Program). **181:** 1 - 146. doi:10.2973/odp.proc.ir.181.106.2000

Ewing, J. and M. Ewing (1967). "Sediment Distribution on the Mid-Ocean Ridges with Respect to Spreading of the Sea Floor." Science **156**(3782): 1590 – 1592. doi:10.1126/science.156.3782.1590

Maus, S., U. Barckhausen, et al. (2009). "EMAG2: A 2-arc min resolution Earth Magnetic Anomaly Grid compiled from satellite, airborne, and marine magnetic measurements." Geochemistry, Geophysics, Geosystems **10**(8): Q08005. doi:10.1029/2009GC002471

Molnar, P., T. Atwater, et al. (1975). "Magnetic Anomalies, Bathymetry and the Tectonic Evolution of the South Pacific since the Late Cretaceous." Geophysical Journal International **40**(3): 383 – 420. doi:10.1111/j.1365-246X.1975.tb04139.x

Weigelt, E. and G. Uenzelmann-Neben (2007). "Orbital forced cyclicity of reflector strength in the seismic records of the Cape Basin." Geophysical Research Letters **34**(1): L01702. doi:10.1029/2006gl028376

5. Nonlinear sediment thickness increase on the western East Pacific Rise flank, 45°S

Horn, M. and G. Uenzelmann-Neben (2013). "Nonlinear sediment thickness increase on the western East Pacific Rise flank, 45°S." Geo-Marine Letters **33**(5): 381 - 390. doi:10.1007/s00367-013-0335-1

5.1 Abstract

Sediment thickness was evaluated on the western flank of the East Pacific Rise (EPR) at 45°S, based on high-resolution seismic data gathered during cruise 213/2 of R/V *Sonne* in 2011. Two zones with distinctly different sediment thickness were identified, separated by a transitional zone bordering a pseudo-fault. Sediment in the more distal zone is almost twice as thick (~120 m) as in the zone close to the EPR (~60 m). This is in contrast to the expected sedimentary column thickening with seafloor age and distance to the spreading axis. The younger of two seismic units detected within the sedimentary column (EPR-2) occurs mainly in the distal zone on crust older than 9 Ma, whereas on younger crust it is present only in small isolated bodies. Both sedimentary units identified drape the basement. The drape is interpreted to represent particle settling from suspension and a generally low regional primary productivity. The spatial variation in sediment thickness cannot be explained by existing models, and other processes considered in the present case are (1) higher productivity in the western sector of the survey area, where thicker sediments were observed (zone 2), (2) the formation of sediment drifts near basement highs ('seamount effect'), due to flow of Lower Circumpolar Deep Water affecting sediment deposition, and (3) erosion and/or non-deposition of the younger EPR-2 unit, due to elevated bed shear stresses associated with eddies transferring kinetic energy to the seafloor.

5.2 Introduction

Sedimentary deposits of continental margins and upwelling zones have been studied intensively and have provided valuable information on past climate behaviour and regional ocean circulations patterns (see Rebesco et al. (2008) for overview). By contrast, settings characterised by mid ocean ridges (MORs) have received less attention since the pioneering work of, for example, Ewing and Ewing (1967) and Ewing et al. (1969). More recent studies mostly concentrate on the Mid Atlantic Ridge (Marks 1981; Mitchell et al. 1998; Alves et al. 2004) and the equatorial zone of the East Pacific Rise (EPR) and the Galapagos Spreading Centre (Lonsdale 1977; Mitchell 1998). In theory, sediments deposited in the vicinity of MORs are expected to thicken systematically with distance from the spreading axis and seafloor age (Ewing et al. 1969; Kearey and Vine 1996). In reality, however, sediment thickness variations do not strictly reflect crustal age because they may also be controlled by complex spatiotemporal changes in surface primary productivity, hydrothermal activity and carbonate compensation depth (CCD). Furthermore the chemical characteristics and dynamics of local water masses may lead to local dissolution, erosion and redistribution of sediments (e.g. Faugères and Stow (2008)). These processes vary geographically and temporally and show a complex interrelation.

The sedimentary history has been well studied for the equatorial region of the EPR. Since the 1970s, the Deep Sea Drilling Project (DSDP; e.g. (Tracey et al. 1971; Hays et al. 1972; Rosendahl et al. 1980; Mayer et al. 1985)), Ocean Drilling Program (ODP; e.g. Pisias et al. (1992)) and Integrated Ocean Drilling Program (IODP; e.g. Lyle et al. (2009)) along with seismic studies (e.g. Mitchell et al. (2003); Tominaga et al. (2011)) targeted the equatorial zone with their enhanced primary productivity because of upwelling of nutrient rich waters. Mayer et al. (1986) correlated DSDP borehole physical property data to seismic horizons and newer studies revealed the influence of bottom currents on the depositional environment in the equatorial area (e.g. Dubois and Mitchell (2012)). With decreasing influence of the high productivity zone to the south other processes become important. Results from DSDP Leg 92 (Leinen et al. 1986) showed that the hydrothermal influence at 19°S is higher than in the equatorial zone. Hauschild et al. (2003) for example related the higher sediment accumulation at the western flank of the EPR at 15°S to a hydrothermal plume. The change in controlling sediment deposition is evident from the equatorial zone to 19°S, but it is not clear which processes control the sedimentation further to the south.

This paper investigates high-resolution seismic reflection data from the western flank of the East Pacific Rise at ~45°S. Profiles were surveyed along the seafloor-spreading direction in order to study the sedimentary column on young oceanic crust. This region of the Pacific Ocean at ~45°S (here referred to as EPR region) has hardly been surveyed at all. Sediment is provided by low primary productivity and eventually by a contribution of hydrothermal activity while wind-blown dust is a neglectable component (Rea et al. 2006). The acquired data cover oceanic crust of 4 – 19 Ma (Molnar

et al. 1975) and can provide information about processes influencing sedimentary distribution and accumulation on the lower flank of a MOR such as modifications in sediment supply and erosion/re-deposition due to the activity of oceanic currents. The main aim is to identify processes shaping the sedimentary deposits near MORs and how these processes are linked to the regional environment.

5.3 Physical setting

The area of investigation is located at ~45°S on the western flank of the EPR, an ultra-fast spreading ridge (DeMets et al. 1990). The age of the seafloor for the EPR region can be estimated from magnetic isochrons identified by Molnar et al. (1975) (Fig. 5.1, grey contours and numbers). Seismic profiles were collected across oceanic crust spanning isochrons C3 (4.0 Ma) to C6 (20.2 Ma; (Cande and Kent 1992). The EPR crest forms a topographic barrier (Chen and Morgan 1990) that blocks deep ocean flow and redirects it to the northeast (Reid (1997) see Fig. 5.1). World Ocean Circulation Experiment profile P17A shows that the EPR-region is strongly influenced by Lower Circumpolar Deep Water (LCDW) in water depths of 3,200–4,000 m (Talley (2007), blue arrow, Fig. 5.1, inset).

The sediment flux to the EPR region is estimated as low. Sources of terrigenous material are more than 3000 km away from the EPR-region (Fig. 5.1, inset). Due to low primary productivity (Antoine et al. 1996) and organic carbon in the water column (Stramski et al. 2008) only a small amount of biogenic sediment is presently exported to the seabed. Likely most of the material deposited is of carbonate origin (Seibold and Berger 1996) as siliceous material flux is estimated also to be low (Berger and Herguera 1992). The borehole location closest to the EPR-region is IODP Expedition 329 Site U1369 (Fig. 5.1, inset). This site still is approximately 2,000 km away from the EPR-region, located on significantly older crust (~58 Ma), and cores were drilled only up to 17 m below the seafloor (D'Hondt et al. 2011). No correlation of the seismic data to the borehole data can hence be carried out.

5.4 Materials and methods

Five high resolution seismic reflection data (profiles AWI-20110001 to AWI-20110005) with a sample rate of 1 ms and a vertical resolution of approximately 10 m were acquired during cruise SO 213/2 of R/V *Sonne* in 2011. This article is based on the profiles AWI-20110001 and -20110003 as well as on parts of profiles AWI-20110004 and -20110005 (for the sake of completeness, profile AWI-20110002 is also shown). Profile AWI-20110001 was chosen to define the seismic stratigraphy because its position is on the oldest oceanic crust in our survey area. The profiles AWI-20110003 to AWI-20110005 allow displaying the evolution of the sediment cover with increasing crustal age because these profiles are perpendicular orientated to the spreading direction of the EPR. Their locations are given in Figure 5.1 (coloured lines). As a seismic source, a cluster of four GI-Guns with 2.8 l volume in total was used. The seismic signal was recorded with a 3,000 m streamer containing

240 channels. Five seismic reflection profiles with a total length of about 560 km (Fig. 5.1) were acquired with this configuration.

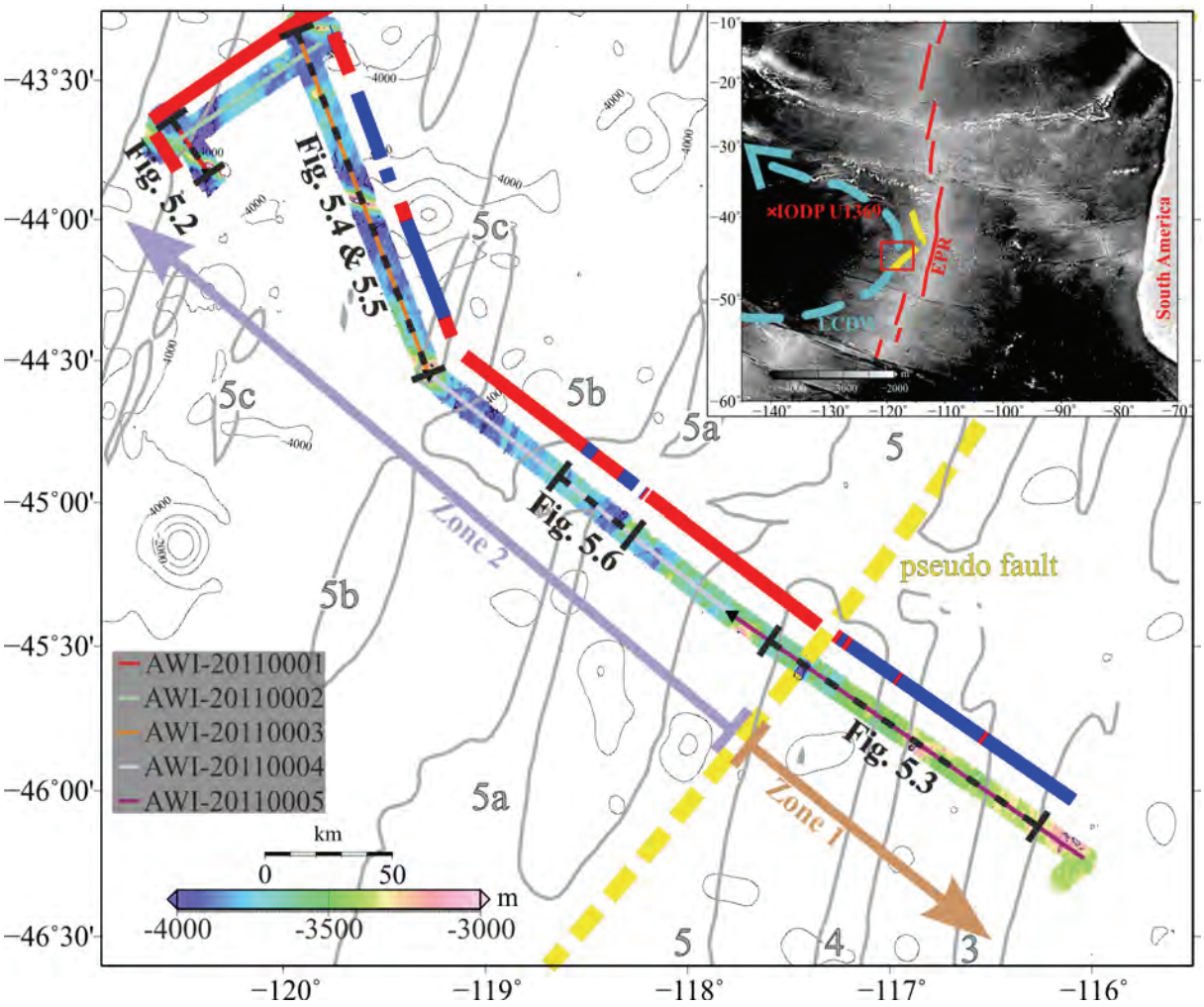

Figure 5.1: Overview of the survey area, locations of profiles (cruise SO 213/2), local swath bathymetry colour coded parallel to the track line(Tiedemann et al. 2012), and regional bathymetry (Smith and Sandwell 1997). *Thick grey contours* Magnetic anomalies (Maus et al. 2009), with corresponding isochron number (Molnar et al. 1975); *yellow dashed line* pseudo-fault identified from satellite derived gravity data inside the survey area; *grey and brown arrows* two zones of sediment thickness described in the text; *black dashed lines* locations of parts of profiles shown in Figs. 5.2-5.6. *Red* (unit EPR-2) and *blue* (unit EPR-1) lines near profiles represent extents of seismic units. *Inset* Locations of survey area, the closest deep sea borehole, and the bottom geostrophic current flow of the LCDW (*blue arrow*, Reid (1997))

Standard data processing included common depth point (CDP) sorting (25 m interval), velocity analysis (every 50 CDPs) for normal moveout correction, deconvolution with a predictive gap operator to suppress surface ghosts, stacking, post stack migration, frequency filtering (band pass filter) between 10 and 250 Hz, and a time-variant signal amplitude scaling. For conversions of two-way travel time (TWT) to depths, a velocity of 1,500 m/s was used for the water column and 1,600 m/s for the sediments.

The age of the oceanic crust covered by the acquired profiles was calculated using the magnetic anomalies identified by Molnar et al. (1975) assuming a constant spreading rate between pairs of chrons.

5.5 Results

5.5.1 Definition of seismic stratigraphy

Three seismostratigraphic units can be distinguished: the acoustic basement (marked brown in Figs. 5.2, 5.3, 5.4, 5.5, and 5.6) and two sedimentary units defined by two pronounced reflectors EPR-A (blue) and EPR-B (red, the seafloor). Reflector EPR-A is a prominent regional reflector of high amplitude identifiable on all profiles while EPR-B is only present at certain spots (see Fig. 5.1). The acoustic basement appears rough with hummocky, high amplitude reflectors (e.g. Fig. 5.2, profile AWI-20110001) and is interpreted as top of the oceanic crust. Another possibility is that the acoustic basement consists of chert that masks the oceanic crust (Moore 2008). However, the occurrence of chert near the basement is not expected because of generally low siliceous input in the area (Berger and Herguera 1992). In addition the basement does not show a strong horizontal reflection, which would indicate a chert layer. The crust is characterised by large basement highs ranging in height from 0.6 – 1.4 s TWT (approx. 450 – 1,050 m) above the surrounding seafloor (prominent example in Fig. 5.2a, profile AWI-20110001, CDPs 100 – 650). All basement highs in the survey area break through the sedimentary cover. They show only a very thin or no resolvable sedimentary cover. The acoustic basement reflector and reflector EPR-A (blue, Fig. 5.2b) delimit stratigraphic unit EPR-1. Unit EPR-1 varies in thickness between 0 and 0.18 s TWT (0 – 145 m), typical values range between 0.076 s TWT and 0.12 s TWT (60 – 100 m). The unit contains low amplitude parallel internal reflectors. Seismostratigraphic unit EPR-2 is delimited by reflectors EPR-A und EPR-B (red reflector, Fig. 5.2b). EPR-2 has an almost constant thickness of ~0.03 s TWT (20 – 25 m) but can reach a maximum vertical dimension of 0.14 s TWT (~115 m). Where unit EPR-2 reaches a thickness of above 0.1 s TWT (~80 m), few internal reflections are visible in this unit. A strong reflection can be present between defining reflectors EPR-A and EPR-B where the unit is only approximately 0.03 s TWT thick (see, for example, Fig. 5.2, profile AWI-20110001, CDPs 1,100–1,230).

Unfortunately, no drill location providing an age-depth model exists to date the seismic reflectors and seismostratigraphic units.

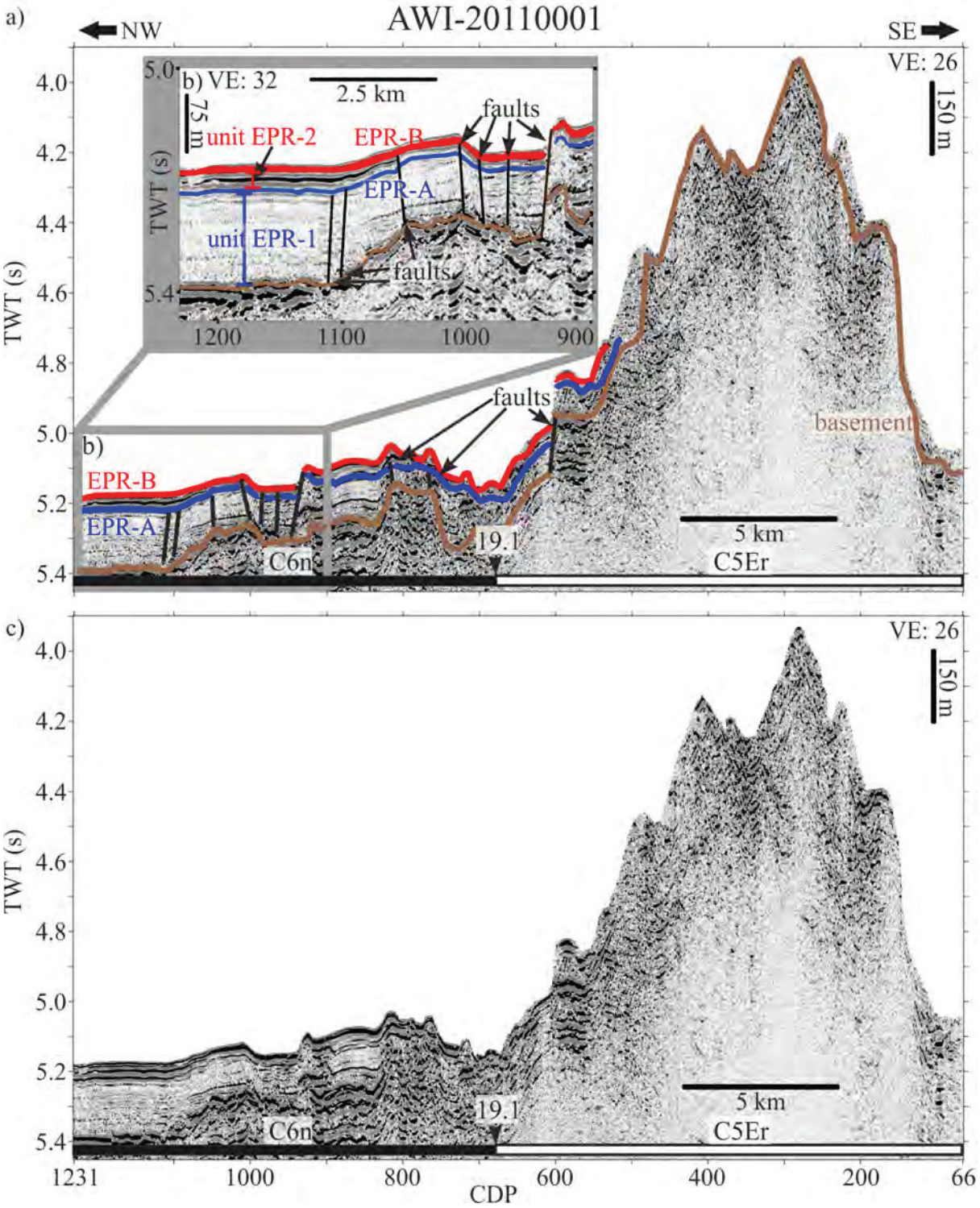

Figure 5.2 a Seismic profile AWI-20110001. At the bottom, the *black* (normal) and *white* (reversed) lines mark the approximate position and polarity of the identified chrons (Molnar et al. 1975). Magnetic polarity change ages are given in Ma (Cande and Kent 1992). **b** Seismic stratigraphy including digitised basement for sediments near the EPR. The basement (*brown*) and two reflectors EPR-A (*blue*) and EPR-B (*red*, seafloor) define two stratigraphic units. **c** Uninterpreted profile corresponding to **a**. *VE* Vertical exaggeration at seafloor

5.5.2 Application of seismostratigraphic model

The observed sedimentary cover can be divided into two zones based on the thickness of the whole sedimentary column. Zone 1 comprises the south-eastern part of the survey area with a crustal age of 4–8.5 Ma (Figures 5.1 and 5.3, profile AWI-20110005 east of CDP 2250). Within zone 1 we observe unit EPR-1 draping the basement, while unit EPR-2 is identified only at five isolated spots (see below). Zone 2 covers the north-western part of our area of investigation (9-18.5 Ma crustal age) (Figures 5.1 and 5.3, profile AWI-20110005 west of CDP 1400). There, we observe both stratigraphic units with a more frequent occurrence of unit EPR-2. However, unit EPR-2 does not form a continuous layer (see Figure 5.1). Between those two zones, a roughly 20 km wide zone with almost no resolvable sedimentary cover can be identified, here referred to as transitional zone (Fig. 5.3, profile AWI-20110005, CDPs 1400 – 2250).

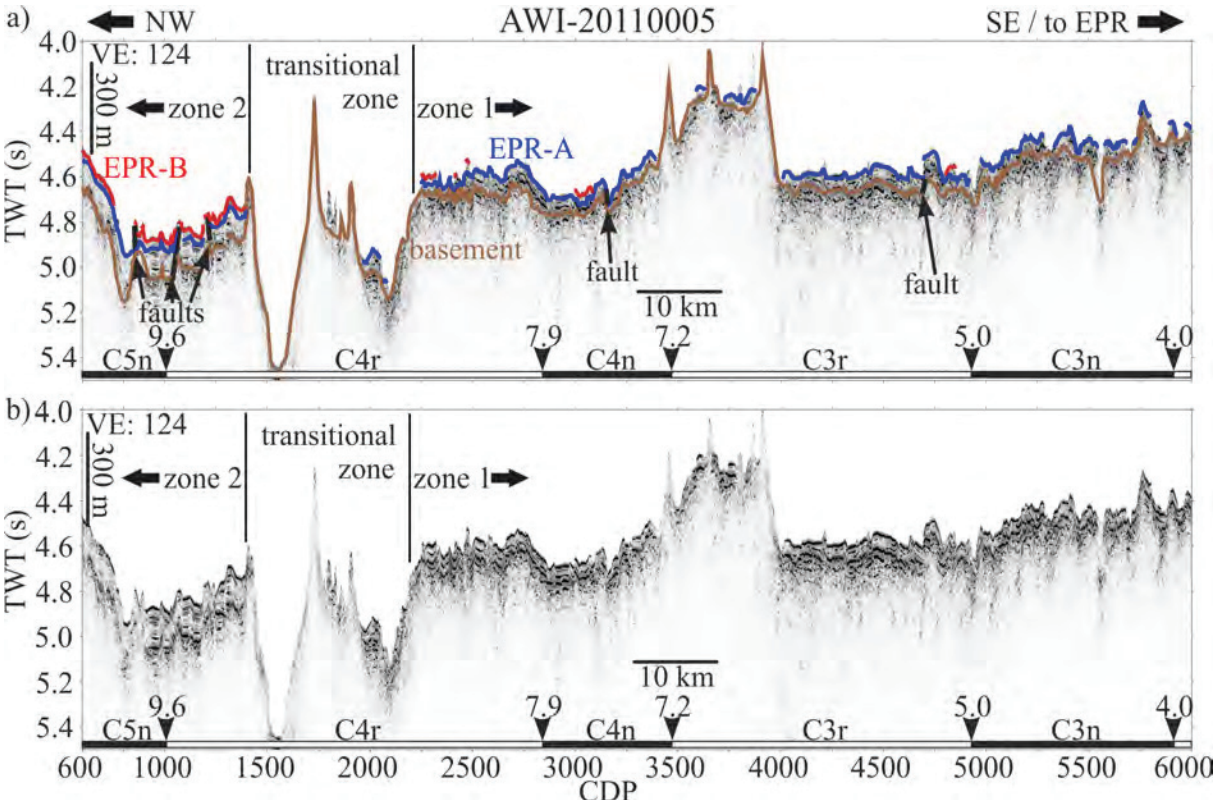

Figure 5.3 a Part of seismic profile AWI-20110005, showing the transitional zone located between zones 1 and 2 (CDP 1450 – 2250), and the age of the underlying oceanic crust. The *black* (normal) and *white* (reversed) lines mark the approximate position and polarity of the identified chrons (Molnar et al. 1975); magnetic polarity change ages in Ma (Cande and Kent 1992). **b** Corresponding uninterpreted profile

5.5.2.1 Unit EPR-1

Unit EPR-1 can be observed throughout the survey area. Inside zone 1 unit EPR-1 shows a mean thickness of 0.076 s TWT (~ 60 m, Figure 5.3, profile AWI-20110005 CDPs 2250 – 6000) and is disturbed only by one basement high. In zone 2, unit EPR-1 is observed with a fairly constant thickness of approximately 0.12 s TWT (~ 100 m). Unit EPR-1 in general drapes the basement thus

reflecting basement topography. Sediments at certain spots (cf. thin black arrows in, e.g. Fig. 5.2, profile AWI-20110001, CDP 600; Fig. 5.3, profile AWI-20110005, CDPs 800, 1100, 1250, 3250, 4750; Fig. 5.4, profile AWI 20110003, CDPs 2050, 2620, 4100, 4400, 4700 5100) thin and wedge out towards basement highs. These features are interpreted as off-axis faults, which extend into the basement. Differential compaction can be ruled out because the sediment composition is uniform and not thick enough for differential compaction. Their origin may be the thermal subsidence of the crust because of deviations in sediment cover, occurrence of basement highs and local differences in crust thickness.

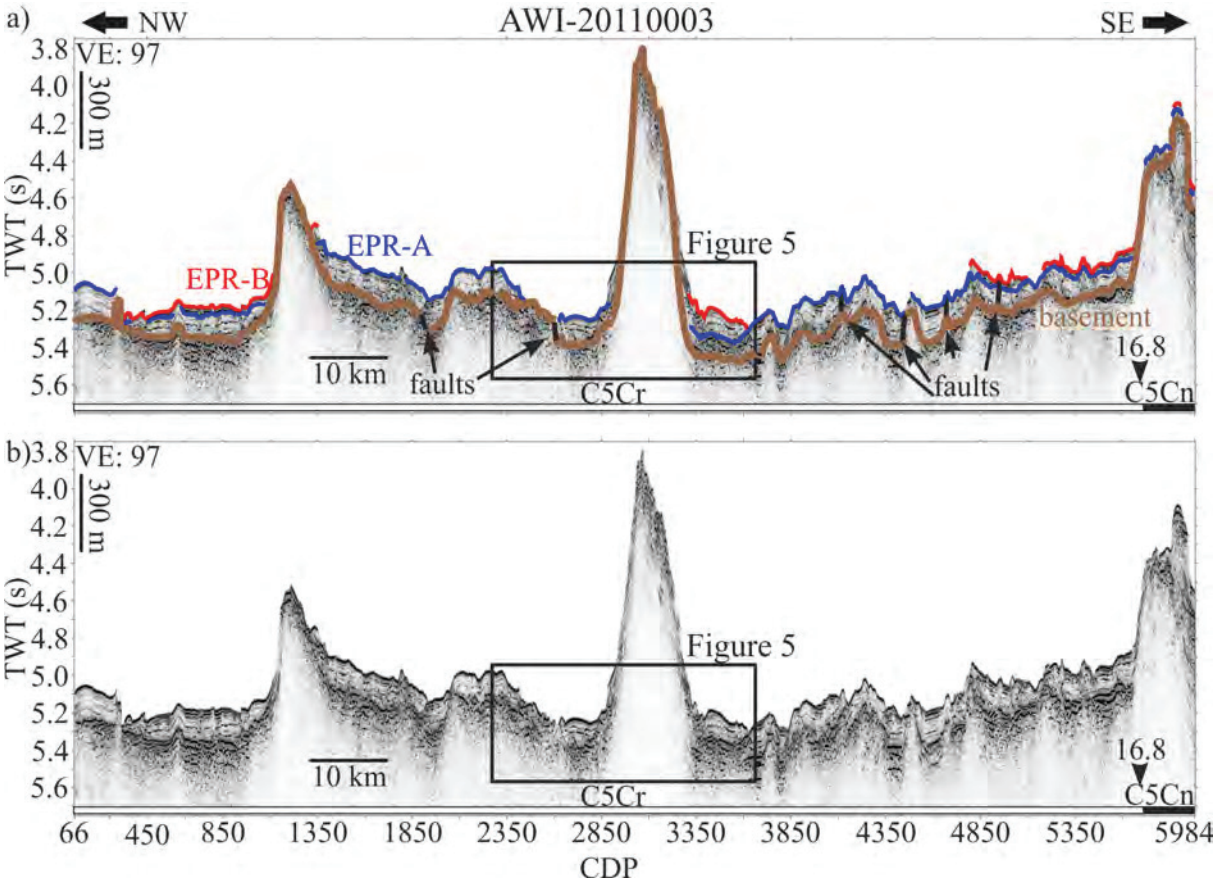

Figure 5.4 a Seismic profile AWI-20110003 in the north-western, oldest sector of the survey area. The *black* (normal) and *white* (reversed) lines mark the approximate position and polarity of the identified chrons (Molnar et al. 1975); magnetic polarity change ages in Ma (Cande and Kent 1992). No polarity changes were identified by Molnar et al. (1975) between chron C5Cn and C6n, which is why the polarity is marked as C5Cr. *Box* Profile section shown in more detail in Fig. 5.5. **b** Corresponding uninterpreted profile

5.5.2.2 Unit EPR-2

The occurrence of unit EPR-2 is different to EPR-1. Inside zone 1 unit EPR-2 appears only in five isolated spots (Figure 5.3, profile AWI-20110005, CDP 2250 – 2500, CDP 3000 – 3100 and CDP 4750 – 4850). Reflector EPR-B can only be traced for short distances and terminates against reflector EPR-A. The thickness of unit EPR-2 is about 0.02 s TWT to 0.05 s TWT (15 m – 40 m). In zone 2 unit EPR-2 is more abundant. Its thickness range is approximately the same as in zone 1, 0.02 to 0.05 s

TWT (15 m – 40 m). Southeast of a basement high (Figure 5.5a, profile AWI-20110003, CDPs 3300 – 3600) however, the unit reaches a thickness of approximately 0.14 s TWT (~ 115 m). Internal reflections and top reflector EPR-B here are of upward convex shape and terminate against reflector EPR-A forming an isolated sediment body. In general, the appearance of unit EPR-2 is rather patchy, and it does not form a continuous layer (Figure 5.1). The absence of unit EPR-2 cannot be correlated with basement highs. Unit EPR-2 still reflects the basement topography indicating draping. The faults observed in unit EPR-1 continue into unit EPR-2.

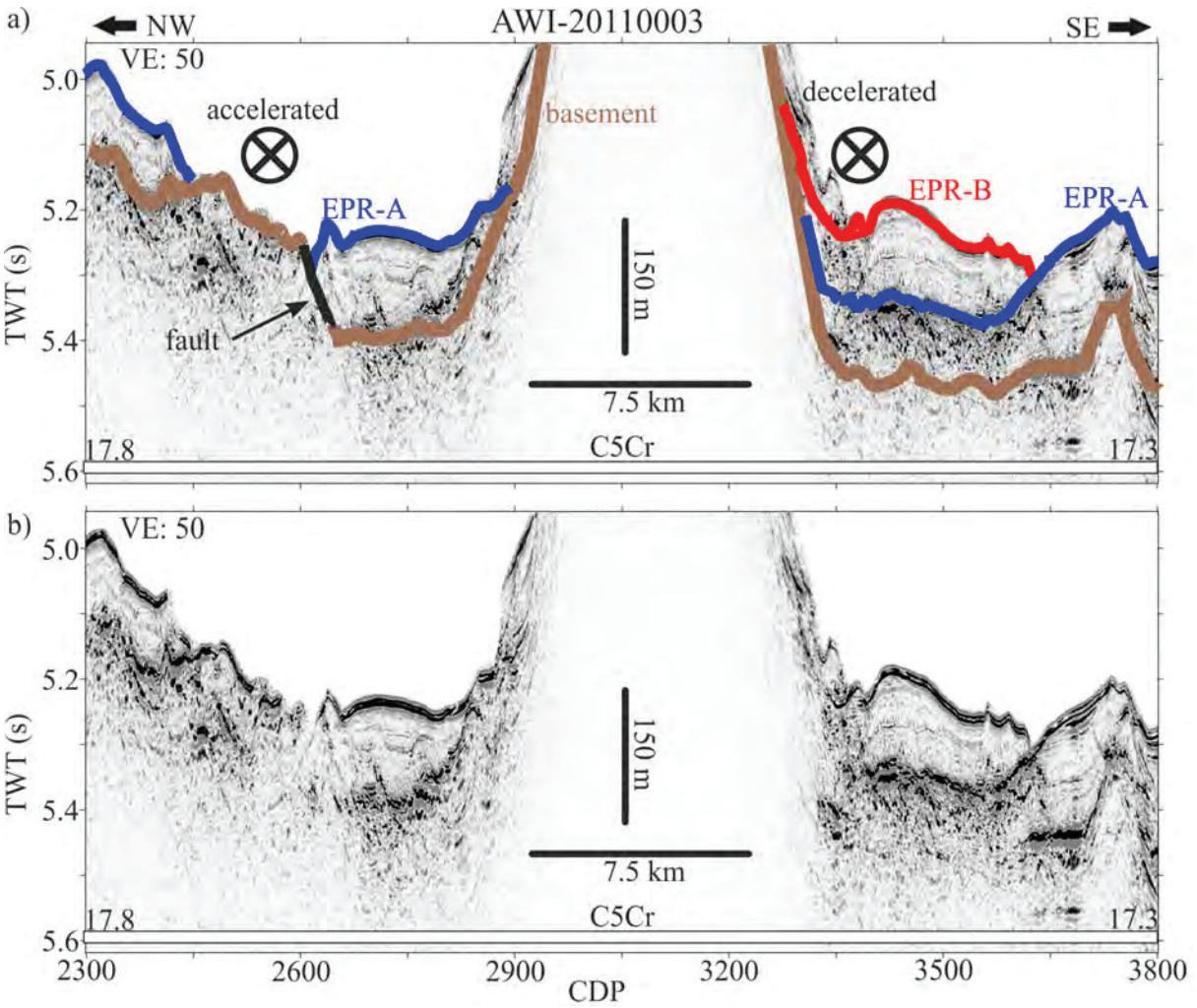

Figure 5.5 a Enlarged section of profile AWI-20110003 (cf. Fig. 5.4), showing a local disturbance interpreted to result from the "seamount effect" associated with the positions of flow cores. *White line C5Cr* Reversed polarity after chron C5Cn, the values being extrapolated ages for CDP 2300 and 3800 in Ma. **b** Corresponding uninterpreted profile section

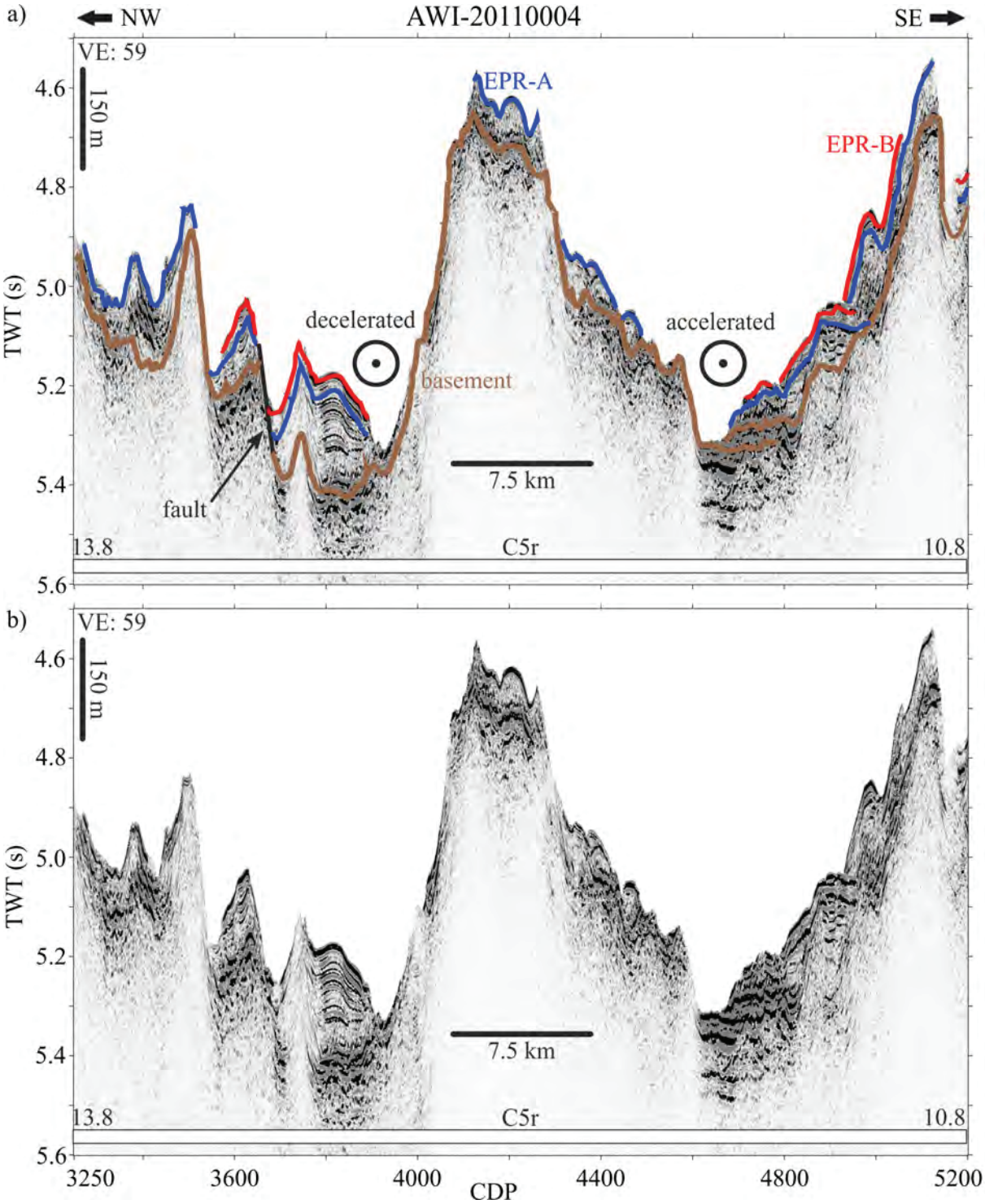

Figure 5.6 a Part of seismic profile AWI-20110004, showing a local disturbance of sedimentary cover due to a split flow pattern at a basement high (Hernández-Molina et al. 2006). The decelerated and accelerated flow paths are marked, and flow direction is out of the plane. *White line* Reversed polarity after chron C5r, as the identification of chron C5An was not possible (Molnar et al. 1975); values are extrapolated ages in Ma for CDP 3250 and CDP 5200. **b** Corresponding uninterpreted profile

5.6 Discussion

The zonation of the sedimentary cover west of the EPR is one of the main features revealed by the seismic stratigraphy reported in the present study. The sedimentary units are about twice as thick in

the distal zone 2 as in the proximal zone 1 with unit EPR-2 there present in about 340 km of 450 km profile distance. A transitional zone separates the two sedimentary zones, which is almost void of sedimentary deposits (Figure 5.3, profile AWI-20110005, CDPs 1400 – 2250). This transitional zone comprises oceanic crust of 9 Ma and shows a topography similar to fracture zones (Kearey and Vine 1996). The satellite derived bathymetry (Smith and Sandwell 1997) does not show evidence for a fracture zone in this area (Figure 5.1). Nevertheless, Tebbens and Cande (1997) identified a pseudo-fault from satellite derived gravity in this area (chrons 5r to 3n) resulting from propagating ridge segments, which may explain the topography of the observed transitional zone. Unfortunately, Tebbens and Cande (1997) do not provide information on the structure and/or nature of their pseudo fault.

The sedimentary column in zone 2, the more distal zone, is about twice as thick as in the EPR proximal zone 1. Both zones show a sedimentary column with a more or less constant thickness interrupted by basement highs, which are mostly void of a resolvable sedimentary cover. While unit EPR-1 is observed in both zones the younger unit EPR-2 can be identified frequently only in the distal Zone 2 (Figures 5.1, 5.3 and 5.4). The occurrence of EPR-2 in the proximal zone 1 is limited to isolated spots. Generally, the sedimentary cover over MORs is expected to steadily thicken with seafloor age and distance from the spreading centre (Ewing et al. 1969; Kearey and Vine 1996). The sedimentary distribution presented here thus contradicts this general pattern.

Ewing and Ewing (1967) also interpreted seismic profiles from all major ridge systems and observed a general pattern with two zones of different sediment thickness. Their proximal zone covers seafloor of crustal age 0–10 Ma with a linear increase in sediment thickness (~13 m/10^{-6} years). The distal zone shows a 2–4 times thicker sedimentary column and an increase of only 3 m/10^{-6} years. This second zone extends basinwards until it intersects with the CCD. Sediments deeper as the CCD accumulate at a much smaller rate because of carbonate dissolution. Ewing and Ewing (1967) explain their observations by (1) a change in spreading rate affecting sediment accumulation, and (2) a lack of modifications in sedimentation rate. The observations presented here differ from those of Ewing and Ewing (1967) in two aspects: (1) the two zones distinguished here do not show a significant increase in sediment thickness with seafloor age and distance to the EPR, and (2) the younger unit EPR-2 is only present in a few places in the proximal zone. Due to these differences the hypotheses of Ewing and Ewing (1967) cannot be applied to explain the sedimentary distribution presented here.

Hauschild et al. (2003) collected a seismic profile at the western flank of the EPR at 15°S, which covers oceanic crust of 0-7 Ma. They observed a distinct asymmetry in sediment distribution between the eastern and western flank of the EPR: a slow increase in sediment thickness (mean sedimentation rate of 4 m/10^{-6} years) with a drape of the basement on the eastern flank and a stronger increase in sediment thickness with a mean sedimentation rate of 10 m/10^{-6} years on the western flank (Hauschild et al. 2003). The draping sequences at the eastern flank were interpreted as the result of accumulation from particles locally settling from suspension. For the western flank Hauschild et al. (2003) observed

a ponding of the sedimentary sequences indicating sediment transport processes due to bottom currents. These westward setting bottom currents (Reid 1997) distribute the material produced by a hydrothermal plume at the EPR inferred from enhanced He^3 concentrations.

The sedimentary coverage observed at ~45° S strongly differs from the one reported by Hauschild et al. (2003) for 15° S. The sedimentary column at 45° S is generally thinner than at 15° S. This can be explained following Laske and Masters (Laske and Masters 1997), who show that, while the highest productivity of surface waters is observed near the equator, productivity and hence sediment thickness decreases towards the north and south. Both sedimentary units observed on the western EPR flank at 45° S reflect the basement topography suggesting sediment drape as a primary depositional mechanism. Applying Hauschild et al.'s (2003) interpretation of draping sediments on the eastern EPR flank (15° S) indicates sedimentation by particle settling for the western flank of the EPR at 45° S. Still, cited observations do not observe or explain the existence of two zones, each with a constant but very different sediment thickness (Figure 5.7a).

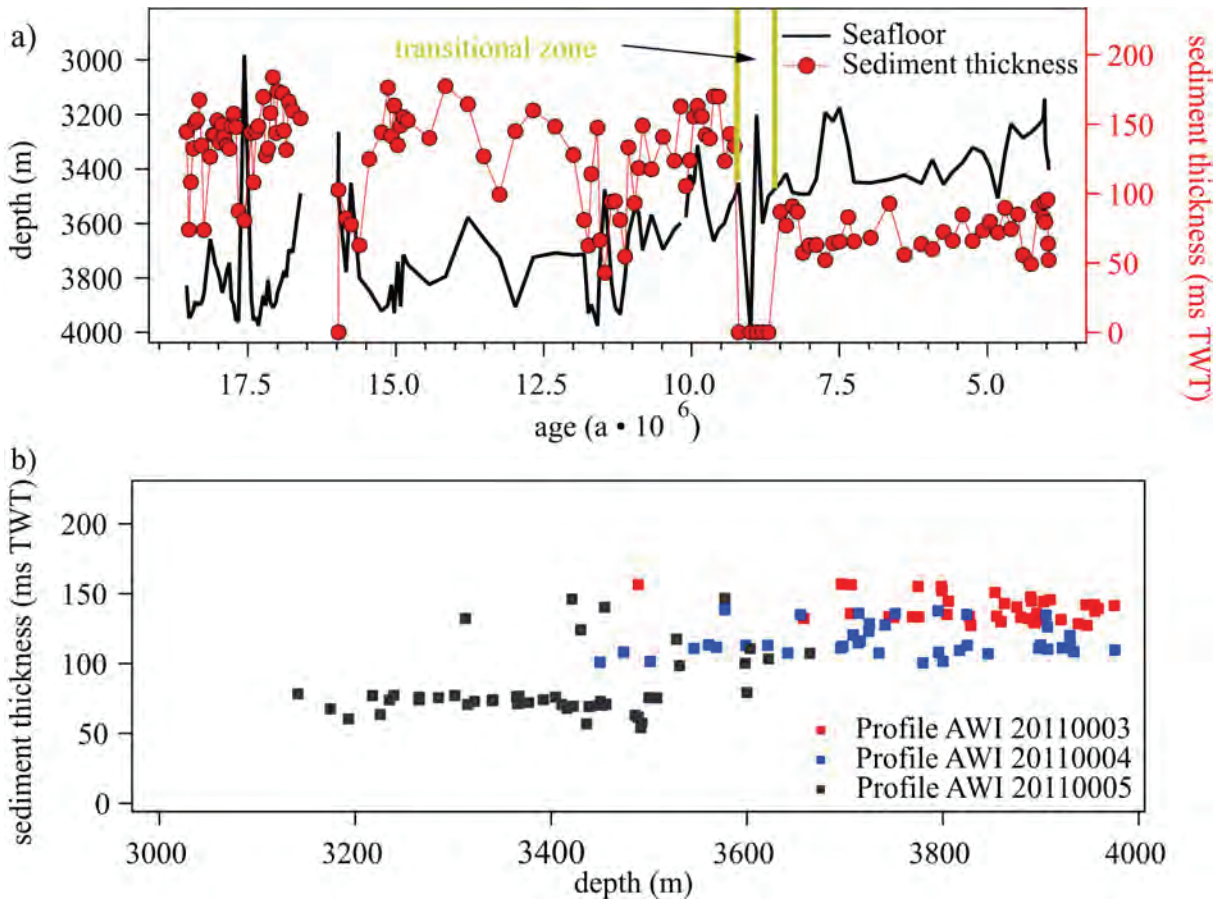

Figure 5.7 a Interrelationships between average sedimentary cover for profiles AWI-20110003, AWI-20110004 and AWI-20110005, the depth of the seafloor based on swath bathymetry (Tiedemann et al. 2012) and the age of the underlying crust, the latter calculated from the magnetic anomalies of Fig. 5.1 assuming a constant spreading between anomalies. The pseudo-fault/transitional zone (*dark yellow*) separates two distinct zones. **b** Sedimentary thickness (ms TWT) versus corresponding depth (m) along the three profiles

A dissolution of primarily calcareous sediments due to changes of the CCD as a cause for the observed sedimentary pattern can be ruled out. The topography of our area of investigation varies between 3000 m and 4000 m waterdepth (see Figure 5.7) and thus lies above the present CCD, which has been located at 4400 m (or 5.9 s TWT) since the Miocene-Pliocene boundary (van Andel 1975; Keller and Barron 1983). Furthermore, a CCD effect would likely lead to a thinning of the sedimentary cover with increasing water depth, i.e. distance to the EPR. In the working area a thinner sedimentary column is observed for shallower waters (Figure 5.7b), which also argues against a CCD effect.

A closer look at the sediment distribution hints on a possible cause. Zones of different productivity may be considered leading to thicker sedimentary units with a larger distance to the EPR. There is no direct evidence for such cells of productivity for our area of investigation but the fact that we observe unit EPR-2 mostly in the distal zone 2 may point in this direction. An alternative would be two extreme temporal variations in sediment accumulation leading to higher sedimentation rates around 9-10 Ma and around 4 Ma. However, this is very unlikely and there are no indications for two short periods of high accumulation. Nearest deep sea boreholes with sufficient sediment accumulation are DSDP Leg 35 (Hollister et al. 1976) and DSDP Leg 92 (Leinen et al. 1986). Both locations do not point to two extreme events.

The occurrence of Unit EPR-2 in zone 1 and sedimentary structures near basement highs suggest another explanation. Currents can erode and redeposit sediments and shape sediment bodies (e.g. (Stow et al. 2002; Zenk 2008)). Besides the truncation of reflectors at a basement high (Figure 5.3, profile AWI-20110005, CDPs 3300 – 4000) there are small depositional bodies of unit EPR-2 (Figure 5.3, profile AWI-20110005, CDPs 2250 – 2500, 3000 – 3100 and 4750 – 4850) that point to erosion of unit EPR-2 in zone 1. This indicates either non- or low-deposition as the result of low productivity and transport as suspension or to erosion because of bottom current activity. Erosion or non deposition may also be caused by higher frequency motion in the form of eddies that transfer kinetic energy to the seafloor. This higher energy may then cause erosion or inhibit deposition of sediment. Numerical models of Thoppil et al. (2011) and Faghmous et al. (2012) suggest a higher abundance of eddies at the EPR western flank at the sea surface. Combining this with eddy kinetic energy modelled by Scott et al. (2011) (see their Figure 9), hints on higher kinetic energy near the EPR seafloor. This may indicate that eddies play a role in eroding sediments near the EPR.

Another typical document of current activity are sediment drifts. These are asymmetric, mounded bodies characterised by subparallel internal reflections, which show onlap/downlap onto the base of the mounded body. The internal units of sediment drifts are lenticular and upward convex (Faugères and Stow 1993; Rebesco and Stow 2001; Stow et al. 2002; Shanmugam 2006). Sedimentary features such as sediment drifts are observed near basement highs in the area of investigation (Figure 5.5, profile AWI-20110003 CDPs 2600 – 2900 as well as 3300 – 3630, and 6, profile AWI-20110004, CDPs 3700 – 3920). Kilometre-scale elevations such as knolls and seamounts induce asymmetric local flow fields. In the Southern Hemisphere the flow exhibits acceleration to the left of the basement high

in the downstream direction and decelerated flow to the right (Roberts et al. 1974; Beckmann and Haidvogel 1993; Turnewitsch et al. 2004). These basement highs typically have marginal troughs or moats around their base, which can be observed in the presented data as well (Figure 5.6, profile AWI-20110004, CDPs 3900, 4600). Thus, the Coriolis force leads to more erosion on one side of obstacles, dubbed the 'seamount effect' by (Hernández-Molina et al. 2006).

The LCDW current flows northwards in this part of the South Pacific (Reid 1997; WOCE_International_Project_Office 2003) and therefore is considered as the agent shaping the sediment drifts observed in the present study. In the vicinity of basement highs, the LCDW would show a complex flow pattern and acceleration/deceleration, thereby shaping the sedimentary units into sediment drifts. Furthermore, it is suggested that the LCDW is characterised by stronger flow in areas devoid of unit EPR-2 (those sediments would have been eroded and/or not deposited). Such enhanced flow may be induced by complex interactions between the basement highs and the EPR topography itself.

5.7 Conclusions

High-resolution seismic reflection data from the western flank of the East Pacific Rise have been interpreted with respect to the sedimentary distribution and reveal two zones with sediment draping the basement. Although each zone shows a quite uniform sedimentation pattern, they differ significantly in thickness. This is fundamentally different from an expected linear increase with crustal age. In addition, there are indications for erosion of sedimentary units in the proximal zone to the EPR.

These findings indicate more complex processes taking part in sediment deposition than previously assumed and agree with other studies that show strong variations in sedimentation patterns at MORs (Mitchell et al. 1998; Hauschild et al. 2003). Near the EPR at 45°S there are two causes that have possibly shaped the sedimentary deposits. A factor that may explain the thicker sedimentary column in the distal zone 2 is a deviation of a possible zone of productivity to the west, where unit EPR-2 is present. Unfortunately, there are no publications covering the area of interest that confirm or rule out such zones.

Another main factor possibly influencing sedimentary deposits is bottom current activity. Sediment drifts observed in the vicinity of basement highs plausibly have been formed by enhanced flow of Lower Circumpolar Deep Water, which near the basement highs would show a complex 'seamount effect'. There is evidence that the younger EPR-2 unit may be variably affected by non-deposition and/or erosion due to LCDW activity in zones 1 and 2. Higher-frequency motions may also modulate bottom current activity. It is suggested that eddies are more abundant at the EPR topographic barrier and may take part in shaping sediment deposits.

The present interpretations of seismic units are insufficient to unambiguously identify sedimentary patterns and associated depositional processes on the western flank of the East Pacific Rise at ~45°S. Future studies providing additional information on the lithology and geochemistry of the sediments would help to identify ages of reflectors and correlate these to past changes in oceanographic conditions.

5.8 Acknowledgements

We acknowledge the helpful suggestions by N. Mitchell and B. Davy that improved this paper. In addition, we are grateful for the support of Captain O. Meyer and his crew, as well as Dr. Estella Weigelt, Dr. Jens Grützner and Dietmar Penshorn during cruise SO 213/2 aboard RV *Sonne*. The cruise was funded by the Bundesministerium für Bildung und Forschung under contract number 03G0213A.

5.9 References

Alves, T. M., T. Cunha, et al. (2004). "Surveying the flanks of the Mid-Atlantic Ridge: the Atlantis Basin, North Atlantic Ocean (36°N)." Marine Geology **209**(1 – 4): 199 – 222. doi:10.1016/j.margeo.2004.06.002

Antoine, D., J.-M. André, et al. (1996). "Oceanic primary production: 2. Estimation at global scale from satellite (coastal zone color scanner) chlorophyll." Global Biochemical Cycles **10**(1): 57 – 69. doi:10.1029/95GB02832

Beckmann, A. and D. B. Haidvogel (1993). "Numerical Simulation of Flow around a Tall Isolated Seamount. Part I: Problem Formulation and Model Accuracy." Journal of Physical Oceanography **23**(8): 1736 – 1753. doi:10.1175/1520-0485(1993)023<1736:NSOFAA>2.0.CO;2

Berger, W. H. and J. C. Herguera (1992). "Reading the sedimentary record of the oceans productivity". Published in: Primary Productivity and Biogeochemical Cycles in the Sea. P. G. Falkowski and A. D. Woodhead. New York, Plenum Press**:** 455 – 486.

Cande, S. C. and D. V. Kent (1992). "A New Geomagnetic Polarity Time Scale for the Late Cretaceous and Cenozoic." J. of Geophys. Res. **97**(B10): 13917 – 13951. doi:10.1029/92JB01202

Chen, Y. and W. J. Morgan (1990). "Rift Valley/No Rift Valley Transition at Mid-Ocean Ridges." Journal of Geophysical Research: Solid Earth **95**(B11): 17571 – 17581. doi:10.1029/JB095iB11p17571

D'Hondt, S., F. Inagaki, et al. (2011). "Site U1369". Published in: Integrated Ocean Drilling Program Expedition 329 Preliminary Report. S. D'Hondt, F. Inagaki, C. A. Alvarez Zarikian and Expedition 329 Scientists. Tokyo, Integrated Ocean Drilling Program Management International. **329:** 58. doi:10.2204/iodp.proc.329.107.2011

DeMets, C., R. G. Gordon, et al. (1990). "Current plate motions." Geophys. J. Int. **101**(2): 425 – 478. doi:10.1111/j.1365-246X.1990.tb06579.x

Dubois, N. and N. C. Mitchell (2012). "Large-scale sediment redistribution on the equatorial Pacific seafloor." Deep-Sea Research I: Oceanographic Research Papers **69**: 51 – 61. doi:10.1016/j.dsr.2012.07.006

Ewing, J. and M. Ewing (1967). "Sediment Distribution on the Mid-Ocean Ridges with Respect to Spreading of the Sea Floor." Science **156**(3782): 1590 – 1592. doi:10.1126/science.156.3782.1590

Ewing, M., R. Houtz, et al. (1969). "South Pacific Sediment Distribution." Journal of Geophysical Research **74**(10): 2477 – 2493. doi:10.1029/JB074i010p02477

Faghmous, J. H., L. Styles, et al. (2012). "EddyScan: A Physically Consistent Ocean Eddy Monitoring Application". IEEE Proc Intelligent Data Understanding (CIDU), 2012, Boulder, CO. doi:10.1109/CIDU.2012.6382189

Faugères, J. C. and D. A. V. Stow (1993). "Bottom-current-controlled sedimentation: a synthesis of the contourite problem." Sedimentary Geology **82**(1 – 4): 287 – 297. doi:10.1016/0037-0738(93)90127-Q

Faugères, J. C. and D. A. V. Stow (2008). "Chapter 14 Contourite Drifts: Nature, Evolution and Controls". Published in: Developments in Sedimentology. M. Rebesco and A. Camerlenghi. Amsterdam, Elsevier Science**:** 257 – 288. doi:10.1016/S0070-4571(08)10014-0

Hauschild, J., I. Grevemeyer, et al. (2003). "Asymmetric sedimentation on young ocean floor at the East Pacific Rise, 15°S." Marine Geology **193**(1 – 2): 49 – 59. doi:10.1016/S0025-3227(02)00613-8

Hays, J. D., H. E. I. Cook, et al. (1972). "Initial Reports of the Deep Sea Drilling Project ". Washingtion, DC, US Governmental Printing Office. doi:10.2973/dsdp.proc.9.1972

Hernández-Molina, F. J., R. D. Larter, et al. (2006). "Miocene reversal of bottom water flow along the Pacific Margin of the Antarctic Peninsula: Stratigraphic evidence from a contourite sedimentary tail." Marine Geology **228**(1 – 4): 93 – 116. doi:10.1016/j.margeo.2005.12.010

Hollister, C. D., C. Craddock, et al. (1976). "Initial Reports of the Deep Sea Drilling Project". Washingtion, DC, US Governmental Printing Office. doi:10.2973/dsdp.proc.35.1976

Kearey, P. and F. J. Vine (1996). "Global Tectonics". Oxford, Blackwell Science.

Keller, G. and J. A. Barron (1983). "Paleoceanographic implications of Miocene deep-sea hiatuses." Geological Society of America Bulletin **94**(5): 590 – 613. doi:10.1130/0016-7606(1983)94<590:PIOMDH>2.0.CO;2

Laske, G. and G. Masters (1997). "A Global Digital Map of Sediment Thickness." Eos, Transactions American Geophysical Union **78**: F 483.

Leinen, M., D. K. Rea, et al. (1986). "Initial Reports of the Deep Sea Drilling Project". Washington, DC, US Governmental Printing Office. doi:10.2973/dsdp.proc.92.1986

Lonsdale, P. (1977). "Deep-tow observations at the mounds abyssal hydrothermal field, Galapagos Rift." Earth and Planetary Science Letters **36**(1): 92 – 110. doi:10.1016/0012-821X(77)90191-1

Lyle, M., I. Raffi, et al. (2009). "Pacific Equatorial Transect". Tokyo, Integrated Ocean Drilling Program Management International. doi:10.2204/iodp.pr.321.2009

Marks, N. S. (1981). "Sedimentation on new ocean crust: The Mid-Atlantic Ridge at 37°N." Marine Geology **43**(1 – 2): 65 – 82. doi:10.1016/0025-3227(81)90129-8

Maus, S., U. Barckhausen, et al. (2009). "EMAG2: A 2-arc min resolution Earth Magnetic Anomaly Grid compiled from satellite, airborne, and marine magnetic measurements." Geochemistry, Geophysics, Geosystems **10**(8): Q08005. doi:10.1029/2009GC002471

Mayer, L., F. Theyer, et al. (1985). "Initial Reports of the Deep Sea Drilling Project". Washington, DC, US Governmental Printing Office. doi:10.2973/dsdp.proc.85.1985

Mayer, L. A., T. H. Shipley, et al. (1986). "Equatorial Pacific Seismic Reflectors as Indicators of Global Oceanographic Events." Science **233**(4765): 761 – 764. doi:10.1126/science.233.4765.761

Mitchell, N. C. (1998). "Sediment accumulation rates from Deep Tow profiler records and DSDP Leg 70 cores over the Galapagos spreading centre". Published in: Geological evolution of ocean basins : results from the Ocean Drilling Program. A. Cramp, C. J. MacLeod, S. V. Lee and E. J. W. Jones. London, The Geological Society Publishing House. **131:** 199 – 209. doi:10.1144/GSL.SP.1998.131.01.13

Mitchell, N. C., S. Allerton, et al. (1998). "Sedimentation on young ocean floor at the Mid-Atlantic Ridge, 29 °N." Marine Geology **148**(1 – 2): 1 – 8. doi:10.1016/S0025-3227(98)00018-8

Mitchell, N. C., M. W. Lyle, et al. (2003). "Lower Miocene to present stratigraphy of the equatorial Pacific sediment bulge and carbonate dissolution anomalies." Paleoceanography **18**(2): 1038. doi:10.1029/2002PA000828

Molnar, P., T. Atwater, et al. (1975). "Magnetic Anomalies, Bathymetry and the Tectonic Evolution of the South Pacific since the Late Cretaceous." Geophysical Journal International **40**(3): 383 – 420. doi:10.1111/j.1365-246X.1975.tb04139.x

Moore, T. C. J. (2008). "Chert in the Pacific: Biogenic silica and hydrothermal circulation." Palaeogeography Palaeoclimatology Palaeoecology **261**(1 – 2): 87 – 99. doi:10.1016/j.palaeo.2008.01.009

Pisias, N. G., L. A. Mayer, et al. (1992). "Scientific Results". Texas (Ocean Drilling Program), College Station. doi:10.2973/odp.proc.ir.138.1992

Rea, D. K., M. W. Lyle, et al. (2006). "Broad region of no sediment in the southwest Pacific Basin." Geology **34**(10): 873 – 876. doi:10.1130/G22864.1

Rebesco, M., A. Camerlenghi, et al. (2008). "Contourites ". Amsterdam, Elsevier Science.

Rebesco, M. and D. A. V. Stow (2001). "Seismic expression of contourites and related deposits: a preface." Marine Geophysical Researches **22**(5 – 6): 303 – 308. doi:10.1023/A:1016316913639

Reid, J. L. (1997). "On the total geostrophic circulation of the pacific ocean: flow patterns, tracers, and transports." Progress In Oceanography **39**(4): 263 – 352. doi:10.1016/S0079-6611(97)00012-8

Roberts, D. G., N. G. Hogg, et al. (1974). "Sediment distribution around moated seamounts in the Rockall Trough." Deep Sea Research and Oceanographic Abstracts **21**(3): 175 – 184. doi:10.1016/0011-7471(74)90057-6

Rosendahl, B. R., R. Hekinian, et al. (1980). "Initial Reports of the Deep Sea Drilling Project". Washington, DC, US Governmental Printing Office. doi:10.2973/dsdp.proc.54.1980

Scott, R. B., J. A. Goff, et al. (2011). "Global rate and spectral characteristics of internal gravity wave generation by geostrophic flow over topography." Journal of Geophysical Research: Oceans **116**(C9): C09029. doi:10.1029/2011JC007005

Seibold, E. and W. H. Berger (1996). "The Sea Floor - An Introduction to Marine Geology". Berlin, Springer-Verlag Berlin Heidelberg.

Shanmugam, G. (2006). "Deep-Water Processes and Facies Models: Implications for Sandstone Petroleum Reservoirs". Amsterdam, Elsevier Science.

Smith, W. H. F. and D. T. Sandwell (1997). "Global Sea Floor Topography from Satellite Altimetry and Ship Depth Soundings." Science **277**(5334): 1956 – 1962. doi:10.1126/science.277.5334.1956

Stow, D. A. V., J.-C. Faugères, et al. (2002). "Bottom currents, contourites and deep-sea sediment drifts: current state-of-the-art". Published in: Deep-water contourite systems: Modern drifts and ancient series. D. A. V. Stow, C. J. Pudsey, J. A. Howe, J.-C. Faugères and A. R. Viana. London, Geol. Soc. Lond.**:** 7 – 20. doi:10.1144/GSL.MEM.2002.022.01.02

Stramski, D., R. A. Reynolds, et al. (2008). "Relationships between the surface concentration of particulate organic carbon and optical properties in the eastern South Pacific and eastern Atlantic Oceans." Biogeosciences **5**(1): 171 – 201. doi:10.5194/bg-5-171-2008

Talley, L. D. (2007). "Pacific Ocean". Southampton, U.K., International WOCE Project Office.

Tebbens, S. F. and S. C. Cande (1997). "Southeast Pacific tectonic evolution from early Oligocene to Present." Journal of Geophysical Research: Solid Earth **102**(B6): 12061 – 12084. doi:10.1029/96JB02582

Thoppil, P. G., J. G. Richman, et al. (2011). "Energetics of a global ocean circulation model compared to observations." Geophysical Research Letters **38**(15): L15607. doi:10.1029/2011GL048347

Tiedemann, R., J. O'Conner, et al. (2012). Cruise Report SO213: SOPATRA. Bremerhaven, Alfred Wegener Institute, Helmholtz Centre for Polar and Marine Research**:** 111.

Tominaga, M., M. Lyle, et al. (2011). "Seismic interpretation of pelagic sedimentation regimes in the 18-53 Ma eastern equatorial Pacific: Basin-scale sedimentation and infilling of abyssal valleys." Geochemistry Geophysics Geosystems **12**(3): Q03004. doi:10.1029/2010GC003347

Tracey, J. I. J., G. H. Sutton, et al. (1971). "Initial Reports of the Deep Sea Drilling Project ". Washingtion, DC, US Governmental Printing Office. doi:10.2973/dsdp.proc.8.1971

Turnewitsch, R., J.-L. Reyss, et al. (2004). "Evidence for a sedimentary fingerprint of an asymmetric flow field surrounding a short seamount." Earth and Planetary Science Letters **222**(3 – 4): 1023 – 1036. doi:10.1016/j.epsl.2004.03.042

van Andel, T. H. (1975). "Mesozoic/cenozoic calcite compensation depth and the global distribution of calcareous sediments." Earth and Planetary Science Letters **26**(2): 187 – 194. doi:10.1016/0012-821X(75)90086-2

WOCE_International_Project_Office (2003). WOCE observations 1990-1998; a summary of the WOCE global data resource. W. I. P. Office. Southampton, UK.**:** 52.

Zenk, W. (2008). "Chapter 4 Abyssal and Contour Currents". Published in: Developments in Sedimentology. M. Rebesco and A. Camerlenghi. Amsterdam, Elsevier Science**:** 35, 37 – 57. doi:10.1016/S0070-4571(08)10004-8

6. The Deep Western Boundary Current at the Bounty Trough, east of New Zealand: Indications for its activity already before the opening of the Tasmanian Gateway

Horn, M., and G. Uenzelmann-Neben (2015), The Deep Western Boundary Current at the Bounty Trough, east of New Zealand: Indications for its activity already before the opening of the Tasmanian Gateway Marine Geology, **362:** 60 - 75. Doi: 0.1016/j.margeo.2015.01.011

6.1 Abstract

The Eastern New Zealand Oceanic Sedimentary System is influenced by the main deep cold-water inflow to the Pacific Ocean, the Deep Western Boundary Current (DWBC). ODP Leg 181 targeted this region. The two northern sites ODP 1123 and 1124 are mainly used for interpretation of DWBC flow. Newly acquired high–resolution seismic reflection profiles directly cross ODP Site 1122 in the Outer Bounty Trough area. This has allowed deciphering the first appearance of a branch of the DWBC meandering into the Bounty Trough as early as 20 to 16.7 Ma. We identified four different drift deposits of the DWBC in the Outer Bounty Trough area. The deepest two drifts were formed before the opening of the Tasmanian Gateway and thus provide the first evidence of a pre-Oligocene deep circulation at the eastern New Zealand margin. Additionally, migration of the drift crests to the west and to the east are interpreted to indicate modifications in core flow pathway of the DWBC due to response to climate changes (Eocene cooling, cooling due to West Antarctic Iceshield build-up), tectonic influence (opening of Tasmanian Gateway) and enhanced sediment input (first turbiditic deposits of Bounty Channel).

Keywords: Bounty Trough, seismic stratigraphy, ODP Leg 181 Site 1122, Eastern New Zealand Oceanic Sedimentary System, ENZOSS, Deep Western Boundary Current, DWBC

Highlights:

- First direct link of ODP Site 1122 to multiple multichannel seismic profiles spanning over the whole Outer Bounty Trough region
- Indications of first appearance of the DWBC inside the Bounty Trough west of the Outer Sill during Miocene
- First evidence of a bottom current before the Eocene/Oligocene Boundary
- History of the DWBC between ~65 Ma until 1.7 Ma

6.2 Introduction

The Thermohaline Circulation (THC) is directly linked to global climate. Changes in global climate affect the THC and vice versa (e.g. Clark et al. 2002; Kuhlbrodt et al. 2007). Sedimentary archives recording circulation patterns at key locations of the THC are of great interest for interdisciplinary research. These archives contain valuable information about past changes in oceanic circulation and associated climate. One of these key regions is the Tasmanian Gateway between Antarctica and Australia (Figure 6.1a, insert). At this location the Deep Western Boundary Current (DWBC), the main inflow of deep cold water, enters the Pacific Ocean. The Antarctic Circumpolar Current (ACC) also passes through the Tasmanian Gateway directly affecting the cold water inflow of the DWBC (Carter et al. 2004a; McCave et al. 2008). It is still under debate whether the opening of the Tasmanian Gateway and subsequent establishment of the ACC has been the major cause leading to thermal isolation and Antarctic Glaciation or whether changes in atmospheric carbon dioxide concentration triggered Antarctic Ice Sheet growth (e.g. Zachos et al. 2001; Huber et al. 2004; Sijp et al. 2011). During the Eocene no major tectonic processes such as opening of circum-Antarctic seaways occurred in the Southern Ocean (Cande and Stock 2004), but at least a partial glaciation of East Antarctica is evident pointing towards cooling resulting from CO_2 drawdown (Zachos et al. 2001). Intensive cooling and sea ice enhance the deep water formation (Stocker 2000; van Aken 2007). Thus, cold climate conditions in an ice covered Antarctica caused intensified deep-water formation, which then formed specific sedimentary features in sedimentary archives. Such an archive is located directly downstream of the Tasmanian Gateway, where a major amount of sediment is injected into the DWBC and ACC flow path. The sediments are provided by the Eastern New Zealand Oceanic Sedimentary System (ENZOSS) (Figure 6.1a), a sediment recycling system (Carter et al. 1996a; Carter et al. 1996b). Modern river discharge data suggest ENZOSS has an estimated terrigenous material input of 109 million tonnes per year (Hicks and Shankar 2003). These sediments are transported to the deep sea via three deep sea channels, the Solander Channel, the Bounty Channel and the Hikurangi Channel (Carter et al. 1996a)(Figure 6.1a). Sediments are entrained, transported and deposited by the DWBC regionally influenced by the ACC and form depositional and erosional sequences at the deep sea floor visible in seismic reflection data.

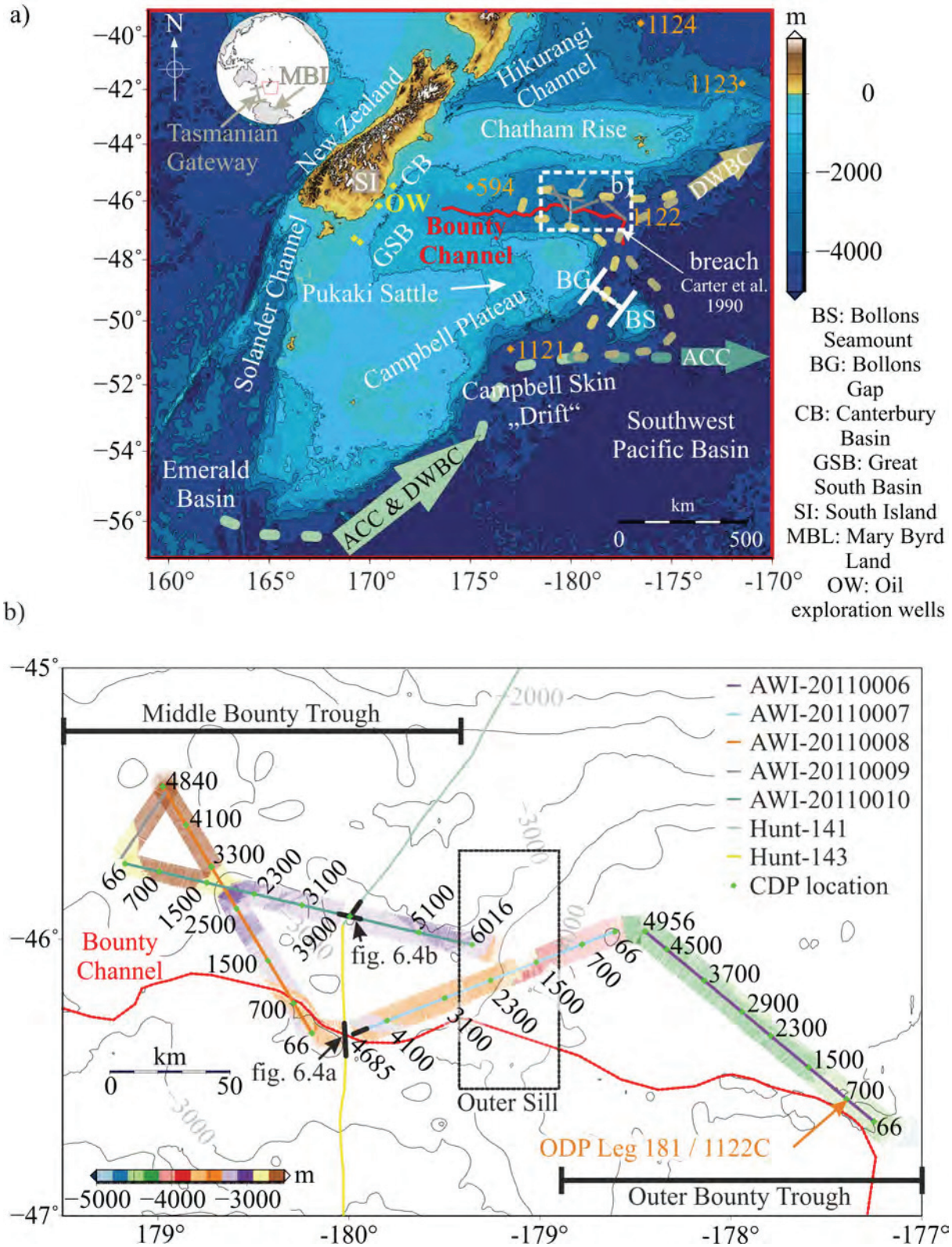

Figure 6.1: **a)** Bathymetry (GEBCO_08 grid; Smith and Sandwell 1997) of the area of interest. Dashed lines and arrows indicate the present deep circulation pattern around the New Zealand Microcontinent. Also shown are deep sea boreholes of ODP Leg 181, DSDP Site 594 and oil exploration wells used to characterise the sediment deposits; **b)** Detailed view of the working area showing profile locations, coloured area shows swath bathymetry acquired during So 213/2 cruise (Tiedemann et al. 2012) with GEBCO_08 contours (Smith and Sandwell 1997) in black. Numbers and green diamonds indicate positions of CDPs of the corresponding figures. Orange diamonds and numbers indicate ODP Sites in the area. Abbreviations: ACC = Antarctic Circumpolar Current, DWBC = Deep Western Boundary Current

Our knowledge of Eocene and older circulation in the ENZOSS region, which help deciphering the oceanic circulation prior and during first Antarctic glaciation during Eocene, is still scarce. The information is mainly based on ODP Leg 181 Site 1124 data. Borehole data suggests a flow of a warm deep water mass from a northern source but no record of cold circulation (Carter et al. 1999d; Carter et al. 2004b). Additionally, most interpretations of the Oligocene and younger circulation originates from north of Chatham Rise (ODP Sites 1123 and 1124, Figure 6.1; (e.g. Hall et al. 2002; Hall et al. 2003; Joseph et al. 2004)). Here the DWBC has been modified due to its journey around the Chatham Rise and has potentially taken up sediments from the Bounty Trough (erosion at the Outer Sill is evident from seismic data (Carter and McCave 1997) implying an intrusion of DWBC into the Bounty Trough taking up sediments). To see the direct influence of the ACC on the DWBC since the opening of the Tasmanian Gateway a location directly upstream of the uncoupling point is desirable. Without the strong erosive activity of ACC and DWBC which occurs south of ~50°S the Bounty Trough represents an ideal location to study the signal of the DWBC. Sediments deposited here are mainly transported by the DWBC to the region and by sporadic isolated turbidities possibly from influxes from the Bounty Trough (Carter et al. 1999b). Since the Bounty Trough is estimated to have formed during late Cretaceous (e.g. Davy 1993; Grobys et al. 2007) its sediment archive may record footprints of a cold current from the south that has passed by the eastern continental margin of New Zealand.

We here present new high-resolution multichannel seismic data from the Middle and Outer Bounty Trough region (Figure 6.1b) including a direct crossing of ODP Site 1122. With these profiles we seek to contribute in resolving the puzzle of the development of the circulation in the South-west Pacific Ocean and decipher the circulation pattern before and after the opening of the Tasmanian Gateway. With our new high-resolution seismic reflection data we can reveal pre-Oligocene circulation as well as post-Oligocene depositional patterns for the Outer Bounty Trough. These circulation patterns are correlated to past global climate fluctuations and tectonic processes. Furthermore, extrapolation of seismic units from the Outer Bounty Trough to the Middle Bounty Trough allows the estimation of the first appearance of a branch of the DWBC inside the Bounty Trough, which Carter and McCave (1997) could only infer from the present oceanic circulation.

6.3 Regional setting

The Eastern New Zealand Oceanic Sedimentary System (ENZOSS) is the generic term for the history of sediment deposition and erosion at the south and eastern New Zealand continental margin (e.g. Carter et al. 1996a). ENZOSS initiation is defined at the opening of the Tasmanian Gateway at ~ 33.7 Ma (Carter et al. 2004b). Since then ACC and DWBC have influenced the ENZOSS region and left their footprints in the sedimentary deposits. Sedimentary ages and a geological interpretation are available via ODP Leg 181 (Sites 1121 -1124, Figure 6.1a). The following description focuses on the Bounty Trough region, between the Campbell Plateau (south) and the Chatham Rise (north).

6.3.1 Tectonic and oceanic framework in the Bounty Trough area

The Bounty Trough is located east of the South Island of New Zealand (Figure 6.1a). Refraction/wide angle reflection data (Grobys et al. 2007) infer that the Bounty Trough is situated on thinned continental crust. Its formation resulted from a failed rift arm during the separation of New Zealand and Antarctica (Cook et al. (1999) and references therein). Davy (1993) recognised a zone of steeper basement gradient of unknown origin at the mouth of the Bounty Trough (his Figure 8, Zone D2). This zone is termed the Outer Sill (Carter et al. 1994) (Figure 6.1b), which also marks a transition from thinned continental crust in the west to oceanic crust east of the Outer Sill (Davy 1993). The Outer Sill separates the Bounty Trough into two zones, the Middle Bounty Trough and the Outer Bounty Trough. The Outer Bounty Trough comprises the Bounty Fan (Carter et al. 1994). Tectonic reconstructions (Eagles et al. 2004; Wobbe et al. 2012) suggest an opening of Bounty Trough around 80 Ma. Davy (2006) shows a potential anomaly c34n indicating that the Bounty Trough formation is older than 85 Ma. These publications suggest the late Cretaceous as the upper limit for the age of the oldest sedimentary deposits.

The present oceanic conditions are dominated by the DWBC, the major flux of deep cold water into the Pacific Ocean (presently 35 – 40%, Figure 6.1a (Warren 1973; Warren 1981; McCave et al. 2008)). The ACC influences the DWBC during their combined flow along the Campbell Plateau slope (Carter and Wilkin 1999; Stanton and Morris 2004; McCave et al. 2008). At ~50° S, south of Bollons Seamount (Figure 6.1a) the DWBC uncouples from the ACC continuing its journey along the New Zealand microcontinent (now referred to as Zealandia) to enter the Bounty Trough region. The main flow of the ACC turns east to flow through the South Pacific south of Bollons Seamount (between 55°S and 49°S; Carter and Wilkin 1999). The northward flow of the DWBC splits into two different branches. The eastern branch flows eastward around Bollons Seamount to enter the Outer Bounty Trough region, where it flows directly across the Bounty Channel deposits (Carter et al. 2004a). The western branch passes through a 4300 m deep gateway, the Bollons Gap, between Bollons Seamount and Campbell Plateau (Figure 6.1a; Davy 2006). Seismic reflection data (Carter and Carter 1996; Carter and McCave 1997) shows erosion at the top of the Outer Sill. It is likely that the western branch has created these erosional features after leaving the influence of the ACC at Bollons Gap and entering the Bounty Trough near the boundary between the inner and Middle Bounty Trough (Figure 6.1a; Carter and Wilkin 1999).

The oceanic setting between the rifting of New Zealand and Antarctica until the opening of the Tasmanian Gateway at the Eocene/Oligocene boundary is not well understood. A deep flow in the Bounty Trough area during this period has not been reported as ODP Site 1122 retrieved material as old as early Miocene (Carter et al. 1999b). Results of ODP Leg 189 from the Tasmanian Gateway indicate only a surface circulation for the Eocene flowing from the south along the coast of Antarctica to the north along the east Australian coast (Exon et al. 2001; Stickley et al. 2004). Numerical models of Eocene ocean circulation support this assumption (Huber et al. 2004; Sijp et al. 2011) by proposing

a clockwise deep circulation passing Zealandia from west to east. The oceanic conditions are better resolved for the time after the opening of the Tasmanian Gateway at ~33.7 Ma (Stickley et al. 2004). After its establishment, the DWBC dominated sedimentation in the Outer Bounty Trough region, as suggested by the results of ODP Site 1122 (Carter et al. 1999b). The DWBC itself is modified by the ACC causing episodic fluctuations of DWBC strength (Carter and Wilkin 1999; Morris et al. 2001; Stanton and Morris 2004; McCave et al. 2008). The Outer Bounty Trough area has been affected by two strong episodic flows. Directly after the onset of the ACC, strong deep flows prevailed because the presence of an East Antarctic ice sheet (EAIS) favoured enhanced deep-water production (Zachos et al. 2001; Carter et al. 2004a). The duration of an ACC/DWBC flow affecting the Bounty Trough region has not yet been determined but probably lies between 6 myrs at ODP site 1124 (Carter et al. 1999d) and 13 myrs at ODP site 1123 (Carter et al. 1999c). This strong flow was followed by more tranquil conditions with less energetic flow conditions until the late Miocene. A second strong episodic deep flow was inferred from ODP Site 1122 between 10.4 Ma and ~ 5 Ma (Carter et al. 1999b). This second event is attributed to the build-up of the West Antarctic Ice Sheet after the Miocene Climate Optimum (Carter et al. 1999b; Carter et al. 2004a; Carter et al. 2004b). Late Miocene to Pliocene oceanic conditions have been dominated by DWBC strong flows due to climate cooling (Carter et al. 2004a). Changes of current flow during the Plio-/Pleistocene were controlled by glacial interglacial cycles initially paced by obliquity but around 0.8 Ma transitioned to eccentricity driven cycles (Carter et al. 2004a).

6.3.2 Sedimentary framework

The previously described oceanic conditions are recorded in the sedimentary column inside the Bounty Trough region. That record includes (1) biopelagic sediments (2) sediments transported by the DWBC, and (3) terrigenous sediment input via turbidity currents within the Bounty Channel during glacial low stands (Carter et al. 1999b; Carter et al. 2004a). During interglacial high stands turbidity currents bypass the Bounty Trough head and flow directly into the Hikurangi Channel (Carter et al. 2004b). The turbidity flows of the Bounty Channel are the main sediment source sediments younger than ~ 1.7 Ma of the Outer Bounty Trough (Carter et al. 1999b). However, this sediment input has only been present since ~2.2 Ma when the first turbidites accumulated at the deep sea at the mouth of Bounty Trough as revealed by ODP Site 1122 (Carter et al. 1999b). Before 2.2 Ma the sedimentary sources are restricted to pelagic sedimentation and DWBC transported sediments and few isolated turbidities originating from the Bounty Trough(Carter et al. 1999b), that have been eroded from deposits upstream of the DWBC, e.g. in the Emerald Basin or the Campbell Skin Drift (Joseph et al. 2004). Current controlled sedimentation pre-dates the onset of Bounty Channel turbidities. The upper sedimentary column (up to 617 metres below seafloor (mbsf)) at ODP 1122 has three lithological units (I to III, Figures 6.2a and 6.3 (Carter et al. 1999b)). Unit I (early Pleistocene to recent) contains terrigenous sediments transported by turbidity currents via the Bounty Channel. Four sub-units (Ia to Id) represent turbidity deposits of different grain size and thickness (Carter et al. 1999b). The lower

part of unit Id (below 360 m) marks the change in depositional environment from turbidity-dominated to contourite-dominated deposits. Unit II (early Pliocene to early Pleistocene) contains pelagic/hemipelagic sediments with interbedded bottom current deposits of sand and muds. Turbidity occurrence within subunit IIa is restricted to isolated beds of fine sand, probably deposited during weak contour current activity (Carter et al. 1999b). Turbidite occurrence is further reduced in subunits IIb and IIc. Here hemi-/pelagic sediments dominate. The boundary between unit IIb and IIc is defined by a hiatus in deposition (at 494 mbsf, from 10.4 Ma to 5 Ma). It is attributed to the intensified flow of ACC and DWBC. Unit III (middle Miocene) consists of coarser grained pelagic/hemipelagic sediments of contouritic origin. Turbidites are rare. ODP Site 1122 terminates at 617 mbsf approximately 50 m above a pronounced regional unconformity.

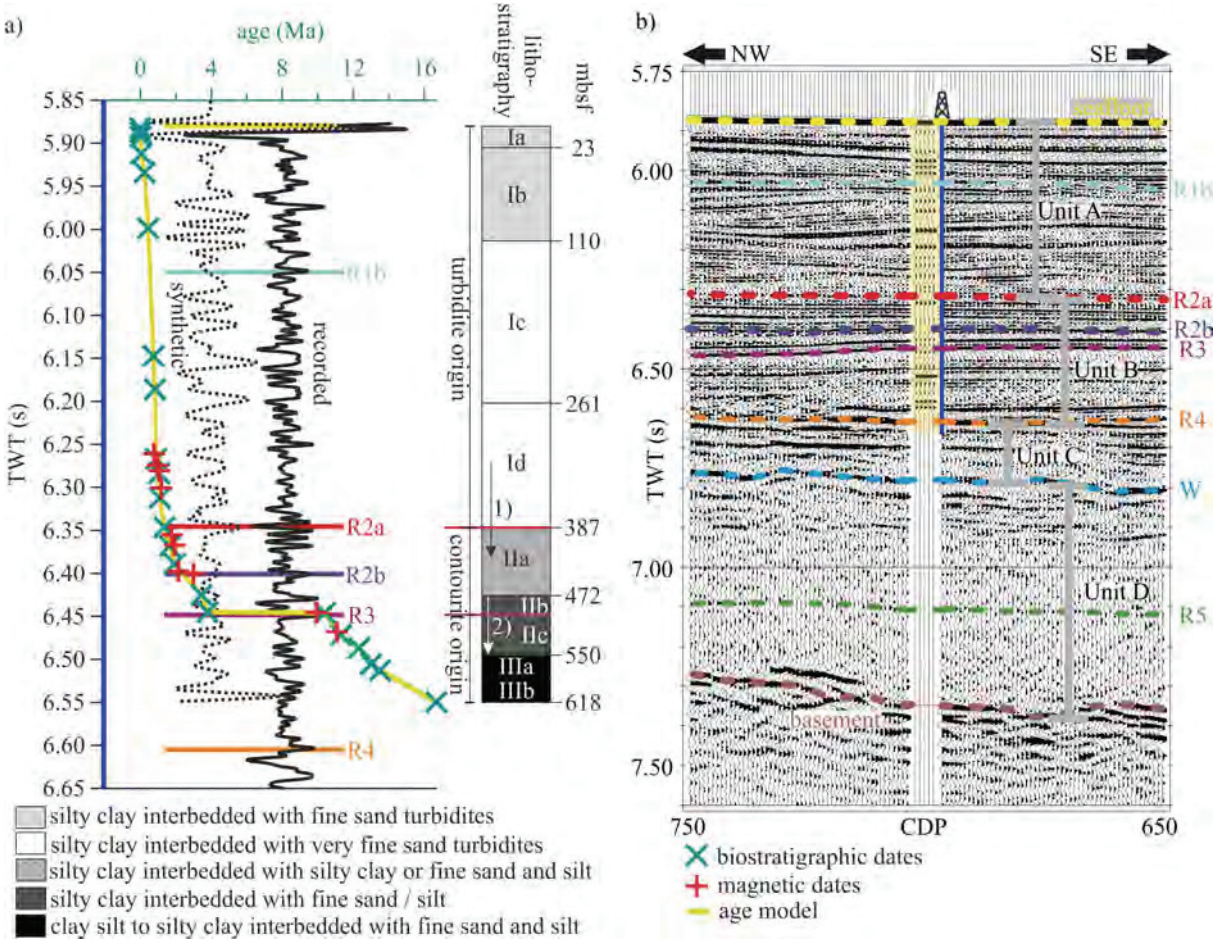

Figure 6.2: **a)** Graphical sketch of results of ODP Site 1122 (Carter et al. 1999b) with link of the synthetic seismogram to the measured trace at CDP 700, the location of ODP Site 1122 in Figure 6.3. The computed age model is presented in dark yellow, crosses represent dated events from biostratigraphy (green) and magnetic data (red). Numbered arrows: 1) transition from turbiditic to contouritic deposits, 2) increasing detrital chlorite content; **b)** computed synthetic seismogram linked to the seismic data presented here. Location of borehole is marked in Figure 6.1b.

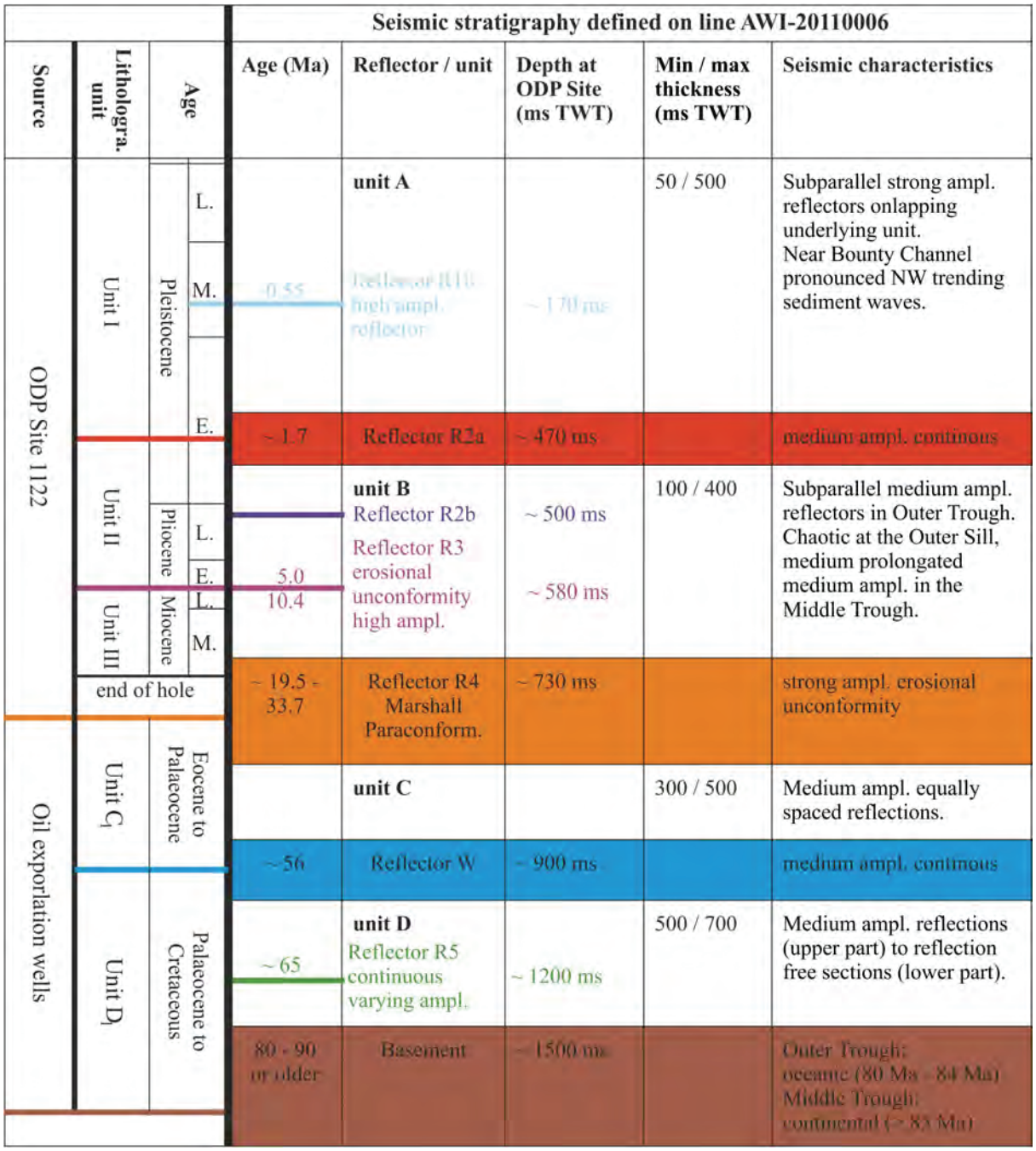

Figure 6.3: Summary of the seismic stratigraphy as described in Section 6.4.1 and 6.4.2; ampl. = amplitude.

Sedimentary rocks below the sampled strata of ODP Site 1122 can be characterised from oil exploration wells from the Canterbury Basin and the Great South Basin (Carter 1988; Carter et al. 1994). The observations have been traced into the Bounty Trough area using single channel seismic lines (Carter et al. 1994). The sediments below the regional unconformity are divided into two different lithological units (C_l and D_l) separated by a regional unconformity W, possibly representing the Palaeocene/Eocene Boundary (Carter 1988). Unit C_l above unconformity W consists of coastal plain coal measures followed by shallow marine sandstone-siltstone shale, marl and biopelagic chalk deposited during marine transgression of New Zealand (Carter 1988). The age estimation for this group is Palaeocene to Eocene. Below unconformity W, unit D_l still originates from marine

transgression until approximately half way between reflector W and the basement. The lower part of unit D_l is of terrigenous origin, deposited during initial rifting during the Cretaceous (Carter 1988).

6.4 Methods

Five high-resolution seismic reflection profiles (Profiles AWI-20110006 to AWI-20110010, with a total profile length about 571 km) were acquired during cruise SO 213/2 with R/V *Sonne* in Febuary 2011 (Fig. 6.1). These profiles, as well as excerpts of lines Hunt-141 and Hunt-143, were interpreted by Uenzelmann-Neben et al. (2009) and are used to describe the seismostratigraphy of the Middle Bounty Trough, the Outer Sill Region and the Outer Bounty Trough. The end of profile AWI-20110007 is 3.25 km near profile Hunt-143 (approximately CDP 8830, see Figure 7 in Uenzelmann-Neben et al. (2009)). Profile AWI-20110010, CDP 3900, and line Hunt-141 (both correlation points are indicated in Figure 6.1b) are 2.25 km apart.

Profiles recorded during SO 213/2 were acquired with a 3000 m long digital streamer containing 240 channels. As a seismic source, four GI-Guns (total volume 2.8 l) with a central frequency of 40 Hz were used. This setup allows a vertical resolution of about 10m at the seafloor. Data processing comprised Common Depth Point (CDP) sorting (25 m spacing), velocity analysis (every 50 CDPs), filtering in F-K space (except profile AWI-20110006), normal move out correction, stacking, omega-x migration, frequency filtering (band pass filter for 0 to 9000 ms TWT with 10 – 250 Hz, only up to 150 Hz for all CDPs of Profiles AWI-20110007 and AWI-20110008 because of high frequency noise) and muting of the water column. For display purposes an automatic gain control (AGC) of 1000 ms was applied to profile AWI-20110008.

To link the borehole information of ODP Leg 181 Site 1122 to the seismic data, a synthetic seismogram was computed. For this purpose ODP shipboard measurements of density, porosity, and P-wave velocity were used (Carter et al. (1999b)). As P-wave velocities were only determined for the interval 390-608 mbsf (Carter et al. (1999b), the missing velocities were calculated using an empiric formula for P-wave velocity of normal consolidated sediments (Erickson and Jarrard (1998)). Measured and calculated velocities were merged and multiplied with density to derive a continuous down core profile of seismic impedance values. This dataset was convolved with a 40 Hz Ricker wavelet to simulate the seismic source signal of the GI-Guns. For age estimation we used the age model constrained by biostratigraphic events analogue to Figure F25 and palaeomagnetic data of Figure F21 of Carter et al. (1999b) and computed a corresponding age curve for our analysis (dark yellow curve in Figure 6.2, tie points to ODP 1122 biostratigraphy are marked with crosses, palaeomagnetic tie points in red).

Values of thicknesses in metres have been converted assuming a P-wave velocity of 1600 m/s for the units A and B and of 3000 m/s for units C and D.

6.5 Results

6.5.1 Definition of seismostratigraphy at ODP Site 1122

We combined the local seismostratigraphic concept provided for ODP Site 1122 (Carter et al. 1999b) with the regional seismostratigraphy for the whole Bounty Trough (Carter et al. 1994). We used reflectors R2a and R4 of the local seismostratigraphy as a direct link to the borehole and reflector W from the regional seismostratigraphy to constrain four seismic units (Fig. 6.2b). We stuck to the regional concept and the seismic units were accordingly named A (youngest) to D (oldest). We identified four intra unit reflections, three from the local seismostratigraphy, reflectors R1b, R2b and R3, and a newly defined reflection R5 (see Figure 6.3 for summarised seismostratigraphic setup).

Seismostratigraphic unit A at the location of ODP Site 1122 is 0.6s TWT (~ 480 m) thick. The seafloor and reflector R2a, a medium amplitude continuous feature, limit the extent of unit A. The reflection pattern shows the wavy character consistent with sediment waves where internal high amplitude reflections are interbedded with low amplitude reflectors (Figure 6.4 CDP 66 to 1500). Unit A has an intra-unit reflection (reflector R1b), which is also traceable further to the base of the Outer Sill and again in the Middle Bounty Trough within the Bounty Channel levees (Figure 6.4). At ODP Site 1122 we can assign an age of approximately 0.55 Ma to reflector R1b (Figure 6.2a). Via the direct tie (Figures 6.2 and 6.3) to the lithological interpretation of ODP Site 1122 (Carter et al. 1999b) seismostratigraphic unit A is correlated to terrigenous turbidity deposits interbedded with hemi-pelagic to pelagic sediments. The age is estimated to be between Holocene and early Pleistocene (reflector R2a: ~1.6 Ma).

Reflectors R2a and R4 are high amplitude reflectors of regional extent. They constrain seismostratigraphic unit B. At ODP Site 1122 its thickness is 0.4 s TWT (~ 320 m). Internal reflections within unit B are sub-parallel and of medium to low amplitude. Site 1122 penetrated seismostratigraphic unit B and a direct link of seismostratigraphic unit B to the lithological units II and III (Figure 6.2) is possible. Unit B sediments have been deposited mainly by contour currents. Due to the synthetic seismogram, the lithological information can be linked to two intra-unit reflectors. Reflector R2b, a medium amplitude horizon of local extent inside the Outer Bounty Trough, marks the transition from contourite to turbidite deposits (Carter et al. 1999b). Lithological units IIb and IIc are separated by a hiatus (10.4 Ma to 5 Ma) (Figure 6.2). This hiatus appears documented as the second intra-unit reflector R3 (Figure 6.2a), a continuous high amplitude reflection, which points to an unconformity (e.g. Stow and Mayall 2000; Faugères and Stow 2008). Reflector R4 was not cored by ODP Site 1122. With the sedimentation rate from the lowest lithological unit IIIb (~20 m / myr) and age of the oldest sediments retrieved at Site 1122 (16,7 Ma; Carter et al. 1999b) the upper limit of reflector R4 is estimated to be ~19.5 Ma, bearing in mind the limitations of extrapolating sedimentation rates to estimate ages.

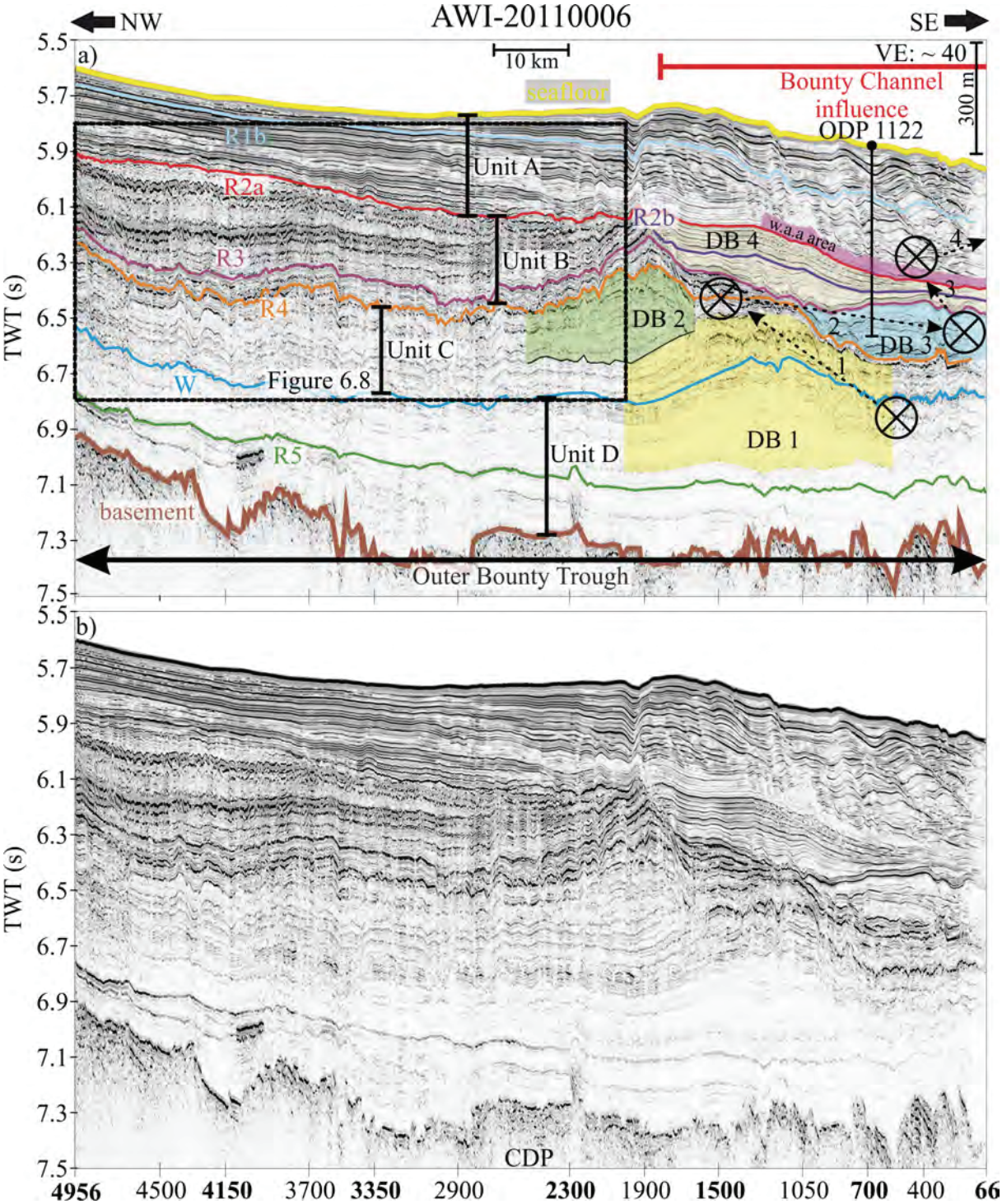

Figure 6.4: Profile AWI-20110006 **a)** Interpreted section of the profile showing the regional relevant reflectors and seismic units A to D. Observed drift bodies (DB 1 - DB 4) are coloured and marked with numbers as defined in the text. Circles with crosses indicate inferred flow cores of a (Proto-) DWBC and the numbered arrows show the displacement of the cores with time. 1: displacement during Palaeocene/Eocene Boundary 2: displacement while initiation of the ACC after opening of Tasmanian Gateway 3: displacement after intensification of deep currents around 10 Ma, 4: displacement after arrival of first turbidites from the Bounty Channel; Abbreviations: DB = drift body, w.a.a. = weak amplitude area (transitional zone), **b)** uninterpreted profile. Bold CDP numbers are marked in Figure 6.1b**.**

Reflectors R3 and R4 are of regional relevance and can be linked to prominent regional reflectors Y and X defined in earlier studies (Davey 1977; Carter et al. 1994). Extrapolation of both reflectors to the Outer Sill allow us to use the formerly interpreted multichannel seismic lines, Hunt-141 and Hunt-

143, located in in the Middle Bounty Trough area (Figure 6.1b) (Uenzelmann-Neben et al. 2009). Reflector R3 can be linked to reflector Y (Figure 6.5), a regional unconformity separating Bounty Channel deposits from the contourite deposits of unit B (Carter et al. 1994). Deep Sea Drilling Project (DSDP) Site 594 (Fig. 6.1) penetrated reflector Y and identified it as a hiatus in deposition between 8.5 Ma and 6.5 Ma (Kennett et al. 1986). The difference to ODP site 1122 (hiatus in deposition between 10.4 and 5 Ma (Carter et al. 1999b)) is easily explained by the location of DSDP Site 594 at the head (away from the main DWBC flow) and Site 1122 at the mouth of the Bounty Trough (close to the DWBC core flow). Reflector R3 was interpreted to result from a stronger DWBC flow during climate cooling initiating the West Antarctic Ice Sheet build-up (Carter et al. 2004b). Reflector R4 corresponds to reflector X (Figure 6.5), which is identified as the Marshall Paraconformity (Carter et al. 1994). This paraconformity is a prominent regional feature observed onshore (e.g. Marshall 1911; Fulthorpe et al. 1996) as well as offshore close to the shore (Carter 1988) and in the substantial drift deposits on the northern flank of Chatham Rise cored at ODP Site 1123 (Carter et al. 1999c) and 1124 (Carter et al. 1999d). It is attributed to the intensified deep flow after opening of the Tasmanian Gateway at the Eocene/Oligocene Boundary (e.g. (Fulthorpe et al. 1996; Exon et al. 2001; Carter et al. 2004b)). The lower limit of the paraconformity is the deep opening of the Tasmanian Gateway (33.5 – 33.7 Ma (e.g. (Stickley et al. 2004; Carter et al. 2004b)).

Seismostratigraphic unit C is bound by reflectors R4 and W. Reflector W is a medium amplitude continuous reflection of regional extent. The thickness of unit C is approximately 0.3s TWT (~ 450 m) at the location of ODP Site 1122. Internal reflections are continuous and of low to medium amplitude. Correlation to lithological unit C_l links seismostratigraphic unit C to hemi-pelagic sediments deposited during marine transgression (Carter et al. 1994). Reflector W was also reached by the exploration wells and assigned a tentative age close to the Palaeocene/Eocene Boundary (Carter 1988; Carter et al. 1994). Although also observed in other regions around New Zealand by DSDP Legs 21 (Edwards 1973) and 29 (Kennett et al. 1975) there are no clear indications for its origin. Davy (1993) interprets it as a sign of change in oceanic circulation pattern around the Palaeocene/Eocene Boundary, an interpretation we adopt.

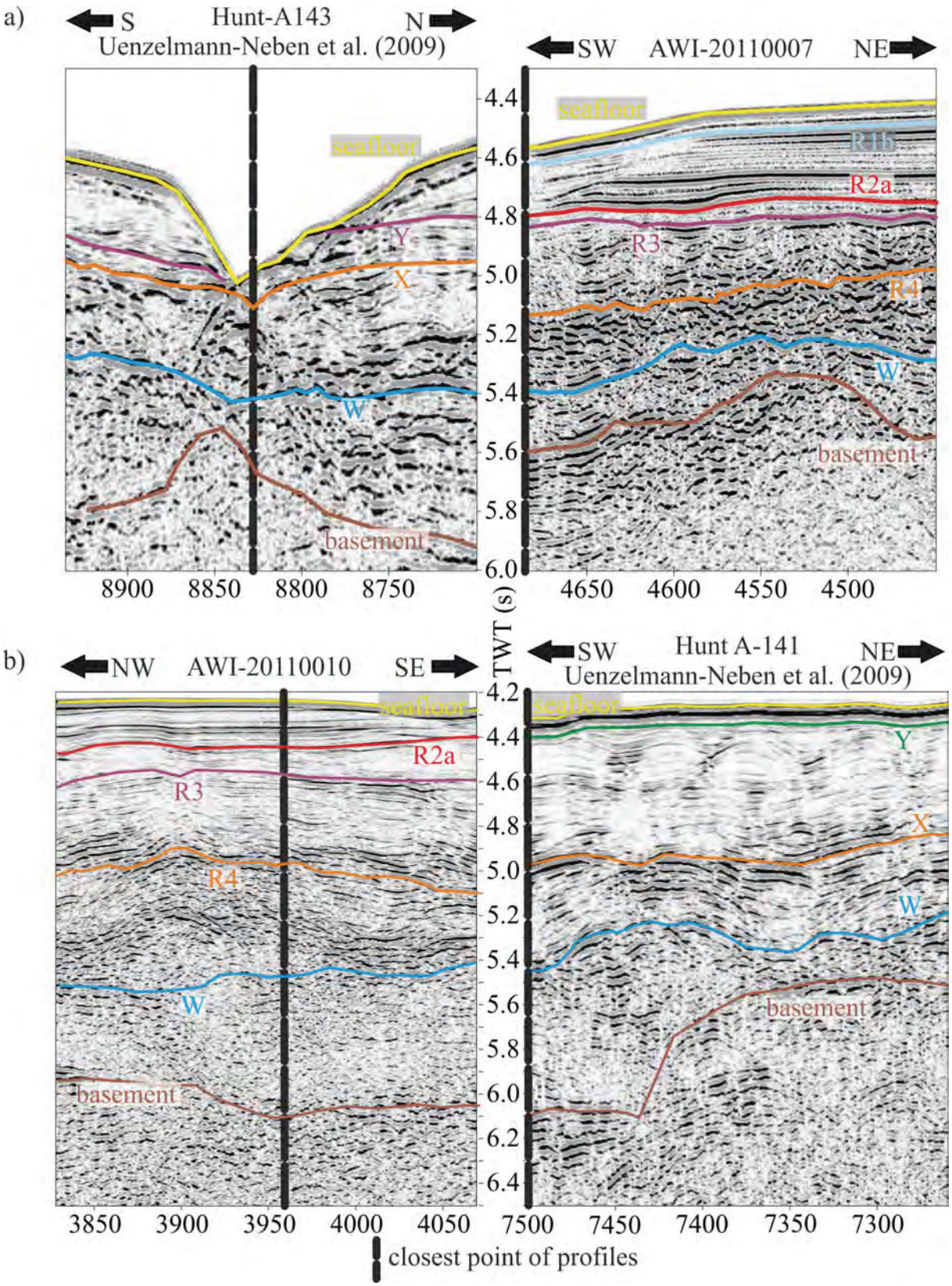

Figure 6.5: **a)** Comparison between interpretation of profile AWI-20110007 and Hunt-143 (Uenzelmann-Neben et al. 2009), **b)** comparison between interpretations of profile AWI-20110010 and Hunt-141 (Uenzelmann-Neben et al. 2009).

The oldest seismostratigraphic unit D is limited by reflector W and the basement reflection. Its thickness is approximately 0.7s TWT (~ 1050 m) at the location of ODP Site 1122. Internal reflection

characteristics show low amplitudes in the upper part to an almost reflector-free lower part. Unit D features an intra-unit reflection within the Outer Bounty Trough, reflector R5. Reflector R5 is a continuous feature of variable amplitude depending on location (compare Figure 6.4 CDP 700 - 2900 to Figure 6.6 CDP 600 – 1000). Seismostratigraphic unit D can be correlated to lithological unit D_l. Strata below reflector W are correlated to the marine transgression analogue to unit C and change to a synrift sediment infill of terrigenous origin in the lower part of unit D (Carter 1988; Carter et al. 1994). Basement age is estimated to be of late Cretaceous age based on the opening of Bounty Trough and magnetic anomaly data (Davy 1993; Grobys et al. 2007). Unfortunately, the description of lithological unit D_l does not report an unconformity to correspond to reflector R5. Age estimation of reflector R5 is difficult but it has to be older than the Palaeocene/Eocene Boundary (reflector W) and younger than the oceanic basement at the location of Site 1122 of approximately 80 Ma (Eagles et al. 2004; Wobbe et al. 2012). If we assume a linear sedimentation rate within seismostratigraphic unit D (depositional period between 80 Ma and 55 Ma, Figure 6.3) we can get a first-order estimate of the age of reflector R5 to be ~ 65 Ma.

6.5.2 Observations

The Outer Bounty Trough, the Outer Sill region and the Middle Bounty Trough (Figure 6.1b) show different patterns in sediment deposition mainly observable in seismic units A and B.

Depositional characteristics of unit A vary between the Outer Bounty Trough and the Outer Sill/Middle Bounty Trough area. Deposits thicker than 0.4 s TWT (~320 m) in the Middle Bounty Trough and Outer Sill region, occur only at the levees bordering Bounty Channel (Figures 6.6, CDPs 4200- 4600, and 6.7, CDPs 1150- 1750). At the levee flanks, accumulation of unit A is significantly reduced to values below 0.2 s TWT (~160 m; Figure 6.6, CDP 2400 to 3200, Figure 6.7, CDP 2200 to 2500). Further away from the Bounty Channel (about 40 – 50 km) unit A is hardly visible and reaches only a thickness of about 0.1 s TWT (< 100 m; see for example patchy sedimentary bodies at the Outer Sill slope (Figure 6.6, CDP 1600 - 2400) or is absent (Figure 6.7, CDP 2600 – 4840). At the Outer Bounty Trough, the influence of the Bounty Channel is evident. The thick sediment wave deposits of unit A drape the underlying unit B (Figure 6.4 CDP 66 – 1400).

Unit B is also present in all three regions and extends further into the Outer Bounty Trough (Figure 6.4 CPD 66 to 1900) than previously reported by Carter et al. (1994). Their data shows that unit B lenses out against a crest of underlying unit C inside the Bounty Fan. We assume that this crest (please refer to Plate 2c and d of Carter et al. 1994) is identical with the crest in Figure 6.4, CDP 1900 .ODP Site 1122 and our new high-resolution multichannel seismic data indicate differences in sediment composition. The reflectivity pattern varies significantly across R2a (Figure 6.4 CDP 66 – 1900 between 6.1 s and 6.4 s TWT) and sedimentary sequences cored at ODP Site 1122 above R2a are of turbidite origin (unit A, lithological unit I), whereas below reflector R2a sediments are of contouritic origin (unit B, lithological unit II and III) (Carter et al. 1999b, see Figure 6.2a).

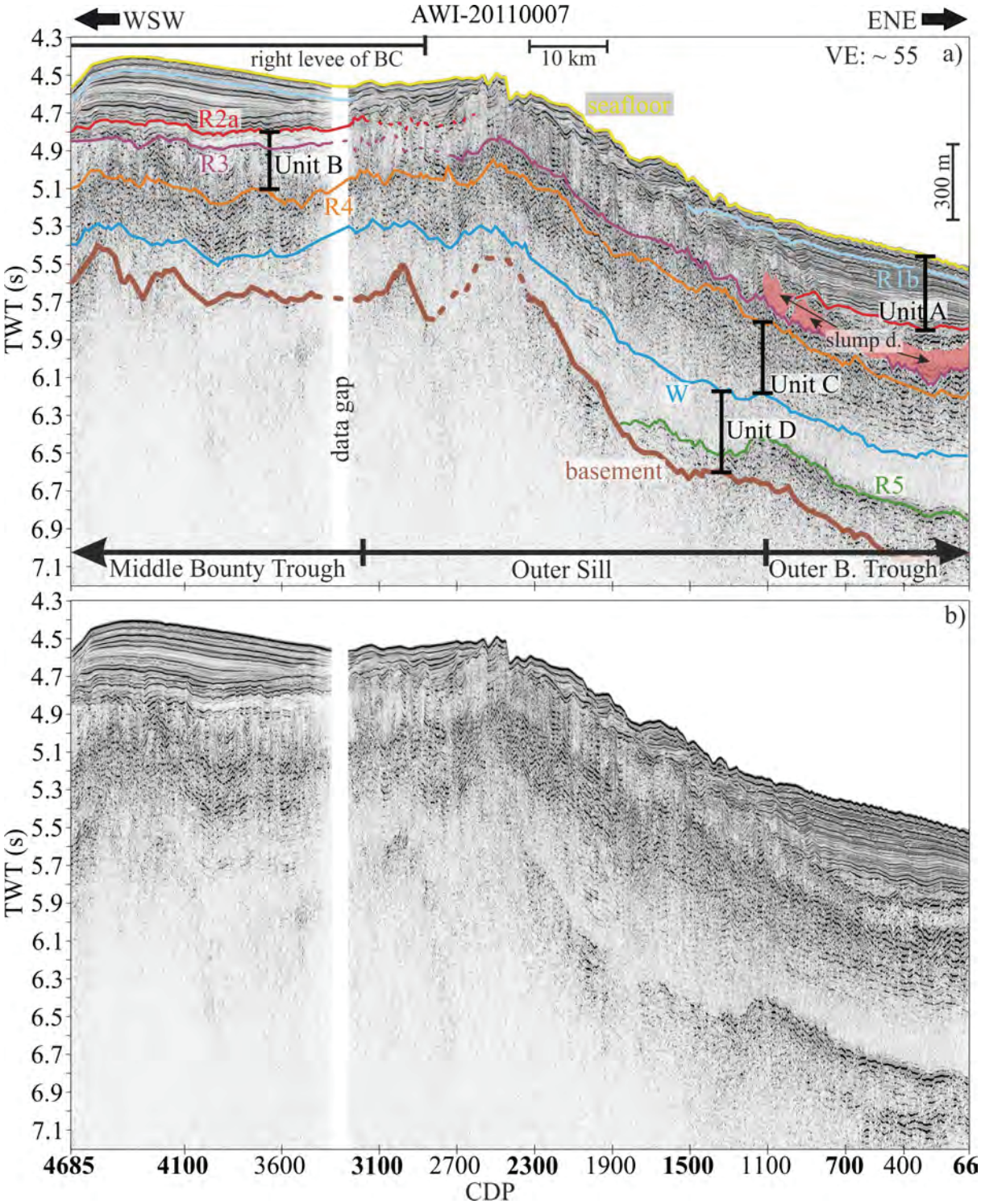

Figure 6.6: Profile AWI-20110007. **a)** Interpreted section of the profile showing the extrapolated reflectors of Profile AWI-20110006, red areas mark identified slump deposits (slump d.); **b)** uninterpreted profile. Bold CDP numbers are marked in Figure 6.1b.

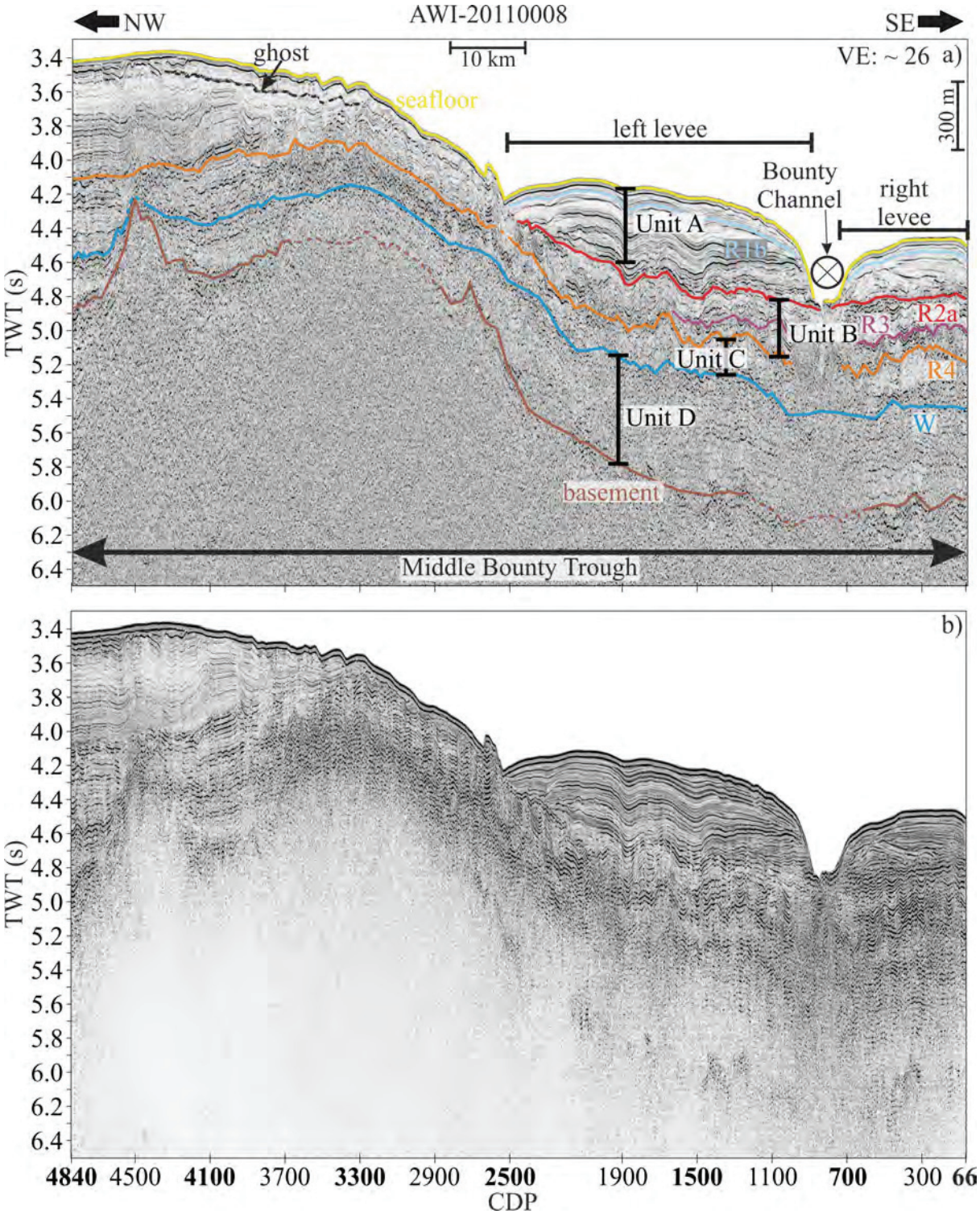

Figure 6.7: Profile AWI-20110008. **a)** Interpreted section of the profile displayed with a 1000 ms Automatic Gain Control (AGC) window showing extrapolated reflection from Profile AWI-20110006 and AWI-20110007, **b)** uninterpreted profile without AGC. Bold CDP numbers are marked in Figure 6.1b.

Unit B shows two different sedimentary bodies (Figure 6.4, CDP 66 – 1050 and CDP 550 to 1950) onlapping the underlying crest slope (Figure 6.4 CDP, 66 to 1900) of unit C. Internal reflection amplitude increase from the bottom to the middle of the two sedimentary bodies and decrease again above the middle. These two characteristics are comparable to elongated mounded drift bodies in the

Canterbury Basin identified by Lu et al. (2003). Northwest of this crest the reflective pattern changes to a semi-continuous pattern visible between this crest and the base of the Outer Sill (Figure 6.6, CDPs 66 – 800 and Figure 6.8). At the Outer Sill region unit B shows chaotic reflections (Figure 6.6, CDPs 800–3800). The chaotic reflection pattern suggests a slump mass (Stow and Mayall 2000) on the Outer Sill slope. At the transition from the Outer Sill to the Middle Bounty Trough the reflection characteristics of unit B change from moderate amplitude chaotic structures (Figure 6.6, CDP 2500 – 4685) to semi-continuous densely spaced reflectors (Figure 6.7b, CDPs 66-2500). In the north-western survey area (end of profile AWI-20110008, Figures 6.1 and 6.7) another change in reflectivity of unit B occurs at the slope of a local basement high (Figure 6.7b CDP 3400 - 4840). Internal reflections weaken in amplitude and form a thicker sedimentary package with seismically transparent sections between weak reflections, in contrast to higher amplitude reflections further southeast (Figure 6.7, CDP 2500 – 3400).

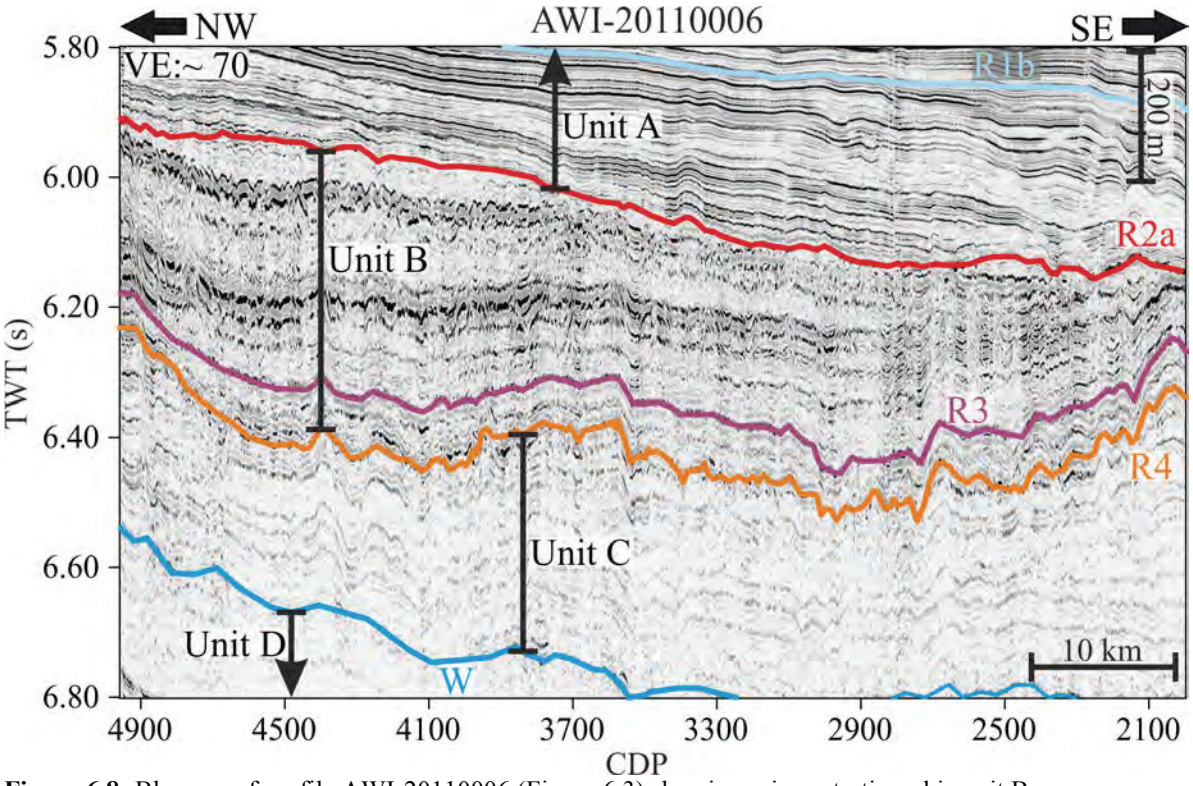

Figure 6.8: Blow-up of profile AWI-20110006 (Figure 6.3) showing seismostratigraphic unit B.

Unit C is less variable than units A and B. Semi continuous reflections of low- amplitude drape the underlying unit D (Outer Bounty Trough, Figure 6.4 and 6.6, CDP 66 – 800) or are of medium to high amplitude chaotic appearance (Outer Sill and Middle Bounty Trough, Figures 6.6, CDP 800 – 4685, and 6.7). Unit C thickness is largest in the Outer Bounty Trough with 0.3 s TWT (~ 450 m), which decreases towards the Middle Bounty Trough (0.2 s TWT, ~300 m). Only one exception of this general pattern is observed. In the Outer Bounty Trough (Figure 6.4 CDP 1700 – 2600), internal reflection characteristics show an upward convex bend lenticular shape. Additionally, reflective amplitude increases from the bottom to the top until reaching reflector R4. This is a typical behaviour for the lower part of an elongated mounded drift, as described by (Lu et al. 2003). The missing

decrease in amplitude is easily explained by the erosion due to the Marshall Paraconformity (R4). Together with the upward convex bend reflections this indicates an elongated mounded drift structure (e.g. Faugères et al. 1999; Stow et al. 2002; Faugères and Stow 2008). Here, unit C also shows its maximum thickness (Figure 6.4, CDP 2000) of ~ 0.45 s TWT (~ 675 m).

Unit D drapes the basement, following its topography. The unit thickness appears almost constant between 0.4 and 0.5 s TWT in the Outer Bounty Trough (~ 600 – 750 m) and decreases when approaching at the Outer Sill (Figure 6.6 west of CDP 1500) where the unit only reaches thicknesses about 0.2 s TWT to 0.4 s TWT (~ 300 - 750 m). An exception of this range is a thickening of unit D in the Outer Bounty Trough (Figure 6.4, near CDP 1500) to more than 0.8 s TWT (~ 1200 m) with internal reflections showing an upward convex shape (Figure 6.4, CDPs 600-2100) as well as an increase in amplitude from the bottom to the centre of these sediment body and decreases again further upward to the top. The upward convex bend reflections (e.g. Faugères et al. 1999; Stow et al. 2002; Faugères and Stow 2008) and the amplitude characteristics (Lu et al. 2003) indicate a mounded elongated drift. A peculiar feature of the Outer Bounty Trough is reflector R5 (Figures 6.4 and 6.6), which occurs 0.2 to 0.4 s TWT above the basement reflector. Its amplitude increases from east to west of the survey area towards the Outer Sill. At the Outer Sill Reflector R5 pinches out against the basement (Figure 6.6, CDP 1900). Such a pattern is also observed in the Atlantic Ocean. There, sediment composition and chert layer thickness have resulted in alternating amplitudes of seismic reflections (Tucholke 1979; Senske and Stephen 1988). As chert is a common feature (multiple layers of chert in the whole core section) in Site 1121 (Carter et al. 1999a) we interpret reflector R5 as a chert layer.

6.6 Discussion

6.6.1 The circulation pattern before the Opening of the Tasmanian Gateway (> 33.7 Ma)

(Carter et al. 2004a) suggest that ENZOSS began to develop at the Eocene/Oligocene boundary. The Marshall Paraconformity (reflector R4) documents this boundary (e.g. Fulthorpe et al. 1996; Stickley et al. 2004; Carter et al. 2004b). Earlier signs of an active cold deep current influence have not been observed in the ENZOSS region so far. Only hints on a warm deep current north of New Zealand were found (Carter et al. 1999d; Carter et al. 2004a). At ODP Site 1124 a hiatus ranging from 58 to 39 Ma is observed. It was possibly caused by a warm, saline, nutrient-rich deep-water mass from a northern source (Carter et al. 1999d; Carter et al. 2004a). ENZOSS by definition is only affected by a cold deep water inflow (Carter et al. 2004a). Any warm northern inflow predated ENZOSS. In contrast to these previous studies our high-resolution seismic reflection data provide new evidence for pre-Oligocene circulation. Above ~ 6.9 s TWT the south-eastern survey area reveals upward convex reflectors with a steeper south-eastern flank (Figure 6.4, CDP 800 to 2000, crest at CDP 1250). Such structures are

commonly interpreted as plastered sediment drifts (e.g. Faugères et al. 1999; Faugères and Stow 2008) and show similar characteristics to the drifts observed in the Canterbury Basin (Lu et al. 2003). Two different drift bodies (drift body 1 and drift body 2 in Figure 6.4a) are observed below the Marshall Paraconformity (reflector R4, Figure 6.4).

6.6.1.1 Drift body 1 (< 65 Ma - 45 Ma)

The upward convex bent reflectors of drift body 1 (DB 1) are observed above reflector R5 (Figure 6.4a). Its internal reflection characteristics show similarities to build-up elongated mounded drifts (Faugères et al. 1999; Stow et al. 2002; Faugères and Stow 2008) and show similar characteristics (strongest amplitude in the middle of the drift body) found by Lu et al. (2003) for elongated mounded drifts. Drift build-up started during the early Palaeocene. The reflector geometry shows a steeper flank on the southeastern side pointing towards a deep current on this side and formed DB 1. We term this flow the Proto-DWBC. We suggest two processes to account for the formation of DB 1. Firstly, oceanic conditions were modified by plate tectonics. New Zealand moved north away from Antarctica (Marie Byrd Land) since the spreading at the Pacific Antarctic Ridge started in the late Cretaceous at ~ 80 Ma (Eagles et al. 2004; Wobbe et al. 2012). Current pathways were reorganised by the submarine crustal expanse of Zealandia. At this time a cyclonic gyre centred in the Ross Sea was active also driving deep-water circulation (e.g. Huber et al. 2004; Sijp et al. 2011). To be able to reach the location of DB 1, the gap between Zealandia and Marie Byrd Land had to be deep enough. Between 80 Ma and 65 Ma the paleo depth of the DB 1 (close to the location of ODP Site 1122, where the paleo depth was calculated for) has been estimated to be between ~ 2600 m (at 85 Ma) and ~ 3000 m (at 65 Ma) depth (Carter et al. 1999b). A first order age estimate indicates the start of drift build-up at DB 1 at 65 Ma giving a paleo depth of the seafloor at ~ 3000 m. This means the gap between Marie Byrd Land and New Zealand probably reached such depth around 65 Ma and allowed a bottom/deep water mass formed near Antarctica to flow north past New Zealand. Secondly, the climate also played a major role. Prior to the Cretaceous/Palaeocene Boundary the global $\delta^{18}O$ isotope curve suggests a decrease in global mean temperature (Cramer et al. 2009; Friedrich et al. 2012). Temperature differences between the high latitudes Southern Ocean and the Pacific Ocean began to increase between 84 Ma and 78 Ma (Friedrich et al. 2012) thus creating a temperature gradient between these two regions. (Cramer et al. (2009 (their Figure 6)) report differences in $\delta^{18}O$ values between the high latitude Southern Ocean and the Pacific up to 0.5 per mill. This may have led to an initiation of a deep-water flow or increasing deep flow speeds creating a current capable of building up DB 1. It is difficult to say whether climate or seafloor spreading initiated deep-water flow east of Zealandia. If climate was the primary driver we would have expected an earlier onset of a deep current if the basin deep enough for such a current. Relative cooling started around 95 Ma (Cramer et al. 2009; Friedrich et al. 2012). Separation of Zealandia and Antarctica did not start before 90 Ma and did not form a significant basin before 80 Ma (Wobbe et al. 2012) allowing any deep current flow between both

continents. We favour a combination of both processes, as no deep north-setting current could have formed without the separation of Zealandia and Antarctica.

Since internal reflections of DB 1 still show an upward convex mounded geometry centred on CDP 1250 (Figure 6.4) and a decrease in amplitude (compare Figure 6.4 CDP 1050 to 1500, high amplitudes between 6.6 and 6.75 s TWT, and lower amplitudes between 6.45 and 6.6 s TWT) above reflector W (marking the Palaeocene/Eocene boundary (Carter 1988; Carter et al. 1994), we can conclude that deposition at DB 1 continued into the early Eocene. After the Cretaceous/Palaeocene Boundary, a relative warming trend of global climate is observed in the global $\delta^{18}O$ isotope curve (Zachos et al. 2008; Cramer et al. 2009; Friedrich et al. 2012). The curve peaks at the Early Eocene Climatic Optimum around 50 Ma (Zachos et al. 2008). This point is either not documented by DB 1, as a decrease in flow speed did not inhibit deposition at DB 1. Possibly the change in amplitude for elongated mounded drifts may represent different phases of drift development (Lu et al. 2003) caused by the warming trend.

After the Early Eocene Climatic Optimum the climate cooled (e.g. Zachos et al. 2008; Cramer et al. 2009). This finally led to at least partial glaciation of Antarctica around 40 Ma (e.g. Zachos et al. 2001). Deposition at DB 1 ceased around 45 Ma (assuming a steady deposition between reflector R4 and W). We suggest that the initiation of deep water flow to have preceded partial glaciation of East Antarctica. Temperatures proxies suggest a linear cooling trend (Zachos et al. 2008; Cramer et al. 2009) that may have allowed sea ice formation during winter earlier than 40 Ma, as suggested from ice rafted debris at Kerguelen Plateau, dated between 36 Ma – 40 Ma (Ehrmann and Mackensen 1992; Zachos et al. 1992). This is also evident from drift formation in the Amundsen Sea as early as Eocene (Uenzelmann-Neben and Gohl 2012). Additionally the Mid Eocene Climate Optimum around 42 Ma (Zachos et al. 2008; Cramer et al. 2009) could have played a role. The short pulse of warming followed by cooling may have affected current pathways and speeds causing a shift away from DB 1. A tectonic effect can be excluded. No major tectonic events affected the New Zealand Region during the Eocene (e.g. Lebrun et al. 2003; Cande and Stock 2004).

6.6.1.2 Drift body 2 (45 Ma – 33.7 Ma)

Above DB 1 we observe a drift crest migration of ~16 km to the west. Here, upward convex bend reflectors are visible indicating a second mounded drift (Figure 6.4, CDP 1500 to 2800, crest at CDP 1900), drift body 2 (DB 2, Figure 6.4). The slight asymmetry (steeper flank to the south east), the increasing amplitudes from bottom to the top of the drift as well the small size (not higher than ~400 m, about 15 km long) fit to the characteristics of a elongate mounded drift (Faugères et al. 1999; Lu et al. 2003). In a similar manner to DB 1, the current flowed at the SE side, a result inferred from drift geometry. Deposition started in the upper part of unit C at ~45 Ma (end of deposition at DB 1, Figure 6.4 above ~ 6.5 s TWT) and continued until the Eocene/Oligocene Boundary (marked by reflector R4). We infer that Proto-DWBC also formed DB 2 between middle Eocene (~ 45 Ma) and the Eocene/Oligocene Boundary. Since the shift from DB 1 to DB 2 global

$\delta^{18}O$ records suggest a general cooling trend since the Mid Eocene Climatic Optimum (Zachos et al. 2008; Cramer et al. 2009). We thus link deposition of DB 2 to a cold contour current caused colder climate conditions as evident from $\delta^{18}O$ records after the Mid Eocene Climatic Optimum (Zachos et al. 2008; Cramer et al. 2009). This also fits to the onset of Antarctic glaciation during the Eocene as deep sea sediment cores at Kerguelen Plateau report terrigenious sediments interpreted as ice rafted debris with ages between 40 Ma – 36 Ma originating from the EAIS (Ehrmann and Mackensen 1992; Zachos et al. 1992). Further it could also be possible that the environmental changes initiating Antarctic glaciations started after the Middle Eocene Climatic Optimum and the Pacific Ocean showed a first response already at ~ 42 - 44 Ma.

6.6.1.3 Evidence for the occurrence of a Proto-DWBC prior to Tasmanian Gateway opening

The interpretation of a Proto-DWBC passing along the eastern flank Zealandia is supported by numerical simulation (Sijp et al. 2011). Their simulation suggests a clockwise circulation with two branches, one passing south and one passing north of Zealandia (Sijp et al. 2011). For the southern limb, deep-sea cores of ODP Leg 189 close to the Tasmanian Gateway confirm the cold water transport. Here, Eocene sediments are dominated by cold water dinocyst/diatom taxa (Huber et al. 2004). As both limbs are part of the same circulation gyre we conclude they transported deep cold water. Figure 6.9 shows the reconstructed positions of Zealandia for the Palaeocene/Eocene boundary (Wobbe et al. 2012) and the simulated flow (Sijp et al. 2011). The cold water also fits with observations of a pre Oligocene East Antarctic Ice Sheet (e.g. Zachos et al. 2001). Glaciation requires cold climate conditions, which favours more deep-water production. The observation of a cold current at the Southwest Pacific Ocean corresponds to the presence of late Eocene Antarctic Glaciation proposed by the global $\delta^{18}O$ isotope curve (Zachos et al. 2008; Cramer et al. 2009) and ice rafted terrigenous debris found in deep sea cores around 40 Ma (Ehrmann and Mackensen 1992; Zachos et al. 1992) A deep cold current with a southern source is also inferred by Hollis et al. (2014) based on a wide spread formation of mudstone enriched in organic carbon content and ^{13}C isotopes. Especially at ODP Site 1121 the appearance of different cold-water taxa indicate a cold bottom current during mid Palaeocene (Hollis 2002; Hollis et al. 2014). This supports to our interpretation of a cold bottom current along the Campbell Plateau slope entering the Outer Bounty Trough where it formed the observed sedimentary drift bodies.

The Campbell Skin Drift south of Campbell Plateau (Fig. 6.1) does not show any current controlled sedimentary structures, which can be explained by the oceanic setting. The Campbell Plateau provides a bathymetric steering for the DWBC and ACC intensifying the flow speeds whereas the Bounty Trough misses such steep flanks favouring lower flow speeds (Carter and Wilkin 1999). This will also have applied to the Proto-DWBC. Stronger flow at the Campbell Plateau slope inhibited deposition whereas inside the Outer Bounty Trough flow speeds were slower due to missing steering bathymetry to create the observed drift bodies DB 1 and DB 2. In addition, depositional features younger than 56

Ma may have been eroded by the onset of the ACC after the opening of the Tasmanian Gateway. At Site 1121 at the Campbell Skin Drift sediments between 56 Ma and 3.26 Ma have been eroded by the vigorous flows during establishment of the ACC and during cooling the since late Miocene (Carter et al. 1999a; Carter et al. 2004a). Thus, any sedimentary structures of the Proto-DWBC may have been destroyed here.

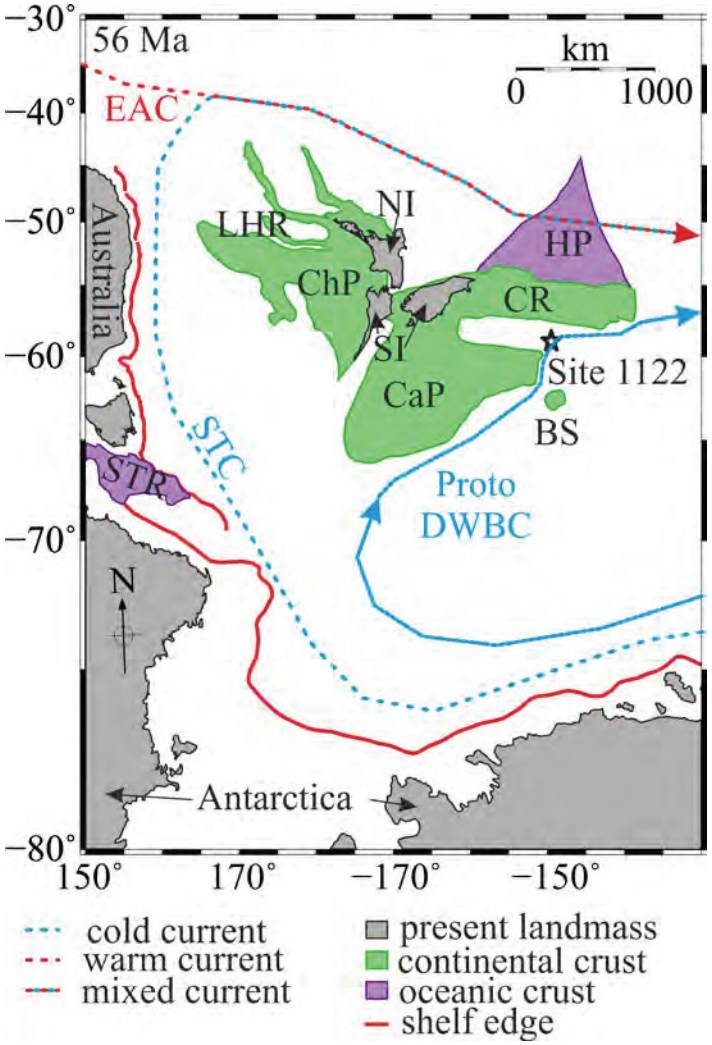

Figure 6.9: Plate tectonic reconstruction of the New Zealand Microcontinent for 56 Ma (modified after Wobbe et al. (2012)) combined with the inferred depth integrated barotropic stream function in the Eocene (Sijp et al. 2011). Abbreviations: BS = Bollons Seamount, CaP = Campbell Plateau, ChP = Challenger Plateau, CR = Chatham Rise, DWBC = Deep Western Boundary Current, EAC = East Australian Current, HP = Hikurangi Plateau, LHR = Lord Howe Rise, NI = North Island, SI = South Island, STC = South Tasmanian Current , STR = South Tasmanian Rise

6.6.2 Circulation pattern since formation of the Marshall Paraconformity (since 33.7 Ma)

Above reflector R4 (Marshall Paraconformity) two sedimentary structures are observed showing the typical upward convex bent reflections of lenticular shape of sediment drifts (Faugères et al. 1999; Faugères and Stow 2008). Additionally, both drifts onlap the palaeoslope, their reflection amplitudes

increase towards the centre of the drift, decrease again to the top of the drift and they both show a pronounced asymmetry. This identifies them as elongated drifts (Lu et al. 2003). We name these structures drift body 3 (DB 3, Figure 6.4a, CDP 66 – 1100 between reflectors R3 and R4) and drift body 4 (DB 4, Figure 6.4a, CDPs 400 – 1900 between reflectors R2a and R3, DB 4). Both drift bodies show typical characteristics for contour currents deposits with a core flow at their south eastern side. ODP Site 1122 cored both sediment drifts confirming their contouritic origin (Carter et al. 1999b). Unfortunately, DB 3 was not completely covered by profile AWI-20110006. As both drift bodies are located above the Marshall Paraconformity (reflector R4) we attribute both drift bodies to activity of the DWBC.

6.6.2.1 Drift body 3 (19.5 Ma - 10.4 Ma)

Below DB 3, the Marshall Paraconformity, reflector R4, clearly indicates a major change in oceanic conditions. Formation of the unconformity is linked to the initiation of the ACC and the DWBC in the Southwest Pacific Ocean (Stickley et al. 2004; Carter et al. 2004b). Due to the erosion associated with these events no sediments were deposited during the Oligocene in the Outer Bounty Trough deposits (Carter et al. 1999b). This is certainly true also for the rest of the area as the Marshall Paraconformity extends over a wide area (see extent of Reflector X in Carter et al. 1994). Following the opening of the Tasmanian Gateway sediment deposition at the Outer Bounty Trough began during the relatively warm climate of the early Miocene (Carter et al. 1999b; Zachos et al. 2001; Carter et al. 2004a). The change in oceanic conditions is observed as drift crest migration from DB 2 to DB 3 (Figure 6.4, CDP 1900 to CDP 500) approximately 35 km to the southeast. Sediment deposition at DB 3 started around 19.5 Ma (upper limit of reflector R4) and has continued under a persistent but variable current, suggested by different pules of well developed winnowing (Carter et al. 1999b; Carter et al. 2004a). This points to distinct pulses of an intensified flow regime of the DWBC. Entirely well-sorted, cold-water sub-/Antarctic diatom taxa point to an erosive cold current (Carter et al. 1999b). The intensification is attributed to the ACC. Such pulses of intensified flow are also observed at Site 1124 (Carter et al. 1999d; Carter et al. 2004a). The end of deposition at DB 3 is marked by a change in colour of sediments, and the biostratigraphy of nannofossils and foraminifers are interpreted as a hiatus in deposition from 10.4 Ma to 5 Ma (Carter et al. 1999b). This hiatus, due to intensified DWBC flow, is correlated to reflector R3. The intensification was likely caused by a more vigorous ACC synchronous to the build-up of the West Antarctic Icesheet (Carter et al. 2004a).

6.6.2.2 Drift body 4 (5 Ma – 1.7 Ma)

Above reflector R3 we observe a further migration of the drift crest. DB 4 has migrated ~25 km to the northwest (Figure 6.4, from CDP 600 to 1600). Sedimentation after the intensified DWBC flow (hiatus associated with reflector R3) started again at ~5 Ma. At this time terrigenous sediment input is still minimal, since the Bounty Channel did not yet extend to the deep sea (Carter et al. 1999b; Carter et al. 2004a). ODP Site 1122 shows DB 4 to be mainly current controlled (fine sand beds with sharp

scoured basal contacts and sharp upper contacts, planar laminations (Carter et al. 1999b)) meaning that these sediments again have been deposited by the DWBC potentially aided by the ACC. Additional support for the contouritic origin is the observed increased detrital chlorite content of sediments at DB 4 (Carter et al. 1999b). This chlorite content is interpreted to have been eroded from the Campbell Skin Drift (Carter et al. 1999b; Carter et al. 2004a). The beginning deposition of DB 4 may have different causes. Either the intensity of the DWBC has decreased or the sediment load of the DWBC has increased so that more tranquil flow conditions in the Outer Bounty Trough favoured deposition. A decrease in current speed of the DWBC is unlikely. The Campbell Skin Drift showed an episode of erosion between 2.2 and 1.8 Ma and an overall sedimentation rate of 1m/myr (Carter et al. 1999a). Additional signs of increased current activity can be found further upstream in the Emerald Basin (Figure 6.1). Here, three different erosional periods have been observed (4 Ma – 3.4 Ma, 2.9 Ma – 2.4 Ma and 2 – 0.8 Ma, (Osborn et al. 1983; Carter et al. 2004a)). This points towards a variable current system with the DWBC and ACC undergoing phases of variable intensity, possibly due to glacial interglacial cycles (Crundwell et al. 2008). A high variability in current speeds is also evident in present day measurements of the DWBC flow at the Campbell Plateau slope with direct influence of the ACC (Stanton and Morris 2004) and north of Chatman Rise without direct ACC influence (Whitworth III et al. 1999). A higher sediment load in combination with lower flow speeds due to the missing steep flanks of the Campbell Plateau at the Outer Bounty Trough (Carter and McCave 1997; Carter and Wilkin 1999) is a preferred explanation for the formation of DB 4. The increased chlorite content of the sediments above reflector R3 is an indication for a sediment origin from the Campbell Skin Drift (Carter et al. 1999a; Carter et al. 1999b). Together with the different erosional surfaces found upstream of the DWBC described above, this indicates a higher sediment load. The geometry of DB 4 classifies it as a plastered drift indicating slow current speeds consistent with this assumption (e.g. Faugères et al. (1999), Faugères and Stow (2008)). These conclusions confirm our interpretation that deposition forming DB 4 is a combination of increased sediment load and lower local flow speeds inside the Bounty Trough area.

DB 4 build-up is divided into two steps. During the first step (below reflector R2b) sedimentation is more or less uniform indicated by the lower amplitude reflections compared to reflections above reflector R2b. Data of ODP Site 1122 confirms this interpretation. Sedimentary rocks below R2b are made up of fine sand beds with sharp scoured basal contacts and sharp upper contacts and uniform sedimentation rate (approx. 25 m/myr (Carter et al. 1999b). Deposits consist almost completely of contourite deposits, also isolated turbidites are a minor component (Carter et al. 1999b). The second step of drift body 4 build-up (above reflector R2b) still shows a lenticular shape of internal reflections typical for a drift body. However, the reflection amplitude increases compared to reflections below reflector R2b. The increase in amplitude coincides with the sporadic occurrence of turbidite deposits (Carter et al. 1999b) (enhanced sedimentation rate to > 100 m/myr (Carter et al. 1999b)). Thus reflector R2b marks the boundary between a constant flow of the DWBC to a more variable current

(Carter et al. 1999b) and contourites are deposited during weaker contour current activity, probably during interglacial stages (Carter et al. 1999b; Crundwell et al. 2008). Deposition at drift body 4 ceased with the deposition of the main turbidites around 1.7 Ma, corresponding to reflector R2a (Carter et al. 1999b).

6.6.2.3 Oceanic conditions since 1.7 Ma

Above drift body 4 a thick wavy sedimentary body (between the seafloor and ~ 380 mbsf or ~ 6.35 s TWT at CDP 700, Figure 6.4) is observed. This body corresponds to seismostratigraphic unit A, characterised by ODP Site 1122 to be mainly of turbidites (Carter et al. 1999b). The observed sediment waves are created by turbidity current overspill of the Bounty Channel levees. Thus, seismostratigraphic unit A does not exhibit any drift bodies that could reveal the history of the DWBC since 1.6 Ma. An exception to this is the almost reflector free zone above reflector R2a (weak amplitude area (w.a.a.) in Figure 6.4, ~ 380 mbsf or 6.35 s TWT and 320 mbsf or ~ 6.25 s TWT (Carter et al. 1999b)) which we call the transitional zone. For this zone, ODP Site 1122 reports a contour current influence on sediment deposition that increased from the top of the zone (~6,25 s TWT, Figure 6.4 CDP 700) down hole. This zone is represented by the lower part of lithological unit Id. Here, Carter et al. (1999b) report abrupt increase in coarser sand and silt beds in lithological unit Id compared to unit IIa below. This part is interpreted as an early stage of Bounty Channel activity (Carter et al. 1999b). Further, we can assume that the reflector free reflection pattern hint on debris flows or slumps and slide deposits (Faugères et al. 1999). Alternatively, this part represents the top of the drift with weaker amplitudes compared to the centre of the drift representing the end of deposition on this drift (Lu et al. 2003). Sediments are normal graded not suggesting any erosive influence of the DWBC (Carter et al. 1999b). Still minimal influence of the DWBC is visible but the drift building core flow is no longer present. We interpret this as another shift in DWBC core flow position. Indeed there is a breach, an erosional structure at the Bounty Channel levee further to the south, which is interpreted as the present core flow position (Carter et al. 1990). The cause of this migration may either be attributed to the onset of the Bounty Channel deposits or to a modification of the oceanic flow conditions. The turbidity currents of the Bounty Channel are rather unlikely to have caused such a shift as they only carried sediments episodically during glacial low stands (Carter et al. 1999b). We rather interpret the migration in core flow position as an indirect or direct influence of the ACC on the DWBC. Multiple researchers have shown the influence of the ACC on the DWBC (e.g. Carter and Wilkin 1999; Morris et al. 2001; Stanton and Morris 2004; McCave et al. 2008). It is also evident that during the early Pleistocene the Emerald Basin and the Tasman Sea showed a hiatus in deposition (Osborn et al. 1983). These hiatuses are attributed to intensified ACC flow due to cooling and reestablishment of the West Antarctic Ice Sheet (Osborn et al. 1983). This intensification also affected the DWBC increasing its power so that it can have formed or enlarged the breach in the Bounty Channel levee reported by Carter et al. (1990).

6.6.3 Implication to the onset of the influence of the DWBC in the Middle Bounty Trough

Presently, a branch of the DWBC (see Figure 6.1a, ochre dots) takes a detour via the Bounty Trough (Carter and McCave 1997). The initiation of this branch is not known. As the DWBC is directly affected by climate as well as topography (e.g. Carter et al. 1999b; Carter et al. 2004a; McCave et al. 2008), climate change may alter the path of this branch. This in turn can have an effect on sediment deposition inside the Bounty Trough. It is important to know whether the DWBC has only sporadic influence during stronger flow periods or a constant influence. Moreover, there information is limited on when the DWBC started to affect sediment deposition in the Bounty Trough as Carter and Carter (1996) sediments have only been surveyed with 3.5 KHz for the modern DWBC effects. Comparing the reflection characteristics of unit B from the Middle Bounty Trough, the Outer Sill Region and the Outer Bounty Trough can help to decipher the onset and duration of DWBC influence. In the Outer Bounty Trough, the reflection characteristics (medium amplitude semi-continuous reflections of lenticular shape, Figure 6.5 CDPs, 66 to 2000) in correlation with results of ODP Site 1122 clearly indicate the contourite origin of the sedimentary sequences correlated with seismostratigraphic unit B. We can trace the defining reflectors R4 and R2a of seismostratigraphic unit B to the west. Here the reflection characteristics change to a more chaotic appearance (Figure 6.6 CDPs 1000 – 4685) indicating slump and slide deposits (Stow and Mayall 2000) or may be due to faulting of Unit B. However we exclude that faulting affected unit B. Faulting, for example by dewatering, should also have affected units A and C as visible by faulting in the Middle Bounty Trough (Uenzelmann-Neben et al. 2009; Davy, personal communication, 2014). As this is not the case, we interpret this as slump or slide deposits. At the base of the Outer Sill slope seismic transparent sections separated by reflectors with small diffraction hyperbolas are observed (Figure 6.4, CDP 3750 to 4956 between reflectors R3 and R2a and Figure 6.6, CDP 66 to 1000 between reflectors R3 and R2a). Such a pattern is typical for debris flow deposits (Faugères et al. 1999). We assume that they originated by slumping and sliding from the Outer Sill slope, that have been triggered by magmatic activity during Miocene (Uenzelmann-Neben et al. 2009). Three small slump or slide deposits can also be identified directly at the base of the Outer Sill ("slump d." in Figure 6.6). Thus possible signs of contourite deposition have been destroyed due to slumping at the Outer Sill slope. However, we can trace reflector R3 (erosional unconformity (Carter et al. (1999b), Figure 6.3) based on unit character on the Outer Sill slope (Figure 6.6, CDP 1000 – 2800) confirming at least a partial influence of the DWBC there. Additionally some sediment between reflectors R3 and R4 are visible as well. We also can identify reflector R3 at the Middle Bounty Trough (Figure 6.6, CDP 3000 – 4685 and Figure 6.7, CDP 66 – 2000). This confirms at least a partial influence of the DWBC inside the Middle Bounty Trough, assuming that in the area covered by our profiles is influenced by the DWBC. Minimum depth is not shallower than 3000 m this is a possible assumption as shallowest extent of the DWBC is limited to 2000 m (Warren 1981; Carter et al. 2004b; McCave et al. 2008). Thus we assume that we can transfer the interpretation of unit B

(contouritic origin by ODP Site 1122 (Carter et al. 1999b)) along our profiles and infer that the DWBC is active inside the Middle Bounty Trough, at least in the area covered by our profiles (Figure 6.1). There is certainly a boundary where the DWBC does not reach further into the Bounty Trough. Seismic data of Uenzelmann-Neben et al. (2009) does not hint on a current entering the Trough from the mouth of Bounty Trough but favours a current coming from the head of the Trough leaving sediment drifts inside unit B, maybe a part of the Southland Current observed by Lu et al. (2003) or a branch of the ACC heading towards the head of Bounty Trough (Neil et al. 2004). However drift bodies of Uenzelmann-Neben et al. (2009) are located in depth of ~2800 m or shallower and the occurrence of unit B on our profiles is below 3000 m. Thus it is possible that the DWBC is overlain by a current from the head of the Bounty Trough that may limit its extent into the Trough. This current is assumed to pass through the Pukaki Saddle (max depth ~ 1500 m (Davey 1977)) and enter the Bounty Trough at least since the last interglacial (e.g. Neil et al. 2004) and also probably before. The Pukaki Saddle limits the maximum depth of this flow and less denser, medium depth water masses are transported by this flow (McCave et al. 2008). This makes it possible that in the deeper regions (deeper than ~3000 m) at mouth of Bounty Trough were influenced by the DWBC, which could have deposited unit B. With the oldest deposits found directly above the Marshall Paraconformity (above reflector R4) it is possible that the DWBC has influenced the Middle Bounty Trough since the formation of the Marshall Paraconformity, whose upper limit is ~19.5 Ma (chapter 4.2).

6.7 Conclusion

High-resolution seismic reflection data of the Bounty Trough, linked with lithological information from ODP Site 1122, enabled a reconstruction of the current and climate regime east of New Zealand. Borehole data, characterised sedimentary rocks below the deposits of the Bounty Channel and fan (seismostratigraphic unit B) to be of contouritic origin. Its is transported by the Deep Western Boundary Current (DWBC). We can trace seismostratigraphic unit B into the Middle Bounty Trough confirming the influence of the DWBC within the Middle Bounty Trough during the Neogene, but the western edge of our profiles limits the extent (~179°E). Thus, the DWBC area of influence appears to be larger than previously assumed and not restricted to the Outer Bounty Trough.

The sedimentary archive of the Outer Bounty Trough has allowed a further reconstruction of the Cenozoic history of deep-water flow at the eastern edge of the New Zealand Microcontinent (Zealandia). Four observed drift bodies in the Outer Bounty Trough present a more complete picture of the influence of palaeoclimate and tectonic events on the (Proto-) DWBC. This includes first evidence for cold deep-water flows before the opening of the Tasmanian Gateway. Drift body 1 and drift body 2 below the Marshall Paraconformity indicate a pre-Oligocene deep circulation east of Zealandia. Build-up of drift body 1 started during the Palaeocene and presumably reflects creation of a deep seaway and current formed by the separation of Zealandia from Antarctica. This deep flow was

probably modified by climate changes during the Eocene, initiating the formation of drift body 2. Timing of drift crest migration coincided with warming during the Mid Eocene Climate Optimum. The next drift crest migration (from drift body 2 to drift body 3) can be linked directly to tectonic processes. The opening of the Tasmanian Gateway has had a major impact of the whole ENZOSS region causing a wide spread erosional event associated with the establishment of the Antarctic Circumpolar Current (ACC). Global cooling along with the establishment of the West Antarctic Ice Sheet interrupted deposition of drift body 3. Deposition started again with the onset of the Pliocene (drift body 4, ~5 Ma). The gentle slope of the Outer Bounty Trough in contrast to the steep flanks of the Campbell Plateau slowed down the DWBC allowing deposition. The last drift crest migration (from drift body 4 to the breach of Carter et al. (1990)) can be attributed to an intensified ACC flow due to cooling during the early Pleistocene recorded in the Emerald - and Tasmanian Basins. The intensification is also evident in the DWBC flow suggesting an indirect influence of the ACC on the DWBC.

6.8 Acknowledgements

We would like to thank Dr. Bryan Davy and a second anonymous reviewer for their helpful comments improving this manuscript. We are grateful for the support of Captain O. Meyer and his crew, as well as Dr. Estella Weigelt, Dr. Jens Grützner and Dietmar Penshorn during cruise SO 213/2 aboard RV *Sonne*. The cruise was funded by the Bundesministerium für Bildung und Forschung under contract number 03G0213A.

6.9 References

Cande, S. C. and J. M. Stock (2004). "Cenozoic Reconstructions of the Austrailia - New Zealand - South Pacific Sector of Antarctica". Published in: The Cenozoic Southern Ocean: Tectonics, Sedimentation, and Climate Change Between Australia and Antarctica. N. F. Exon, J. P. Kennett and M. Malone. Washington, DC, AGU. **151:** 5 - 18. doi:10.1029/gm151

Carter, L., R. M. Carter, et al. (2004a). "Evolution of the sedimentary system beneath the deep Pacific inflow off eastern New Zealand." Marine Geology **205**(1-4): 9-27. doi:10.1016/s0025-3227(04)00016-7

Carter, L., R. M. Carter, et al. (1996a). "Regional sediment recycling in the abyssal Southwest Pacific Ocean." Geology **24**(8): 735-738. doi:10.1130/0091-7613(1996)024<0735:rsrita>2.3.co;2

Carter, L., R. M. Carter, et al. (1990). "Evolution of Pliocene to Recent abyssal sediment waves on Bounty Channel levees, New Zealand." Marine Geology **95**(2): 97-109. doi:10.1016/0025-3227(90)90043-J

Carter, L. and I. N. McCave (1997). "The sedimentary regime beneath the Deep Western Boundary Current inflow to the Southwest Pacific Ocean." Journal of Sedimentary Research **67**(6): 1005-1017. doi:10.1306/d42686b2-2b26-11d7-8648000102c1865d

Carter, L. and J. Wilkin (1999). "Abyssal circulation around New Zealand - a comparison between observations and a global circulation model." Marine Geology **159**(1–4): 221-239. doi:10.1016/S0025-3227(98)00205-9

Carter, R. M. (1988). "Post-breakup stratigraphy of the Kaikoura Synthem (Cretaceous-Cenozoic), continental margin, southeastern New Zealand." New Zealand Journal of Geology and Geophysics **31**(4): 405-429. doi:10.1080/00288306.1988.10422141

Carter, R. M. and L. Carter (1996). "The abyssal Bounty Fan and lower Bounty Channel: evolution of a rifted-margin sedimentary system." Marine Geology **130**(3–4): 181-202. doi:10.1016/0025-3227(95)00139-5

Carter, R. M., L. Carter, et al. (1994). "Seismic stratigraphy of the Bounty Trough, south-west Pacific Ocean." Marine and Petroleum Geology **11**(1): 79-93. doi:10.1016/0264-8172(94)90011-6

Carter, R. M., L. Carter, et al. (1996b). "Current controlled sediment deposition from the shelf to the deep ocean: the Cenozoic evolution of circulation through the SW Pacific gateway." Geologische Rundschau **85**(3): 438-451. doi:10.1007/bf02369001

Carter, R. M., I. N. McCave, et al. (2004b). "1. Leg 181 Synthesis: Fronts, Flows, Drifts, Vocanoes, and the Evolution of the Southwestern Gateway to the Pacific Ocean, Eastern New Zealand". Published in: Proceedings of the Ocean Drilling Programm, Scientific Results. C. Richter. Texas, College Station (Ocean Drilling Program). **181**. doi:10.2973/odp.proc.sr.181.210.2004

Carter, R. M., I. N. McCave, et al. (1999a). "Site 1121: The Campbell "Drift"". Published in: Proceedings of the Ocean Drilling Program, Initial reports:. R. M. Carter, I. N. McCave, C. Richter and L. Carter. Texas, USA, College Station (Ocean Drilling Program). **181:** 1 - 62. doi:10.2973/odp.proc.ir.181.105.2000

Carter, R. M., I. N. McCave, et al. (1999b). "Site 1122: Turbidites with a Contourite Foundation". Published in: Proceedings of the Ocean Drilling Program, Initial reports:. R. M. Carter, I. N. McCave, C. Richter and L. Carter. Texas, USA, College Station (Ocean Drilling Program). **181:** 1 - 146. doi:10.2973/odp.proc.ir.181.106.2000

Carter, R. M., I. N. McCave, et al. (1999c). "Site 1123: North Chatham Drift—a 20-Ma Record of the Pacific Deep Western Boundary Current". Published in: Proceedings of the Ocean Drilling Program, Initial reports:. R. M. Carter, I. N. McCave, C. Richter and L. Carter. Texas, USA, College Station (Ocean Drilling Program). **181:** 1 - 184. doi:10.2973/odp.proc.ir.181.107.2000

Carter, R. M., I. N. McCave, et al. (1999d). "Site 1124: Rekohu Drift—from the K/T Boundary to the Deep Western Boundary Current". Published in: Proceedings of the Ocean Drilling Program, Initial reports:. R. M. Carter, I. N. McCave, C. Richter and L. Carter. Texas, USA, College Station (Ocean Drilling Program). **181:** 1 - 137. doi:10.2973/odp.proc.ir.181.108.2000

Clark, P. U., N. G. Pisias, et al. (2002). "The role of the thermohaline circulation in abrupt climate change." Nature **415**(6874): 863-869. doi:10.1038/415863a

Cook, R. A., R. Sutherland, et al. (1999). "Regional Synthesis". Published in: Cretaceous-Cenozoic geology and petroleum systems of the Great South Basin, New Zealand. A. Sherwood. Lower Hutt, New Zealand, Institute of Geological and Nuclear Sciences monograph**:** 98 - 104.

Cramer, B. S., J. R. Toggweiler, et al. (2009). "Ocean overturning since the Late Cretaceous: Inferences from a new benthic foraminiferal isotope compilation." Paleoceanography **24**(4): PA4216. doi:10.1029/2008pa001683

Crundwell, M., G. Scott, et al. (2008). "Glacial–interglacial ocean climate variability from planktonic foraminifera during the Mid-Pleistocene transition in the temperate Southwest Pacific, ODP Site 1123." Palaeogeography, Palaeoclimatology, Palaeoecology **260**(1–2): 202-229. doi:10.1016/j.palaeo.2007.08.023

Davey, F. J. (1977). "Marine seismic measurements in the New Zealand region." New Zealand Journal of Geology and Geophysics **20**(4): 719-777. doi:10.1080/00288306.1977.10430730

Davy, B. (1993). "The Bounty Trough—Basement Structure Influences on Sedimentary Basin Evolution". Published in: South Pacific sedimentary basins. P. F. Ballance, Elsevier**:** 69-92.

Davy, B. (2006). "Bollons Seamount and early New Zealand–Antarctic seafloor spreading." Geochemistry, Geophysics, Geosystems **7**(6): Q06021. doi:10.1029/2005gc001191

Eagles, G., K. Gohl, et al. (2004). "High-resolution animated tectonic reconstruction of the South Pacific and West Antarctic Margin." Geochemistry Geophysics Geosystems **5**(7): Q07002. doi:10.1029/2003gc000657

Edwards, A. R. (1973). "20. Southwest Pacific Regional Unconformities Encountered during Leg 21". Published in: Initial Reports of the Deep Sea Drilling Project. T. A. Davies. Washington, D.C., US Governmental Printing Office. **21:** 701 - 720. doi:10.2973/dsdp.proc.21.120.1973

Ehrmann, W. U. and A. Mackensen (1992). "Sedimentological evidence for the formation of an East Antarctic ice sheet in Eocene/Oligocene time." Palaeogeography, Palaeoclimatology, Palaeoecology **93**(1–2): 85-112. doi:10.1016/0031-0182(92)90185-8

Erickson, S. N. and R. D. Jarrard (1998). "Velocity-porosity relationships for water-saturated siliciclastic sediments." Journal of Geophysical Research: Solid Earth **103**(B12): 30385-30406. doi:10.1029/98jb02128

Exon, N. F., J. P. Kennett, et al. (2001). "Leg 189 Summary". Published in: Proccedings of the Ocean Drilling Program, Initial Reports. J. M. Scroggs. Texas, College Station (Ocean Drilling Program). **189:** 1 - 98. doi:10.2973/odp.proc.ir.189.101.2001

Faugères, J. C. and D. A. V. Stow (2008). "Chapter 14 Contourite Drifts: Nature, Evolution and Controls". Published in: Developments in Sedimentology. M. Rebesco and A. Camerlenghi. Amsterdam, Elsevier Science**:** 257 – 288. doi:10.1016/S0070-4571(08)10014-0

Faugères, J. C., D. A. V. Stow, et al. (1999). "Seismic features diagnostic of contourite drifts." Marine Geology **162**(1): 1-38. doi:10.1016/s0025-3227(99)00068-7

Friedrich, O., R. D. Norris, et al. (2012). "Evolution of middle to Late Cretaceous oceans—A 55 m.y. record of Earth's temperature and carbon cycle." Geology **40**(2): 107-110. doi:10.1130/g32701.1

Fulthorpe, C. S., R. M. Carter, et al. (1996). "Marshall Paraconformity: a mid-Oligocene record of inception of the Antarctic circumpolar current and coeval glacio-eustatic lowstand?" Marine and Petroleum Geology **13**(1): 61-77. doi:10.1016/0264-8172(95)00033-X

Grobys, J. W. G., K. Gohl, et al. (2007). "Is the Bounty Trough off eastern New Zealand an aborted rift?" Journal of Geophysical Research: Solid Earth **112**(B3). doi:10.1029/2005JB004229

Hall, I. R., L. Carter, et al. (2002). "Major depositional events under the deep Pacific inflow." Geology **30**(6): 487-490. doi:10.1130/0091-7613(2002)030<0487:mdeutd>2.0.co;2

Hall, I. R., I. N. McCave, et al. (2003). "Paleocurrent reconstruction of the deep Pacific inflow during the middle Miocene: Reflections of East Antarctic Ice Sheet growth." Paleoceanography **18**(2): 1040. doi:10.1029/2002pa000817

Hollis, C. J. (2002). "Biostratigraphy and paleoceanographic significance of Paleocene radiolarians from offshore eastern New Zealand." Marine Micropaleontology **46**(3–4): 265-316. doi:10.1016/S0377-8398(02)00066-X

Hollis, C. J., M. J. S. Tayler, et al. (2014). "Organic-rich sedimentation in the South Pacific Ocean associated with Late Paleocene climatic cooling." Earth-Science Reviews **134**(0): 81-97. doi:10.1016/j.earscirev.2014.03.006

Huber, M., H. Brinkhuis, et al. (2004). "Eocene circulation of the Southern Ocean: Was Antarctica kept warm by subtropical waters?" Paleoceanography **19**(4): PA4026. doi:10.1029/2004pa001014

Joseph, L. H., D. K. Rea, et al. (2004). "Neogene history of the Deep Western Boundary Current at Rekohu sediment drift, Southwest Pacific (ODP Site 1124)." Marine Geology **205**(1-4): 185-206. doi:Doi: 10.1016/s0025-3227(04)00023-4

Kennett, J. P., R. E. Houtz, et al. (1975). "44. Cenozoic paleoceanography in the southwest Pacific Ocean, Antarctic glaciation, and the development of the Circum-Antarctic Current". Published in: Initial Reports of the Deep Sea Drilling Project. S. M. White. Washingtion, DC, US Government Priniting Office. **29:** 1155-1169. doi:10.2973/dsdp.proc.29.144.1975

Kennett, J. P., C. C. von der Borch, et al. (1986). "Site 594: Chatham Rise". Published in: Initial Reports of the Deep Sea Drilling Project. J. P. Kennett, C. C. van der Borch and J. H. Blakeslee. Washington DC, US Governmental Printing Office. **90:** 653 - 744. doi:10.2973/dsdp.proc.90.110.1986

Kuhlbrodt, T., A. Griesel, et al. (2007). "On the driving processes of the Atlantic meridional overturning circulation." Reviews of Geophysics **45**(2): RG2001. doi:10.1029/2004rg000166

Lebrun, J.-F., G. Lamarche, et al. (2003). "Subduction initiation at a strike-slip plate boundary: The Cenozoic Pacific-Australian plate boundary, south of New Zealand." Journal of Geophysical Research: Solid Earth **108**(B9): 2453. doi:10.1029/2002jb002041

Lu, H., C. S. Fulthorpe, et al. (2003). "Three-dimensional architecture of shelf-building sediment drifts in the offshore Canterbury Basin, New Zealand." Marine Geology **193**(1–2): 19-47. doi:10.1016/S0025-3227(02)00612-6

Marshall, P. (1911). "New Zealand and Adjacent Islands". Published in: Handbuch der regionalen Geologie. G. Steinmann and O. Wilckens. Heidelberg, C. Winter's Universitätsbuchhandlung**:** 78.

McCave, I. N., L. Carter, et al. (2008). "Glacial–interglacial changes in water mass structure and flow in the SW Pacific Ocean." Quaternary Science Reviews **27**(19–20): 1886-1908. doi:10.1016/j.quascirev.2008.07.010

Morris, M., B. Stanton, et al. (2001). "Subantarctic oceanography around New Zealand: Preliminary results from an ongoing survey." New Zealand Journal of Marine and Freshwater Research **35**(3): 499-519. doi:10.1080/00288330.2001.9517018

Neil, H. L., L. Carter, et al. (2004). "Thermal isolation of Campbell Plateau, New Zealand, by the Antarctic Circumpolar Current over the past 130 kyr." Paleoceanography **19**(4): PA4008. doi:10.1029/2003pa000975

Osborn, N. I., P. F. Ciesielski, et al. (1983). "Disconformities and paleoceanography in the southeast Indian Ocean during the past 5.4 million years." Geological Society of America Bulletin **94**(11): 1345-1358. doi:10.1130/0016-7606(1983)94<1345:dapits>2.0.co;2

Senske, D. A. and R. A. Stephen (1988). A Seismic-Reflection Survey of DSDP Sites 417 and 418. Proceedings of the Ocean Drilling Program, Scientific Results. M. H. Salisbury and J. H. Scott. Texas, College Station (Ocean Drilling Program). **102:** 3 - 17. doi:10.2973/odp.proc.sr.102.116.1988

Sijp, W. P., M. H. England, et al. (2011). "Effect of the deepening of the Tasman Gateway on the global ocean." Paleoceanography **26**(4): PA4207. doi:10.1029/2011pa002143

Smith, W. H. F. and D. T. Sandwell (1997). "Global Sea Floor Topography from Satellite Altimetry and Ship Depth Soundings." Science **277**(5334): 1956 – 1962. doi:10.1126/science.277.5334.1956

Stanton, B. R. and M. Y. Morris (2004). "Direct velocity measurements in the Subantarctic Front and over Campbell Plateau, southeast of New Zealand." Journal of Geophysical Research: Oceans **109**(C1): C01028. doi:10.1029/2002jc001339

Stickley, C. E., H. Brinkhuis, et al. (2004). "Timing and nature of the deepening of the Tasmanian Gateway." Paleoceanography **19**(4): PA4027. doi:10.1029/2004pa001022

Stocker, T. F. (2000). "Past and future reorganizations in the climate system." Quaternary Science Reviews **19**(1–5): 301-319. doi:10.1016/S0277-3791(99)00067-0

Stow, D. A. V., J.-C. Faugères, et al. (2002). "Bottom currents, contourites and deep-sea sediment drifts: current state-of-the-art". Published in: Deep-water contourite systems: Modern drifts and ancient series. D. A. V. Stow, C. J. Pudsey, J. A. Howe, J.-C. Faugères and A. R. Viana. London, Geological Society of London. **22:** 7 - 20. doi:10.1144/GSL.MEM.2002.022.01.02

Stow, D. A. V. and M. Mayall (2000). "Deep-water sedimentary systems: New models for the 21st century." Marine and Petroleum Geology **17**(2): 125-135. doi:10.1016/s0264-8172(99)00064-1

Tiedemann, R., J. O'Conner, et al. (2012). Cruise Report SO213: SOPATRA. Bremerhaven, Alfred Wegener Institute, Helmholtz Centre for Polar and Marine Research**:** 111.

Tucholke, B. E. (1979). "Relationships Between Acoustic Stratigraphy and Lithostratigraphy in the Western North Atlantic Basin". Published in: Initial Reports of the Deep Sea Drilling Project. A. Kaneps. Washingtion, D.C., US Governmental Printing Office. **43:** 827 - 846. doi:10.2973/dsdp.proc.43.141.1979

Uenzelmann-Neben, G. and K. Gohl (2012). "Amundsen Sea sediment drifts: Archives of modifications in oceanographic and climatic conditions " Marine Geology **299-302**: 51-62. doi:10.1016/j.margeo.2011.12.007

Uenzelmann-Neben, G., J. W. G. Grobys, et al. (2009). "Neogene sediment structures in Bounty Trough, eastern New Zealand: Influence of magmatic and oceanic current activity." Geological Society of America Bulletin **121**(1-2): 134-149. doi:10.1130/b26259.1

van Aken, H. M. (2007). "The Oceanic Thermohaline Circulation: An Introduction". New York, Springer Science and Business Media, LLC.

Warren, B. A. (1973). "Transpacific hydrographic sections at lats. 43°S and 28°S: the SCORPIO expedition—II. deep water." Deep Sea Research and Oceanographic Abstracts **20**(1): 9-38. doi:10.1016/0011-7471(73)90040-5

Warren, B. A. (1981). "Deep circulation of the world ocean". Published in: Evolution of physical oceanography. B. A. Warren and C. Wunsch, MIT Press, Caimbridge, Ma**:** 6-41.

Whitworth III, T., B. A. Warren, et al. (1999). "On the deep western-boundary current in the Southwest Pacific Basin." Progress In Oceanography **43**(1): 1-54. doi:10.1016/S0079-6611(99)00005-1

Wobbe, F., K. Gohl, et al. (2012). "Structure and breakup history of the rifted margin of West Antarctica in relation to Cretaceous separation from Zealandia and Bellingshausen plate motion." Geochemistry, Geophysics, Geosystems **13**(4): Q04W12. doi:10.1029/2011gc003742

Zachos, J. C., J. R. Breza, et al. (1992). "Early Oligocene ice-sheet expansion on Antarctica: Stable isotope and sedimentological evidence from Kerguelen Plateau, southern Indian Ocean." Geology **20**(6): 569-573.

Zachos, J. C., G. R. Dickens, et al. (2008). "An early Cenozoic perspective on greenhouse warming and carbon-cycle dynamics." Nature **451**(7176): 279-283. doi:doi: 10.1038/nature06588

Zachos, J. C., M. Pagani, et al. (2001). "Trends, Rhythms, and Aberrations in Global Climate 65 Ma to Present." Science **292**: 686-693. doi:10.1126/science.1059412

7. The spatial extent of the Deep Western Boundary Current into the Bounty Trough: New evidence from Parasound Sub-Bottom Profiling

Michael Horn and Gabriele Uenzelmann-Neben

7.1 Abstract

Deep currents such as the Pacific Deep Western Boundary Current (DWBC) are strengthened periodically in Milankovitch cycles. We studied periodic fluctuations in reflection pattern and reflector amplitude in order to detect cycles in the sedimentary layers. Inside the Bounty Trough area, east of New Zealand, the occurrence of the obliquity frequency is only caused by the DWBC. Therefore, it provides direct evidence for the spatial extent of the DWBC. We can confirm the extent of the DWBC west of the Outer Sill, previously only inferred by erosional features at the Outer Sill. Further our data allows an estimation of the extent of the DWBC into the Bounty Trough, limiting the DWBC presence to east of 178.15°E.

Key words: Parasound sub-bottom profiler, Milankovitch cycles, Deep Western Boundary Current (DWBC), Bounty Trough

Key Points:

- Milankovitch cycles revealed in sub-bottom profiler data by spectral analysis
- Inflow area of the DWBC illustrated by the 41 kyr Milankovitch cycle
- Confirmation that DWBC is present in Bounty Trough area

7.2 Introduction

Thermohaline Circulation is well known to influence global climate and vice versa (e.g. Clark et al. 2002; Kuhlbrodt et al. 2007). One of its components is the Pacific Deep Western Boundary Current (DWBC, Figure 7.1a), the largest deep inflow to the Southwest Pacific Ocean (35 – 40 % of volume transport of deep cold water (e.g. McCave et al. 2008)). Further downstream the DWBC passes along the margin of the New Zealand microcontinent (now referred to as Zealandia). Here, it passes along the steep flanks of the Campbell Plateau until reaching the Bounty Trough. The Bounty Trough cuts into the high relief of Campbell Plateau and Chatham Rise (Figure 7.1b). The upper part of the sedimentary cover at the mouth of Bounty Trough is extensively eroded indicating the presence of the DWBC (Carter and McCave 1997). Extrapolation of seismic units, as defined at ODP Site 1122, into the Bounty Trough has suggested the presence of the DWBC inside the Bounty Trough since about 19.5 Ma. Further the data show that around 1.7 Ma the core flow position shifted to the south (Horn and Uenzelmann-Neben 2014) contemporaneously with an intensification of the DWBC due to global cooling (Osborn et al. 1983). Thus it is uncertain whether the DWBC has continued to be active further inside the Bounty Trough during the late Pleistocene or whether its influence has been limited to east of the Outer Sill.

The upper 400 meters of sedimentary cover inside the Bounty Trough consists of sediments from two different sources. The first source are the New Zealand's South Island riverine sediments transported onwards as turbidity currents via the Bounty Channel into the Bounty Trough. Sediments of turbiditic origin from the Bounty Channel are only deposited during glacial sea level low stands (Carter et al. 2004a; Carter et al. 2004b). These low stands occurred approximately every 100 kyrs during the last 800 kyrs, representing Milankovitch cycles caused by eccentricity (95 kyr - 125 kyr, e.g. Zachos et al. 2001; Miller et al. 2005). The second sediment source is of hemi-/pelagic origin from the water column (Carter et al. 1999b; Carter et al. 2004b) either carried or at least influenced by the DWBC. The DWBC itself shows cyclic variations at the obliquity and eccentricity cycles due to periodic reinforcement of the Antarctic Circumpolar Current (expressed by ODP Site 1123Hall et al. 2001; Crundwell et al. 2008). Thus the occurrence of the obliquity cycle (41 kyr duration) is unique for the sediments deposited under the influence of the DWBC in the Bounty Trough area and is not found in sediments originating from other sources such as the turbidity currents of the Bounty Channel.

Therefore, the presence of specific Milankovitch cycles, i.e. 41 kyr, can be interpreted as an indication for an active influence of the DWBC on Bounty Channel deposits. Here we use the occurrence of specific Milankovitch frequencies in sub-bottom profiler data to reveal the influence of the DWBC on the sedimentary deposits of the Bounty Channel levee. By converting the two way traveltime (TWT) into age using an age-depth model of a deep-sea borehole we can correlate seismic reflections to age and corresponding Milankovitch frequencies. With these data we can show that the DWBC has been present within the Bounty Trough since 1.7 Ma and we can estimate its spatial variability throughout the last 800 kyrs.

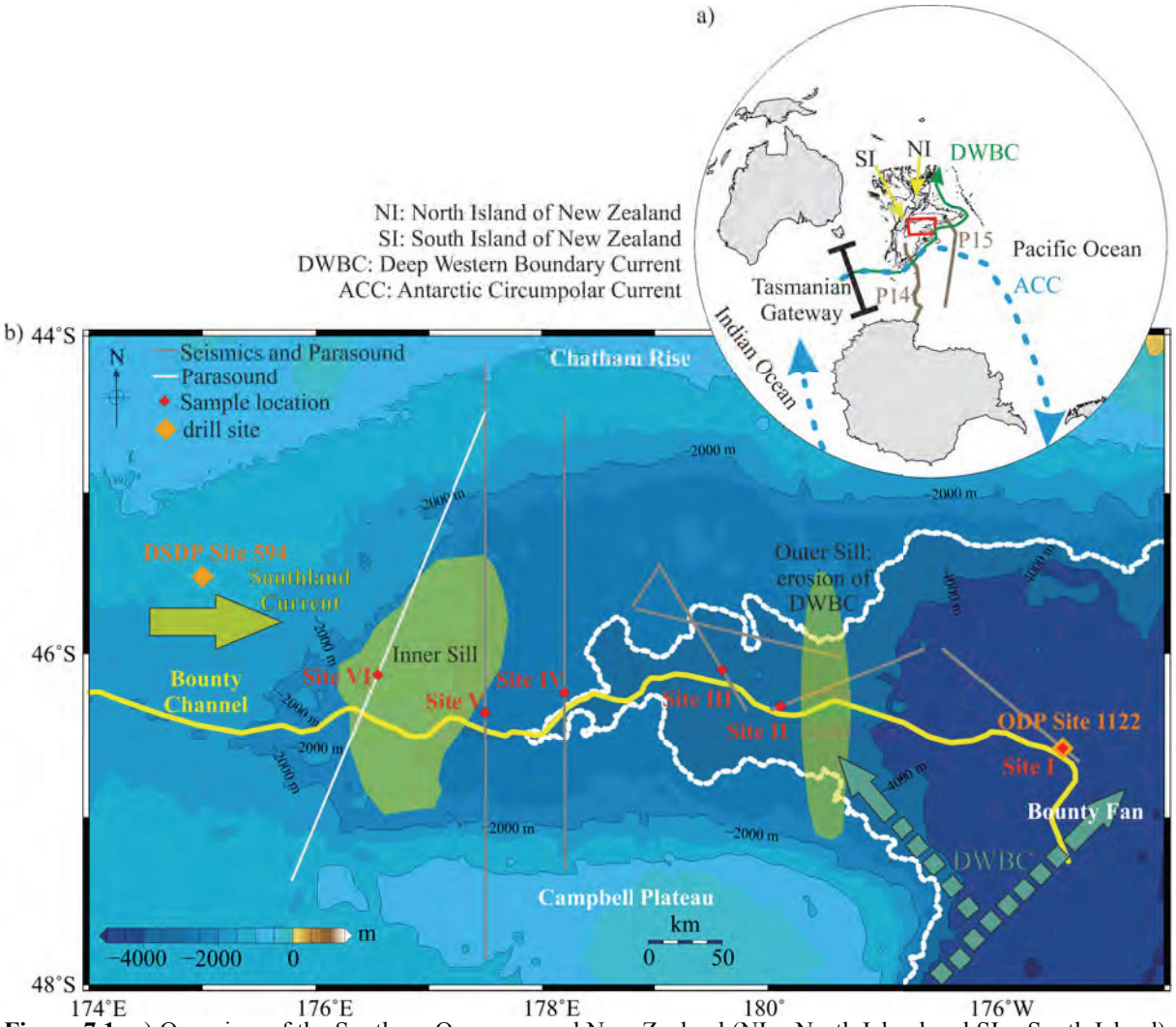

Figure 7.1: a) Overview of the Southern Ocean around New Zealand (NI = North Island and SI = South Island). Black lines indicate the contour lines (every 1000 meters) of the GEBCO_08 grid every 500 meters (Smith and Sandwell 1997), while the blue and dashed arrows indicate the flow paths of the Antarctic Circumpolar Current (ACC) and the green arrows indicate the flow of the Pacific Deep Western Boundary Current (DWBC). Available hydrographic profiles of the World Ocean Circulation Experiment P14 and P15 (Talley 2007) are marked in brown. Ocean Drilling Program (ODP) Site 1123 is marked as orange diamond. **b)** Enlarged map of the Bounty Trough area. Deep-sea core sites from the Ocean Drilling Program (ODP) and Deep Sea Drilling Project (DSDP) are indicated by orange diamonds, sample locations from Site I to Site VI are indicated by red Diamonds. Grey Lines indicate Parasound profiles used for this analysis. White dotted line represents the inferred extent of the DWBC from our analysis. The yellow line marks the axis of the Bounty Channel.

7.3 Regional and tectonic setting

The Bounty Trough, east of South Island (New Zealand, Figure 7.1), is a failed rift arm formed during the Cretaceous. It is situated in thinned continental crust between the Chatham Rise in the north and the Campbell Plateau in the south (Grobys et al. 2007). The Bounty Trough is separated into three different zones by two basement highs showing a significantly greater slope than the surrounding seafloor (Davy 1993). These steps are termed the Inner Sill and Outer Sill (Carter et al. 1994 , Figure 7.1).

7.3.1 Oceanic setting of the Bounty Trough since the Pleistocene

According to Carter et al. (2004a) the general flow path of the DWBC in the Bounty Trough region is almost unchanged since the early Pliocene (~5000 ka), but changes in strengths occurred due to climate effects. We thus assume the present oceanic regime also existed during the Plio-/Pleistocene.

The main oceanic influence at the Bounty Trough area close to the Outer Sill results from the DWBC, which enters the area from the south passing along the Campbell Plateau at the base of the Outer Sill (e.g. Carter and McCave 1997; McCave et al. 2008). Before reaching the Bounty Trough area the DWBC is accompanied by the Antarctic Circumpolar Current (ACC) (south of ~45°S) which has an active influence on flow speed of the DWBC (e.g. Carter et al. 2004b; Crundwell et al. 2008). Compared to warm stages cold glacial periods show intensified winds and ACC flow (McCave et al. 2008). As the ACC directly influences the DWBC the DWBC flow can be expected to have varied similarly (McCave et al. 2008). According to Hall et al. (2001) and Crundwell et al. (2008) these reinforcements of the DWBC correlate with to orbital Milankovitch frequencies. The 41 kyr obliquity cycle in the sediments of ODP Site 1123 has been especially pronounced during the last 1200 kyrs, together with the eccentricity cycles (95 kyr, 125 kyr), as revealed by proxies ($\delta\ ^{18}O$, SST_{ANN-25}) of benthic foraminifers (Crundwell et al. 2008).

The DWBC actively influences sedimentary deposits in its flow path. Examples are a breach in the northern Bounty Channel Levee marking the main core flow of the DWBC (Carter et al. 1990) or the sediment deposition at the Bounty Fan (Carter and Carter 1996). The influence of the DWBC is not limited to the Bounty Fan deposits. The sedimentary cover of the Outer Sill shows erosion of the upper sedimentary unit indicating a vigorous DWBC in recent times. From this area of erosion, a limb of the DWBC is proposed entering the Bounty Trough (Carter and McCave 1997), but its extent is not known. This in turn can influence the shallower flows above the DWBC and may thus affect New Zealand climate conditions.

7.3.2 Sediment supply into the Bounty Trough since the Pleistocene

The Bounty Trough contains a transport system for terrigenous sediments, the Bounty Channel (Carter et al. 2004a; Carter et al. 2004b). Sediment transport in the channel and related deposition started already during the Pliocene (~3.5 Ma) and was fully established by ~ 2.2 Ma (Carter et al. 1999b). Sediments were derived from erosion of the Southern Alps. Rivers transported the sediments to the shelf edge, where they were injected into offshore currents (Carter et al. 1999b; Carter et al. 2004b). During sea-level high stands turbidity currents bypassed the head of the Bounty Trough and were transported via the Southland Current into the Hikurangi Channel (Carter et al. 2004b). At sea level low stands during glacial periods terrigenous sediments reached the deep sea and were deposited as turbidites inside the Bounty Trough and on the Bounty Fan (Carter et al. 1994; Carter et al. 1999b; Carter et al. 2004b). Deposits can be observed as two levees, the northern levee (in flow direction left) being higher than the southern levee due to Coriolis force. Since the Mid Pleistocene Transition (~ 800

ka) the sea level low stands occurred roughly with a 100 kyr frequency (e.g Zachos et al. 2001; Crundwell et al. 2008; Naish et al. 2009). We thus would expect pulses of sediments, which show a cyclicity of roughly 100 kyrs. Further sediment sources for the Bounty Trough area are hemi-/pelagic sediments from the water column. The DWBC itself also transports sediments but no bottom current deposits during the Pleistocene have been reported (Carter et al. 2004b). The upper sedimentary column is primarily dominated by terrigenous sediments interbedded with hemi-/pelagic sediments (e.g. Carter et al. 1994; Carter et al. 1999b).

7.4 Materials and methods

7.4.1 Available data and data processing

Our study is based on sub-bottom profiles acquired during RV Sonne cruises 169 (Gohl 2003) and 213/2 (Ronge et al. 2013) with an Atlas Parasound P70 system. The Atlas Parasound transducer transmits two different frequencies between 18 and 33 kHz and a parametric frequency due to nonlinear interaction of finite amplitudes in the water (Atlas Hydrographic GmbH 2010; Tiedemann et al. 2012). During both cruises this parametric frequency was adjusted to 4 kHz. This paper will use the 4 kHz parametric frequency data, an excerpt of such a profile is shown in Figure 7.2. The 4 kHz signal penetrates deeper into the sedimentary column (up to 200 m, Atlas Hydrographic GmbH 2010) than the other two frequencies. Onboard processing included subtraction of the average amplitude to remove the DC Offset (bias). Further the envelope function of the signal was calculated to increase the coherency of the signal and to reduce disk space needed. We have applied an additional bandpass filtering between 2 kHz and 6 kHz to reduce noise. Evaluation of the occurrence of the DWBC is based on six profiles crossing the Bounty Channel northern levee (Figure 7.1).

7.4.2 Method to reveal Milankovitch cycles in sub-bottom profiler data

We adapt the method of Weigelt and Uenzelmann-Neben (2007) to analyze the occurrence of Milankovitch cycles in our sub-bottom profiler data. According to these authors, Milankovitch cycles can also be revealed within seismic reflection data. To achieve this, first the TWT of the signal must be converted into depth and then into age. This is achieved by using P-wave velocity functions and sedimentation rates, normally derived from bore holes (Weigelt and Uenzelmann-Neben 2007).

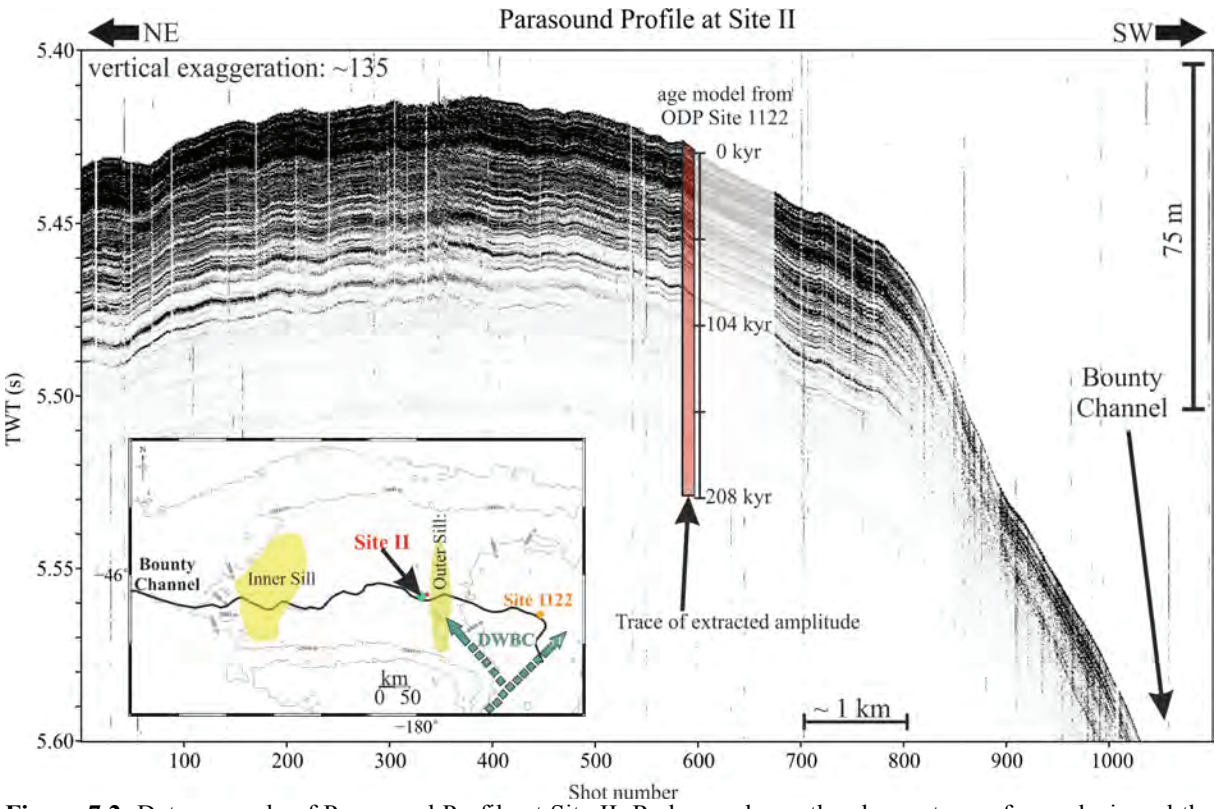

Figure 7.2: Data example of Parasound Profile at Site II. Red area shows the chosen traces for analysis and the corresponding ages as calculated from the sedimentation rate derived from the Ocean Drilling Program (ODP) Site 1122 (Carter et al. 1999b).

To evaluate the frequency spectra we have chosen six different locations along the Bounty Channel axis, each at the crest of the northern levee where a high sedimentation rate prevailed during the Pleistocene (Figure 7.1). The first location (Site I) was chosen at the location of ODP Site 1122 to have a direct connection to the age and velocity models for Site 1122. Conversion of TWT into depth was done by using the sonic velocity calculated from depth samples for the upper sedimentary column (Horn and Uenzelmann-Neben 2014). The subsequent conversion from depth to age was adapted from the age-depth model of ODP Site 1122, giving a sedimentation rate of 38 cm/kyr for the upper sedimentary column (Carter et al. 1999b). In addition to this location five other locations (Site II to Site VI, Figure 7.1) were chosen to evaluate whether the spectrum shows prominent peaks at Milankovitch frequencies. For Sites II and III the same age-depth model and velocity profile were used as for Site I. Sites IV to VI are too far away from ODP Site 1122 to be treated in the same manner. For depth conversion a constant interval velocity of 1550 m/s was used there. Sedimentation rates were set to 20 cm/kyr for location IV, 10 cm/kyr for locations V and 8.5 cm/kyr for Site VI. Sedimentation rates for sites IV and V are calculated based on the depth below sea floor of a specific reflector on seismic reflection data acquired contemporaneously. This reflector represents the Lower Pleistocene of the depth converted seismic reflection data (Uenzelmann-Neben et al. 2009). Site VI was not crossed by seismic reflection data. Sedimentation rate for this location was taken from an old core in the upper Bounty Trough where the highest sedimentation rate was measured to be 8.5 cm/kyr (Griggs et al. 1983).

As we do not use seismic reflection but sub-bottom profiler data differences in resolution and depth penetration have to be taken into account. One critical point is the resolution of Milankovitch cycles with seismic methods. The used setup is capable of penetrating up to 200 meters of unconsolidated sediment (Atlas Hydrographic GmbH 2010). Typical penetration depth achieved is 50 - 150 meters. Sedimentation rates for the area of interest are between 8.5 cm/kyr to 38 cm/kyr. Depending on location and sedimentation rates age ranges of 120 kyr up to 1500 kyr. The frequency (4 kHz) allows a vertical resolution of approximately 10 cm at the seafloor thus theoretically resolving 0.23 kyrs. Uncertainties arise from conversion from TWT to depth and than to age. While the uncertainty by conversion from TWT to depth can be neglected (< 3 % based on a velocity variation of 50 m/s and a TWT uncertainty of 0.001 ms)) error of sedimentation rate plays an important role. For sites I to III the sedimentation rate of 0.38 m/kyr (constant for the first 300 meters) is taken (Carter et al. 1999b). Unfortunately no age error is given, therefor we assume a large uncertainty range of 20 percent. We have chosen this large range to account for errors made during age estimation and to take into account that we use a linear sedimentation rate for the whole lower Pleistocene. For Site IV to V, the sedimentation rate is calculated from depth migrated seismic reflection data (Uenzelmann-Neben et al. 2009). Difference between seafloor and the Lower Pleistocene reflection have been picked from seismic data. This can be done with high accuracy (up to 1 meter) but we will also assume an uncertainty range of 20 percent as we use only one horizon for this estimation and data was converted using picked velocities. The sedimentation rate for site VI is taken from Griggs et al. (1983). We will assume an error of 20% (analogue to ODP Site 1122 age model) as no age error is given. Thus this uncertainty is transferred to the age of different reflections and the theoretical age resolution of 0.23 kyrs cannot be achieved. The finest resolution achievable is thus assumed to be 8.2 kyrs (obliquity) to 20 kyrs (Bounty Channel cyclicity) depending on cycle length. These error ranges are still small enough to get two differentiated peaks around both frequencies.

Calculations were carried out using the spreadsheet application IGOR Pro 5. For Fourier transformation we used the embedded method of Cooley and Tukey (1965).

7.5 Observations

We infer an active influence of the DWBC on deposition at Site I (approx. 4400 m water depth) based on hydrographical findings (Warren 1973; Reid 1997), sediment cores and profiler data (Carter and Carter 1996). Here (Figure 7.3, green curve) a peak around the frequency of $24 * 10^{-3} kyr^{-1}$ (41 kyr obliquity cycle) can be identified. Its width corresponds to the uncertainties of the age-depth model (8.2 kyrs grey area, Figure 7.3) used for the conversion. A spectral peak at a frequency of $10 * 10^{-3} \frac{1}{kyr}$ (100 kyrs cycle) can also be observed.

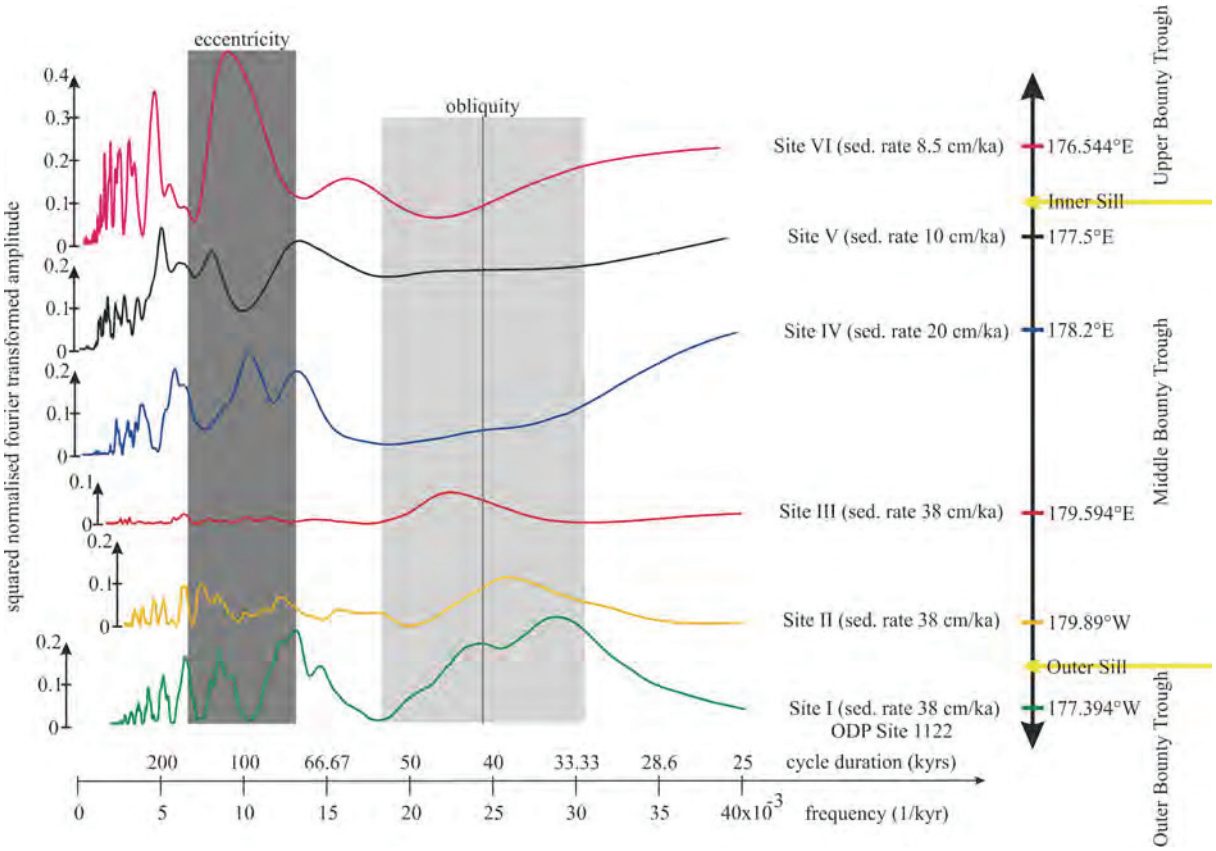

Figure 7.3: Spectral analysis of the Site I (lowermost) to Site VI (uppermost). The grey areas indicate the uncertainty ranges for the obliquity cycle and the range of the eccentricity cycle of the frequency bands.

The other investigated sites have been chosen west of the Outer Sill. Site II (approx. 3400 meters water depth, yellow in Figure 7.3) and Site III (approx. 3200 meters water depth, red in Figure 7.3) are located close to the Outer Sill. Both Site II and Site III show a frequency peak near $24 * 10^{-3} kyr^{-1}$ well inside the error margin of 10 kyrs (grey area in Figure 7.3). Site II shows no pronounced peak at a frequency of $10 * 10^{-3} kyr^{-1}$ (100 kyrs) while frequencies lower than $15 * 10^{-3} kyr^{-1}$ almost completely absent at Site III. Site IV (blue in Figure 7.3) is located at approximately 2800 meters depth. Here different frequencies appear. A first frequency peak is observed around $13 * 10^{-3} kyr^{-1}$ and a second around $10 * 10^{-3} kyr^{-1}$. Higher frequencies, especially the obliquity frequency of $24 * 10^{-3} kyr^{-1}$, are not observed. Site V at 2700 meters water depth (black in Figure 7.3) shows a similar pattern to Site IV. The first peak also is observed at ~ $13 * 10^{-3} kyr^{-1}$ and a second peak at a lower frequency of approximately $8 * 10^{-3} kyr^{-1}$ (~125 kyr cycle length). Site VI at approximately 2500 m water depths is the most western site of our analysis. Here, the main frequency peak is around $10 * 10^{-3} kyr^{-1}$ (100 kyr cycle) and the peak around $13 * 10^{-3} kyr^{-1}$ almost disappears compared to Sites IV and V. Sites IV to VI exhibit a second peak between 5 to 6 $* 10^{-3} kyr^{-1}$. These peaks represent cycle lengths of approximately double the length of 100 kyrs cycles.

7.6 Discussion

7.6.1 Resolution of cycles

Our main goal is to use Parasound sub-bottom profiler data to resolve the presence of the 41 kyr obliquity cycle. Thus, we have to make sure our data can resolve these cycles. Three important parameters are crucial for a cycle to be resolved, (1) minimum vertical resolution, (2) the sampled interval of sub bottom profiler data and (3) the accuracy of the age-depth model.

(1) Vertical resolution is limited by the used frequency of the Parasound system. To fulfill the Nyquist criterion two different reflective horizons have to be spaced of at least 10 cm apart to be recognized as individual events. With sedimentation rates between 8.5 cm/kyr and 38 cm/kyr, 41 kyrs are represented by sedimentary deposits of ~ 3.5 m, thus meeting the Nyquist criterion of 10 cm.

(2) The imaged interval has to be long enough to incorporate at least two full cycles of the cyclicity we want to observe. For the specific example of the 41 kyr obliquity cycle we need an age range of more than 82 kyrs penetrated by sub bottom profiler data. This is fulfilled at all six sites as the minimum age range imaged is ~ 100 kyrs at Site I. All other sites exhibit at least 170 kyrs of age range and can contain four full cycles or more.

(3) The uncertainties in the age-depth models used for age conversion are also a source of discrepancies. In our case uncertainties are estimated to be 20% of the age value. This uncertainty range is small enough to distinguish the 41 kyr Milankovitch cycle (± 8.2 kyrs) from other cycles such as 100 kyrs (± 20 kyrs). However, peaks will not be as pronounced but exhibit a broader appearance. The corresponding uncertainty ranges are marked in grey in the corresponding frequency analyses (Figure 7.3).

For the 100 kyr cyclicity of the Bounty Channel only the second point needs further consideration as longer time periods have to be sampled to observe such cyclicity. For Site I to III the sampled interval is not long enough, as it does not reach an age interval of 200 kyrs. Thus spectral analysis of Sites I to III cannot unequivocally identify these frequencies. For Sites IV to VI depth penetration reaches values between 800 and 1200 kyrs. Here, the Bounty Channel cyclicity can be resolved.

7.6.2 Validation of the method at Site I (ODP Site 1122)

ODP Site 1122 lies directly under the influence of the DWBC, which is confirmed by borehole (Carter et al. 1999b), hydrographical (Warren 1973) and seismic data (Carter and McCave 1997). The spectral analysis should show a peak at 41 kyr frequency ($24 * 10^{-3} kyr^{-1}$). The corresponding curve of the frequency analysis (Figure 7.3, green cure) shows this peak. Thus the spectral analysis is capable to reveal the presence of the DWBC influence on sediment deposition. The frequency peak around 24 $* 10^{-3} kyr^{-1}$is split into two peaks. This can be explained with the resolution and linearity of the age-depth model of ODP Site 1122. Both peaks are in a range of the ± 8.2 kyrs of the 41 kyr frequency. We take this result as a validation of our method. Like Weigelt and Uenzelmann-Neben (2007) we are

able to reveal climate forcing by changes in sediment compositions expressed as impedance contrasts. We thus do not rely on sediment components such as benthic foraminifers to reveal a periodic forcing as done by Crundwell et al. (2008), and the areal extent of processes caused by Milankovitch cycles can be assigned to definite areas just by surveying an area and information of sedimentation rate is available. This in turn can lead to further inferences, as described in the next section.

7.6.3 Spatial extent of the DWBC into the Bounty Trough

Frequency analyses at Sites II and III clearly show the 41 kyr frequency peak (Figure 7.3, yellow and red curves). It is shifted a bit to the lower frequencies at Site III and a bit to higher frequencies at Site II, but within the expected uncertainty. This observation confirms the influence of the DWBC inside the Bounty Trough west of the Outer Sill. Due to low penetration and resulting age range it is not possible to examine the presence of cycles of 100 kyr length.

Sites IV to VI have a higher penetration of at least 150 ms TWT (~ 120 m) and a lower sedimentation rate, which extends the age range to 800 kyrs or even more. Therefore, we expect the 100 kyrs cycle to be more pronounced and the 41 kyr cycles should be clearly visible if present. Figure 7.3 shows that Sites IV to VI (curves in blue, black and purple) all show a spectral peak around the 100 kyr frequency implying the influence of the Bounty Channel deposits. A spectral peak around $24 * 10^{-3} kyr^{-1}$ (41 kyr obliquity) is not evident. Thus, we do not have an influence of the DWBC at Sites IV to VI, which implies that the DWBC does not reach that far into the Bounty Trough. We do observe a frequency of $13 * 10^{-3} kyr^{-1}$ corresponding to twice the obliquity cycle at sides IV and V. We attribute this observation to different periods between pairs of sea level low stands and age errors. For the last 800 kyr the general trend has hinted on an approximately 100 kyr cyclicity but the sea level curve of Miller et al. (2005) is far from being regular. We infer that the peak at $13 * 10^{-3} kyr^{-1}$ (representing 80 kyrs cycle duration) is caused by shorter periods between some sea level low stands than 100 kyrs and the corresponding age uncertainties. We further conclude that Site IV documents a boundary and the DWBC does not cross further to the west.

Observing the influence on sediment deposition of the DWBC at Sites I to III and not at Sites IV to VI allows an estimation of the activity depth of the DWBC. Considering Figure 7.4 we can constrain the depth range to > 3000 meters depth (marked in Figure 7.1 as white dashed line). Our findings confirm the presence of a deep cold limb of the DWBC inside the Bounty Trough, previously only inferred from observed erosion at the Outer Sill (Carter and McCave 1997). We thus conclude that the DWBC takes an active part in influencing the Bounty Trough sedimentary cover and is present west of the Outer Sill even if the today's core flow lies south of the sampled locations (Carter et al. 1990).

The depth limit of the DWBC conforms to the shallowest extent of the Lower Circumpolar Deep Water (LCDW Figure 7.4, e.g. Carter et al. (2004b)) at about 2900 m (Carter et al. 2004b; McCave et al. 2008). We do not observe the influence of the Upper Circumpolar Deep Water (UCDW), also transported by the DWBC (Orsi et al. 1995; McCave et al. 2008), which has been identified in up to

2500 meters water depth in this area (Carter et al. 2004b; McCave et al. 2008)). This hints at a different water mass stratification inside the Bounty Trough compared to the flanks of the Campbell Plateau and Chatham Rise where the hydrological measurements (Profiles P14 and P15, see Figure 7.1; Talley 2007). The Bounty Trough is more confined and a current, the Southland Current, transporting Antarctic Intermediate Water (AAIW; Figure 7.4), flows from west to east through the area (see Figure 7.1, e.g. Reid 1997; McCave et al. 2008). We suggest the influence of the Southland Current has prevented shallower UCDW from entering Bounty Trough (Reid 1997). Thus we can limit the influence of the DWBC to east of ~178.2°E. Further to the west the DWBC has not influenced sediment deposition during the late Quaternary. Sedimentary rocks there mainly drape the underlying sedimentary bodies and no erosion has been reported west of 178.2°E (e.g. Carter et al. 1994; Uenzelmann-Neben et al. 2009). The presence of a defined dense water mass of LCDW inside the Bounty Trough may affect the overlying AAIW inhibiting the lighter AAIW from descending to deeper regions when transported through the Bounty Trough. This in turn may affect the local surface waters thus and may have a feedback on local climate.

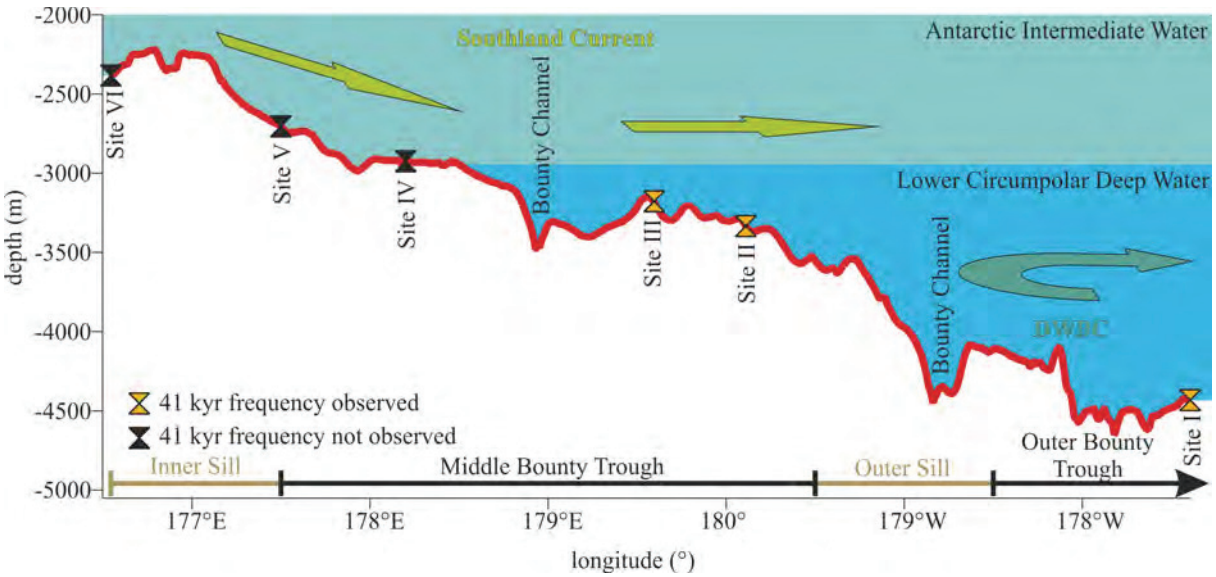

Figure 7.4: Depth profile along the Bounty Trough. Beginning with Site I, a straight line was drawn between each site. Site location is indicated by two triangles. Blue colors indicate the depth ranges of the Antarctic Intermediate Water and the Circumpolar Deep Water in the Southwest Pacific Ocean (Carter et al. 2004b; McCave et al. 2008)

7.7 Conclusion

Spectral analysis of high-resolution Parasound sub-bottom profiler data is capable of identifying the influence of the Pacific Deep Western Boundary Current (DWBC) within late Pleistocene sedimentary deposits of the Bounty Trough.

We suggest a limb of the DWBC enters the Bounty Trough and is limited to east of 178.2 °E (east of Site IV). Previous studies had not established any estimate of this extent of the DWBC into Bounty Trough; its existence was only inferred. With the knowledge of this extent we can assume that the DWBC was active inside the Bounty Trough during the last 100 kyrs, i.e. during the last glacial

maximum and further into the past. This implies that cold waters were carried closer to New Zealand's South Island by the DWBC than presently assumed. Our findings may hence revise paleoclimate models for the New Zealand region. We infer that the upper boundary of the DWBC follows the 3000 meters deep isobath (Figure 7.1, white dashed line).

7.8 Acknowledgements

We are grateful for the support of Captain H. Anderson and his crew during RV Sonne cruise 169 and Captain O. Meyer and his crew during RV Sonne cruise 213/2 as well as the Parasound watch keepers during both cruises. The cruises were funded by the Bundesministerium für Bildung und Forschung under contract number 03G0169A and 03G0213A. The Parasound data this paper is based on can be found in the PAGEA (www.pangea.de) Database. Please look for the corresponding cruises with RV Sonne.

7.9 References

Atlas Hydrographic GmbH (2010). ATLAS PARASOUND Deep-Sea parametric sub-bottom profiler. Bremen, http://www.atlas-elektronik.com/what-we-do/hydrographic-systems/parasound/.

Carter, L., R. M. Carter, et al. (2004a). "Evolution of the sedimentary system beneath the deep Pacific inflow off eastern New Zealand." Marine Geology **205**(1-4): 9-27. doi:10.1016/s0025-3227(04)00016-7

Carter, L., R. M. Carter, et al. (1990). "Evolution of Pliocene to Recent abyssal sediment waves on Bounty Channel levees, New Zealand." Marine Geology **95**(2): 97-109. doi:10.1016/0025-3227(90)90043-J

Carter, L. and I. N. McCave (1997). "The sedimentary regime beneath the Deep Western Boundary Current inflow to the Southwest Pacific Ocean." Journal of Sedimentary Research **67**(6): 1005-1017. doi:10.1306/d42686b2-2b26-11d7-8648000102c1865d

Carter, R. M. and L. Carter (1996). "The abyssal Bounty Fan and lower Bounty Channel: evolution of a rifted-margin sedimentary system." Marine Geology **130**(3–4): 181-202. doi:10.1016/0025-3227(95)00139-5

Carter, R. M., L. Carter, et al. (1994). "Seismic stratigraphy of the Bounty Trough, south-west Pacific Ocean." Marine and Petroleum Geology **11**(1): 79-93. doi:10.1016/0264-8172(94)90011-6

Carter, R. M., I. N. McCave, et al. (2004b). "1. Leg 181 Synthesis: Fronts, Flows, Drifts, Vocanoes, and the Evolution of the Southwestern Gateway to the Pacific Ocean, Eastern New Zealand". Published in: Proceedings of the Ocean Drilling Programm, Scientific Results. C. Richter. Texas, College Station (Ocean Drilling Program). **181**. doi:10.2973/odp.proc.sr.181.210.2004

Carter, R. M., I. N. McCave, et al. (1999b). "Site 1122: Turbidites with a Contourite Foundation". Published in: Proceedings of the Ocean Drilling Program, Initial reports:. R. M. Carter, I. N. McCave, C. Richter and L. Carter. Texas, USA, College Station (Ocean Drilling Program). **181:** 1 - 146. doi:10.2973/odp.proc.ir.181.106.2000

Clark, P. U., N. G. Pisias, et al. (2002). "The role of the thermohaline circulation in abrupt climate change." Nature **415**(6874): 863-869. doi:10.1038/415863a

Cooley, J. W. and J. W. Tukey (1965). "An algorithm for the machine calculation of complex Fourier series." Mathematics of Computation **19**(90): 297-301.

Crundwell, M., G. Scott, et al. (2008). "Glacial–interglacial ocean climate variability from planktonic foraminifera during the Mid-Pleistocene transition in the temperate Southwest Pacific, ODP Site 1123." Palaeogeography, Palaeoclimatology, Palaeoecology **260**(1–2): 202-229. doi:10.1016/j.palaeo.2007.08.023

Davy, B. (1993). "The Bounty Trough—Basement Structure Influences on Sedimentary Basin Evolution". Published in: South Pacific sedimentary basins. P. F. Ballance, Elsevier**:** 69-92.

Gohl, K. (2003). Structure and dynamics of a submarine continent: Tectonic-magmatic evolution of the Campbell Plateau (New Zealand) Report of the RV SONNE cruise SO-169, Project CAMP 17 January to 24 February 2003 Reports on Polar and Marine Research. Bremerhaven, Alfred Wegner Institut, Helmholtz Centre for Polar and Marine Reseach, Bremerhaven. **457:** 88. doi:10.2312/BzPM_0457_2003

Griggs, G. B., L. Carter, et al. (1983). "Late Quaternary marine stratigraphy southeast of New Zealand." Geological Society of America Bulletin **94**(6): 791-797. doi:10.1130/0016-7606(1983)94<791:lqmsso>2.0.co;2

Grobys, J. W. G., K. Gohl, et al. (2007). "Is the Bounty Trough off eastern New Zealand an aborted rift?" Journal of Geophysical Research: Solid Earth **112**. doi:doi:10.1029/2005JB004229

Hall, I. R., I. N. McCave, et al. (2001). "Intensified deep Pacific inflow and ventilation in Pleistocene glacial times." Nature **412**(6849): 809-812. doi:10.1038/35090552

Horn, M. and G. Uenzelmann-Neben (2014). "The Deep Western Boundary Current at the Bounty Trough, east of New Zealand: Indications for its activity already before the opening of the Tasmanian Gateway " submitted to Marine Geology in 2014.

Kuhlbrodt, T., A. Griesel, et al. (2007). "On the driving processes of the Atlantic meridional overturning circulation." Reviews of Geophysics **45**(2): RG2001. doi:10.1029/2004rg000166

McCave, I. N., L. Carter, et al. (2008). "Glacial–interglacial changes in water mass structure and flow in the SW Pacific Ocean." Quaternary Science Reviews **27**(19–20): 1886-1908. doi:10.1016/j.quascirev.2008.07.010

Miller, K. G., M. A. Kominz, et al. (2005). "The Phanerozoic Record of Global Sea-Level Change." Science **310**(5752): 1293-1298. doi:10.1126/science.1116412

Naish, T., R. Powell, et al. (2009). "Obliquity-paced Pliocene West Antarctic ice sheet oscillations." Nature **458**(7236): 322-328. doi:10.1038/nature07867

Orsi, A. H., T. Whitworth III, et al. (1995). "On the meridional extent and fronts of the Antarctic Circumpolar Current." Deep Sea Research Part I: Oceanographic Research Papers **42**(5): 641-673. doi:10.1016/0967-0637(95)00021-w

Osborn, N. I., P. F. Ciesielski, et al. (1983). "Disconformities and paleoceanography in the southeast Indian Ocean during the past 5.4 million years." Geological Society of America Bulletin **94**(11): 1345-1358. doi:10.1130/0016-7606(1983)94<1345:dapits>2.0.co;2

Reid, J. L. (1997). "On the total geostrophic circulation of the pacific ocean: flow patterns, tracers, and transports." Progress In Oceanography **39**(4): 263 – 352. doi:10.1016/S0079-6611(97)00012-8

Ronge, T. A., R. Tiedemann, et al. (2013). SO213 SOPATRA – Fahrtbericht und erste Ergebnisse SONNE Statusseminar. Kiel**:** 24. doi:10013/epic.42135

Smith, W. H. F. and D. T. Sandwell (1997). "Global Sea Floor Topography from Satellite Altimetry and Ship Depth Soundings." Science **277**(5334): 1956 – 1962. doi:10.1126/science.277.5334.1956

Talley, L. D. (2007). "Pacific Ocean". Southampton, U.K., International WOCE Project Office.

Tiedemann, R., J. O'Conner, et al. (2012). Cruise Report SO213: SOPATRA. Bremerhaven, Alfred Wegener Institute, Helmholtz Centre for Polar and Marine Research**:** 111.

Uenzelmann-Neben, G., J. W. G. Grobys, et al. (2009). "Neogene sediment structures in Bounty Trough, eastern New Zealand: Influence of magmatic and oceanic current activity." Geological Society of America Bulletin **121**(1-2): 134-149. doi:10.1130/B26259.1

Warren, B. A. (1973). "Transpacific hydrographic sections at lats. 43°S and 28°S: the SCORPIO expedition—II. deep water." Deep Sea Research and Oceanographic Abstracts **20**(1): 9-38. doi:10.1016/0011-7471(73)90040-5

Weigelt, E. and G. Uenzelmann-Neben (2007). "Orbital forced cyclicity of reflector strength in the seismic records of the Cape Basin." Geophysical Research Letters **34**(1): L01702. doi:10.1029/2006gl028376

Zachos, J. C., M. Pagani, et al. (2001). "Trends, Rhythms, and Aberrations in Global Climate 65 Ma to Present." Science **292**: 686-693.

8. Comparison of the two limbs of deep inflow into the Southwest Pacific Basin

The influence of the ACC on the DWBC has been shown by numerous studies (e.g. Carter and Wilkin 1999; Morris et al. 2001; Stanton and Morris 2004). The eastern limb leaves the ACC flow south of the EPR region. Here, no direct evidence for the influence of the ACC on the eastern limb is given. However, the flow through the survey area is attributed to the LCDW (Horn and Uenzelmann-Neben 2013), and the ACC also transports this water mass (e.g. Orsi et al. 1995; McCave et al. 2008). This allows the conclusion that the eastern limb is also affected by the ACC flow, analogue to the DWBC. Thus, the sedimentary structures from the EPR region (chapter 5) can be compared to the interpretations derived from the sediment drifts and borehole information east of Zealandia (chapter 6). The findings of chapters 5 and 6 since ~ 19 Ma are summarised in Table 8.1.

	Western limb, DWBC (chapter 6) Eastern Edge of Zealandia		Eastern limb (chapter 5) West of the EPR	
	Age (Ma)		Age (Ma)	
1	19.5 – 10.4	Initiation of sediment drift DB 3. Slow down of current speeds during warm Miocene but still persistent and variable current speeds due to ACC	> 9	Constant cover of older sedimentary unit EPR-1 in the distal zone hints on a steady flow allowing the accumulation of EPR-1 due to pelagic sedimentation
2	10.4 - 5.0	Erosional unconformity caused by intensification of West Antarctic Ice Sheet	~ 9	Erosive structures and abrupt increase in sedimentary cover hint on changes in oceanic circulation
3	5.0 – 1.7	Formation of sediment Drift DB 4 due to increased sediment load of DWBC caused by upstream erosion	< 9	Sediments on oceanic crust between 9 Ma and 4 Ma do not show any other structures indicating another change in oceanic setup
	< 1.7	Flow shifts again to the south east, turbiditis dominate	-	-

Table 8.1: Comparison between the two different cold water inflows into the Southwest Pacific Basin. The findings for the Deep Western Boundary Current (DWBC; western limb)) are constrained by findings of ODP Leg 181 Site 1122 (Carter et al. 1999b). For the eastern limb close to the East Pacific Rise (EPR) changes in oceanic circulation are inferred from changes in the sedimentary cover (Horn and Uenzelmann-Neben 2013).

Both regions indicate changes in paleoceanographic setup since the Miocene. I examine the first three points of Table 8.1 in order to find out if the causes for the paleoceanographic changes are comparable:

1. Between 19 Ma and 10 Ma – 9 Ma deposition dominates in both regions with almost no signs of erosion. During that time the global temperature increase during the Mid Miocene Climate Optimum causing a relative global warming (e.g. Zachos et al. 2008; Cramer et al. 2009) led to decreasing deep water formation and thus to diminished deep cold flow (van Aken 2007) favouring deposition. Beneath the DWBC a sediment drift body is observed (Carter et al. 2004a; see also DB 3 in Figure 6.4). Below the eastern limb in the distal zone pelagic sedimentation formed unit EPR-1 (older sedimentary unit; Horn and Uenzelmann-Neben 2013). Unit EPR-1 is almost undisturbed in the distal zone 2 (see Figures 5.2 – 5.4). This indicates a steady flow of LCDW allowing accumulation of pelagic sediments. Thus both limbs show comparable flow conditions that may have the same cause, the warm Mid Miocene Climate Optimum decreasing the flow speeds of the ACC. Winnowing of sediments below the DWBC flow path may indicate variations in flow speed due to East Antarctic Ice Sheet growth after the Mid Miocene Climate Optimum (Carter et al. 2004a). Such variations are not observed for the eastern limb. During cruise SO 213/2 no sediment samples have been taken in the EPR region that reached the older sedimentary unit (EPR-2; longest core about 15 m Tiedemann et al. 2012). In general, both limbs showed similar and tranquil flow conditions during the Middle Miocene.
2. The proximal zone in the EPR region shows almost no sign of the younger unit EPR-2 and its general sedimentary cover is almost half as thick as in the distal zone. In addition, the distal zone exhibits erosional features of the younger unit EPR-2 and small sediment drifts formed around obstacles (seamount effect, Figures 5.5 and 5.6) only on top of unit EPR-1. This suggests that the eastern limb flow has been accelerated at some point back in time, when the deposition of unit EPR-1 ceased. A transitional zone on approximately 9 Ma old oceanic crust separates the two zones. Thus, I assume that this change in oceanic setup happened around 9 Ma or earlier. Comparing this change in oceanic circulation to the DWBC supports this assumption. Close to Zealandia the Outer Bounty Trough shows an erosive episode of 10.4 Ma to 5 Ma. The hiatus is attributed to intensification of the DWBC and the ACC due to West Antarctic Ice Sheet build-up (climate cooling, e.g. Carter et al. 1999b; Carter et al. 2004a; Horn and Uenzelmann-Neben 2014). This period fits to the estimation of the change of the oceanic setup in the EPR region. I also attribute this change to the build-up of the West Antarctic Ice Sheet as the timing of the intensification is of the same age for both limbs. Its source is probably again the ACC.
3. Since the change in oceanic setup the sedimentary deposits below the eastern limb do not hint on a further change in oceanic setup. The flow speed of the DWBC also does not change significantly; it remains high since the formation of the hiatus between 10.4 Ma – 5 Ma (e.g. Carter et al. 1999b; Carter et al. 2004a and chapter 6). At 5 Ma deposition of drift body DB 4 (Figure 6.4) starts. However, the build-up is not attributed to slower flow speed but to an

increased sediment load taken up by the DWBC further upstream at the slope of the Campbell Plateau (Carter et al. 1999a; Carter et al. 1999b and chapter 6). The ACC flow remained high since 5 Ma (Osborn et al. 1983). Both branches were intensified by its flow. However, the record of the oceanic setup is different. The sedimentary archive below the western branch received a higher sediment load due to the erosion at the base of the Campbell Plateau allowing additional deposition (DB 4, Figure 6.4). Below the eastern branch sediments have been eroded by the stronger flows and no additional deposition of sediments is observable, except small depositional features around obstacles (seamount effect, Figures 5.5 and 5.6).

This leads me to the following conclusion: Keeping in mind that the EPR-region and Bounty Trough are more than 4000 km distant from each other (Figure 1.2) this comparison is only a first indication of similarities in both regions and need further investigation. Nevertheless both limbs of deep cold inflow show similarities and a comparable history of intensification of deep cold inflow around 10 Ma – 9 Ma. These changes in paleoceanographic setup are all caused by the ACC that is intensified due to cooling and establishment of the West Antarctic Ice Sheet.

References

Carter, L., R. M. Carter, et al. (2004a). "Evolution of the sedimentary system beneath the deep Pacific inflow off eastern New Zealand." Marine Geology **205**(1-4): 9-27. doi:10.1016/s0025-3227(04)00016-7

Carter, L. and J. Wilkin (1999). "Abyssal circulation around New Zealand - a comparison between observations and a global circulation model." Marine Geology **159**(1–4): 221-239. doi:10.1016/S0025-3227(98)00205-9

Carter, R. M., I. N. McCave, et al. (1999a). "Site 1121: The Campbell "Drift"". Published in: Proceedings of the Ocean Drilling Program, Initial reports:. R. M. Carter, I. N. McCave, C. Richter and L. Carter. Texas, USA, College Station (Ocean Drilling Program). **181:** 1 - 62. doi:10.2973/odp.proc.ir.181.105.2000

Carter, R. M., I. N. McCave, et al. (1999b). "Site 1122: Turbidites with a Contourite Foundation". Published in: Proceedings of the Ocean Drilling Program, Initial reports:. R. M. Carter, I. N. McCave, C. Richter and L. Carter. Texas, USA, College Station (Ocean Drilling Program). **181:** 1 - 146. doi:10.2973/odp.proc.ir.181.106.2000

Cramer, B. S., J. R. Toggweiler, et al. (2009). "Ocean overturning since the Late Cretaceous: Inferences from a new benthic foraminiferal isotope compilation." Paleoceanography **24**(4): PA4216. doi:10.1029/2008pa001683

Horn, M. and G. Uenzelmann-Neben (2013). "Nonlinear sediment thickness increase on the western East Pacific Rise flank, 45°S." Geo-Marine Letters **33**(5): 381 - 390. doi:10.1007/s00367-013-0335-1

Horn, M. and G. Uenzelmann-Neben (2014). "The Deep Western Boundary Current at the Bounty Trough, east of New Zealand: Indications for its activity already before the opening of the Tasmanian Gateway " submitted to Marine Geology in 2014.

McCave, I. N., L. Carter, et al. (2008). "Glacial–interglacial changes in water mass structure and flow in the SW Pacific Ocean." Quaternary Science Reviews **27**(19–20): 1886-1908. doi:10.1016/j.quascirev.2008.07.010

Morris, M., B. Stanton, et al. (2001). "Subantarctic oceanography around New Zealand: Preliminary results from an ongoing survey." New Zealand Journal of Marine and Freshwater Research **35**(3): 499-519. doi:10.1080/00288330.2001.9517018

Orsi, A. H., T. Whitworth III, et al. (1995). "On the meridional extent and fronts of the Antarctic Circumpolar Current." Deep Sea Research Part I: Oceanographic Research Papers **42**(5): 641-673. doi:10.1016/0967-0637(95)00021-w

Osborn, N. I., P. F. Ciesielski, et al. (1983). "Disconformities and paleoceanography in the southeast Indian Ocean during the past 5.4 million years." Geological Society of America Bulletin **94**(11): 1345-1358. doi:10.1130/0016-7606(1983)94<1345:dapits>2.0.co;2

Stanton, B. R. and M. Y. Morris (2004). "Direct velocity measurements in the Subantarctic Front and over Campbell Plateau, southeast of New Zealand." Journal of Geophysical Research: Oceans **109**(C1): C01028. doi:10.1029/2002jc001339

Tiedemann, R., J. O'Conner, et al. (2012). Cruise Report SO213: SOPATRA. Bremerhaven, Alfred Wegener Institute, Helmholtz Centre for Polar and Marine Research**:** 111.

van Aken, H. M. (2007). "The Oceanic Thermohaline Circulation: An Introduction". New York, Springer Science and Business Media, LLC.

Zachos, J. C., G. R. Dickens, et al. (2008). "An early Cenozoic perspective on greenhouse warming and carbon-cycle dynamics." Nature **451**(7176): 279-283. doi:doi: 10.1038/nature06588

9. Summary and Conclusions

The main aim of this thesis was the attempt to fill some white spots on the paleoceanographic map of the South Pacific Ocean. As presented in the previous three chapters I have found several new indications for ancient bottom current flows in the sedimentary deposits of the South Pacific Ocean.

9.1 The eastern limb close to the East Pacific Rise

The first paper (Chapter 5) has targeted the centre of the South Pacific Ocean close to the East Pacific Rise (EPR). Here, the eastern limb of the deep flow entering the Southwest Pacific Basin turns north leaving the Antarctic Circumpolar Current (ACC) flow path to enter the survey area. The acquired seismic profiles (Figure 2.1b) have been analysed with respect to three different objectives:

1. **Sedimentary cover with respect to the model prediction:**

   Ewing and Ewing (1967) proposed a linear increase of the sedimentary cover at the flanks of oceanic spreading ridges, which is symmetric on both flanks of the ridge. The thickness of the cover increases until calcareous sediments start to dissolve at the Carbonate Compensation Depth (CCD). As already revealed, this symmetric sedimentary cover at both flanks of the ridge is not observed at the EPR (Hauschild et al. 2003). Data from this thesis now show that the increase in sedimentary cover is not linear. Instead the sedimentary deposits can be divided into two zones (a distal and a proximal zone) of uniform thickness. The distal zone has an almost twice as thick sedimentary cover as in the proximal zone.

2. **Processes that have shaped the sedimentary cover:**

   The differences from the model predicted by Ewing and Ewing (1967) can be explained with structures found in the seismic reflection data. The distribution of sediments, sedimentary structures around basement highs and erosive structures indicate the influence of bottom currents. These currents took an active influence in shaping the sedimentary deposits creating the observed differences between the proximal and the distal zone. However, I cannot totally rule out that the thicker sedimentary column in the distal zone may have been created by a higher primary production cell. Missing data makes it impossible to rule out or confirm this explanation but remote sensing (see Figure 9.1) shows low primary productivity in the South Pacific Ocean today. Thus under the assumption that primary production in the South Pacific Ocean was also weak over geological time scales, I assume that the observed structures have been caused by bottom currents.

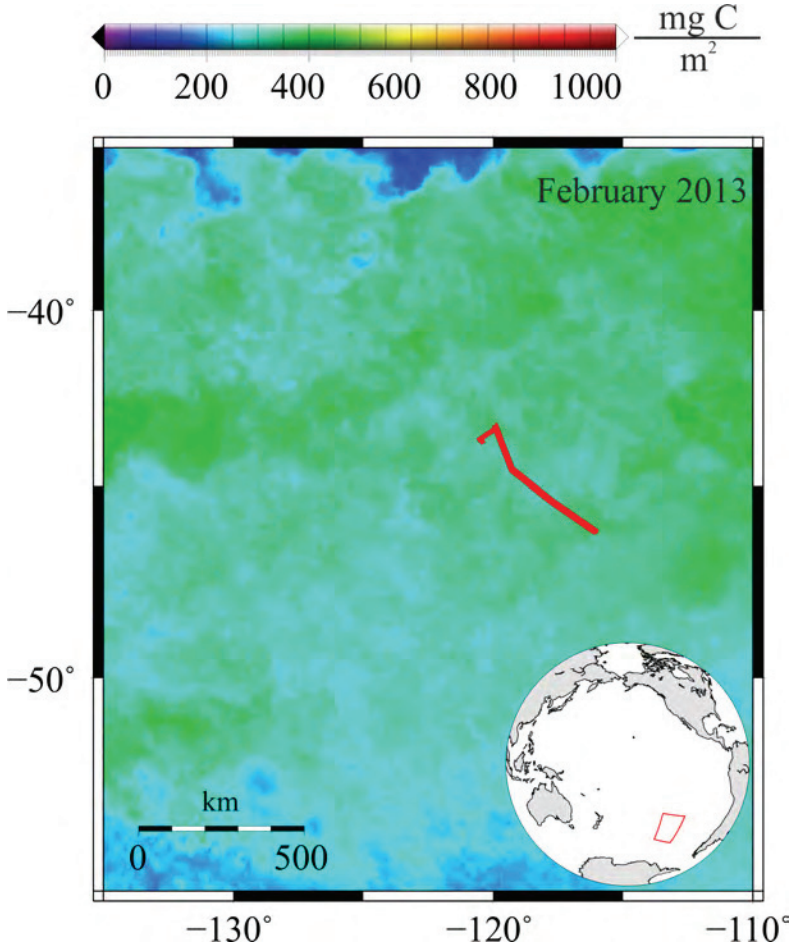

Figure 9.1: Net primary production expressed by the Vertically Generalised Production Model (Behrenfeld and Falkowski 1997). Data shown in this figure is the monthly average from February 2013, available at http://www.science.oregonstate.edu/ocean.productivity/index.php (O'Malley 2014). Primary Production is around 300 mg carbon (C) per square metre. This is the lower edge of the global primary productivity scale. Red lines indicate the position of the seismic reflection profiles.

9.2 The Deep Western Boundary Current

9.2.1 Past oceanic setup at the eastern edge of Zealandia

My second contribution to the paleoceanographic map of the South Pacific Ocean targeted the Pacific Deep Western Boundary Current (DWBC) close to Zealandia at the Bounty Trough region (chapter 6). Here, a larger sedimentary archive recording the DWBC history has formed, which can be used to reveal paleoceanographic changes since the late Cretaceous. This manuscript covers three different topics:

1. **Paleoceanographic setup before the opening of the Tasmanian Gateway:**

   I have found indications for an active proto-DWBC below the Eocene/Oligocene boundary. Two sediment drift bodies in the Outer Bounty Trough are the first evidence of a deep cold flow in the South Pacific Ocean during Eocene and older times in the Southwest Pacific Ocean. Initiation of a deep flow forming the first drift body (DB 1) is probably linked to a combination of climate cooling observed during the late Cretaceous (Cramer et al. 2009; Friedrich et al. 2012) and separation of Antarctica and Zealandia (Wobbe et al. 2012). Further, the shift from DB 1 to the

second drift body (DB 2) is probably caused by colder climate conditions in the Late Eocene. The drift crest migration from DB 1 to DB 2 occurs at the same time as the East Antarctic Glaciation around 44 - 42 Ma. This supports the theory that Antarctic Glaciation was not caused by the opening of the Tasmanian Gateway. Cooling already began before the opening, favouring a dropping CO_2 level as a cause for glaciation rather than the opening of Circumantarctic seaways.

2. The history of the DWBC in the Bounty Trough area:

I have compiled a complete scenario of the DWBC history at the Outer Bounty Trough region. In addition to drift bodies DB 1 and DB 2 I have found two additional drift bodies (DB 3 and DB 4) above the Eocene/Oligocene boundary. The history since the Oligocene can be summarised as follows: The Oligocene sediments have been removed during a long lasting erosional phase, creating the Marshall Paraconformity (33.7 - ~19.5 Ma). This vigorous flow of the DWBC, enforced by the ACC, was followed by a phase of slower flow speed creating DB 3. This period was followed by stronger flows due to climate cooling and West Antarctic Ice Sheet build-up leading to another phase of erosion between 10.4 Ma and 5.0 Ma. Between 5.0 Ma and 1.7 Ma, deposition started again, creating DB 4. Build–up was caused by the intensified load of the DWBC that has been taken up further upstream. Finally at 1.7 Ma the DWBC shifted away from the Outer Bounty Trough to a breach in the northern levee of the Bounty Channel.

3. The occurrence of the DWBC west of the Outer Sill since the Miocene:

I can estimate the extent and timing of the DWBC flow into the Bounty Trough. Up to now evidence was only found for a limb affecting the youngest sedimentary unit (Unit A) at the Outer Sill. Using the distribution of seismostratigraphic Unit B (of contouritic origin as confirmed by ODP Site 1122) I have shown that the DWBC may have influenced the Bounty Trough already since ~19.5 Ma as its deposits can be found also west of the Outer Sill inside the Bounty Trough.

9.2.2 Present influence of the DWBC inside the Middle Bounty Trough

The third manuscript (chapter 7) again targeted the occurrence of the DWBC west of the Outer Sill inside the Middle Bounty Trough. In Chapter 6 I have shown that sediments below the deposits of the Bounty Channel (unit B, contouritic origin) are also present inside the Middle Bounty Trough. Sedimentary structures within Unit B suggest the influence of the DWBC was present west of the Outer Sill from 19.5 Ma to 1.7 Ma. Additionally, Pleistocene DWBC variability on orbital (20 to 400 ka) timescales is recorded in unit A. High-resolution Parasound sub-bottom profiler data can be used to analyse the upper sedimentary column with the detail needed to detect these orbital cycles. The Bounty Channel turbiditis show a different cyclicity (only deposited during glacial lowstands, since 800 ka approximately every 100 kyrs) than the DWBC (prominent strengthening every 41 ka). Thus the occurrence of the 41 kyr obliquity cycle can be used to trace the influence area of the DWBC inside the Bounty Trough as the turbiditiy current of the Bounty Channel is the only other source that takes active part in shaping the sediments in the Bounty Trough area since 800 ka.

1. **Revealing cyclic signals from Parasound sub-bottom profiler data:**

   Weigelt and Uenzelmann-Neben (2007) have shown that a spectral analysis with a Fourier transformation algorithm can reveal cyclic signals from seismic reflection data, which have been converted from TWT into age of the deposits. These signals can be related to climate cycles on orbital frequencies (Milankovitch cycles). I have adapted this method to Parasound sub-bottom profiler data. Spectral analysis shows that in the working area the method is capable to resolve Milankovitch cycles caused by obliquity (41 kyr) and longer periods.

2. **Presence of the DWBC west of the Outer Sill:**

   Spectral analysis performed at six different sites along the Bounty Channel axis are used to map the spatial occurrence of the 41 kyr obliquity cycle documented by the deposits. The mapping reveals the presence of the DWBC west of the Outer Sill but its presence is limited to east of 178.2°E. These results provide the first direct evidence on the occurrence of the DWBC inside the Bounty Trough during late Pleistocene to recent times. Up to now the presence of the DWBC was only inferred due to erosional structures at the Outer Sill.

9.3 The deep inflow into the Southwest Pacific Basin since the Miocene

The structure of the sedimentary column at the western flank of the EPR and the occurrence of bottom current derived features presented in chapter 5 can be further interpreted to gain information about paleoceanic changes in the EPR region (Chapter 8). This allows me to provide first insights into the Miocene paleoceanography of the South Pacific Ocean far away from any land mass. Between 19 Ma and 9 Ma sedimentary structures suggest a steady flow of the eastern limb, which has allowed the formation of the first seismostratigraphic unit. Around 9 Ma a change in oceanic setup is suggested by the distribution of sediments. Erosional structures in the upper sedimentary column indicate an increase in flow speeds of the bottom currents from the eastern limb.

The western limb (DWBC) shows a comparable behaviour: A depositional phase creating drift body 3 (DB 3) begins during the Early Miocene (19.5 Ma). This phase is interrupted by an erosional unconformity (reflector R3) created by the DWBC between 10.4 Ma - 5 Ma. Cooling due to the West Antarctic Ice Sheet build-up increased the flow speed of the DWBC. The expansion of the West Antarctic Ice Sheet and the resulting cold climate around Antarctica keeps the flow speeds high until the present day. Although another drift body (DB 4) has formed beneath the DWBC deposition is only possible due to erosion further upstream by the combined DWBC and ACC.

The comparison of the history of both of deep cold inflow into the South Pacific Ocean shows many similarities since the early Miocene. It is reasonable to extrapolate the findings of the Bounty Trough region to the EPR region. Both limbs are influenced by the ACC and thus its intensification due to the

changes caused by the West Antarctic Ice Sheet build-up are not only visible close to Zealandia but also in the open South Pacific Ocean.

9.4 References

Behrenfeld, M. J. and P. G. Falkowski (1997). "Photosynthetic rates derived from satellite-based chlorophyll concentration." Limnology and Oceanography **42**(1): 1-20.

Cramer, B. S., J. R. Toggweiler, et al. (2009). "Ocean overturning since the Late Cretaceous: Inferences from a new benthic foraminiferal isotope compilation." Paleoceanography **24**(4): PA4216. doi:10.1029/2008pa001683

Ewing, J. and M. Ewing (1967). "Sediment Distribution on the Mid-Ocean Ridges with Respect to Spreading of the Sea Floor." Science **156**(3782): 1590 – 1592. doi:10.1126/science.156.3782.1590

Friedrich, O., R. D. Norris, et al. (2012). "Evolution of middle to Late Cretaceous oceans—A 55 m.y. record of Earth's temperature and carbon cycle." Geology **40**(2): 107-110. doi:10.1130/g32701.1

Hauschild, J., I. Grevemeyer, et al. (2003). "Asymmetric sedimentation on young ocean floor at the East Pacific Rise, 15°S." Mar. Geol. **193**(1 – 2): 49 – 59. doi:10.1016/S0025-3227(02)00613-8

O'Malley, R. (2014). "The Ocean Productivity Homepage." Retrieved 20.10.2014, 2014, from http://www.science.oregonstate.edu/ocean.productivity/index.php.

Weigelt, E. and G. Uenzelmann-Neben (2007). "Orbital forced cyclicity of reflector strength in the seismic records of the Cape Basin." Geophysical Research Letters **34**(1): L01702. doi:10.1029/2006gl028376

Wobbe, F., K. Gohl, et al. (2012). "Structure and breakup history of the rifted margin of West Antarctica in relation to Cretaceous separation from Zealandia and Bellingshausen plate motion." Geochemistry, Geophysics, Geosystems **13**(4): Q04W12. doi:10.1029/2011gc003742

10. Outlook

I have presented new evidence for paleoceanographic changes of the deep inflow into the Pacific Ocean. Nevertheless there are still white spots that have to be filled.

10.1 Further research close to the EPR

Seismic reflection profiles at the western flank of the EPR cover only oceanic crust younger than the beginning of chron C6n, (~19 Ma, see Figure 5.1) and thus sediments documenting the paleoceanographic setup of the region before ~19 Ma have not been surveyed. Likely, sediments deposited on older oceanic crust can reveal further structures of the eastern limb of deep cold inflow into the South Pacific Ocean.

Therefore I suggest the acquisition of two additional profiles perpendicular to the ridge axis. Figure 10.1 shows two sample locations of such profiles. These two profiles would allow analysing a longer history of the eastern limb of deep Pacific inflow, because they also cover older parts of the oceanic crust and older sediment deposits. Further, one of these perpendicular profiles should completely cross the EPR (as shown with the northern profile in Figure 10.1) to survey sediments on the eastern side of the EPR. The main purpose would be to test the hypothesis that the EPR really has a symmetric sedimentary cover on both sides of the rise crest (Ewing and Ewing 1967) or whether asymmetric sedimentation, which has been observed 30° further north of the EPR-region (Hauschild et al. 2003), is also present in this area. An additional profile extending from the northeast to the southwest should cross the previously proposed profiles. This profile would allow a correlation of findings made on the profiles perpendicular to the EPR and extrapolate prominent reflections to the whole area.

For planning the western extent of the new profiles, the present and former Carbonate Compensation Depth (CCD) should be taken into account because the $CaCO_3$ inside the sediments at the EPR flank start to dissolve when the depth of the CCD is reached. Thus, potential new profiles should only extent into the Southwest Pacific Basin until they reach the depth of the present CCD at ~ 4400 metres (Figure 10.1, drak gray line; van Andel 1975). Further we have to take into account that the paleo CCD was shallower than today. The shallowest CCD was reached during the late Miocene when the CCD rose to about 3900 metres (Figure 10.1, light gray line; van Andel 1975). Thus possible bottom current footprints in carbonate sediments may have been dissolved in depth of 3900 m or deeper. Nevertheless sediment on crust older than 20 Ma may have preserved potential footprints as only the upper sediments may have been affected. Thus, oceanic crust in 3900 m to 4400 metres depth may give new information on the paleoceanographic setup when interpreted with caution concerning dissolved sediments. By comparing the CCD with the age of the oceanic crust, it is possible to derive new information from sediments deposited on ~30 Ma old crust (Figure 10.1 shows age colour-coded oceanic crust (Mueller et al. 2008) and the present CCD as dark grey contour). These three additional

profiles may give further insights into the history of the deep Pacific inflow back to about 30 Ma. Further, they can be used to refine the old model of sedimentation at the flanks of spreading ridges.

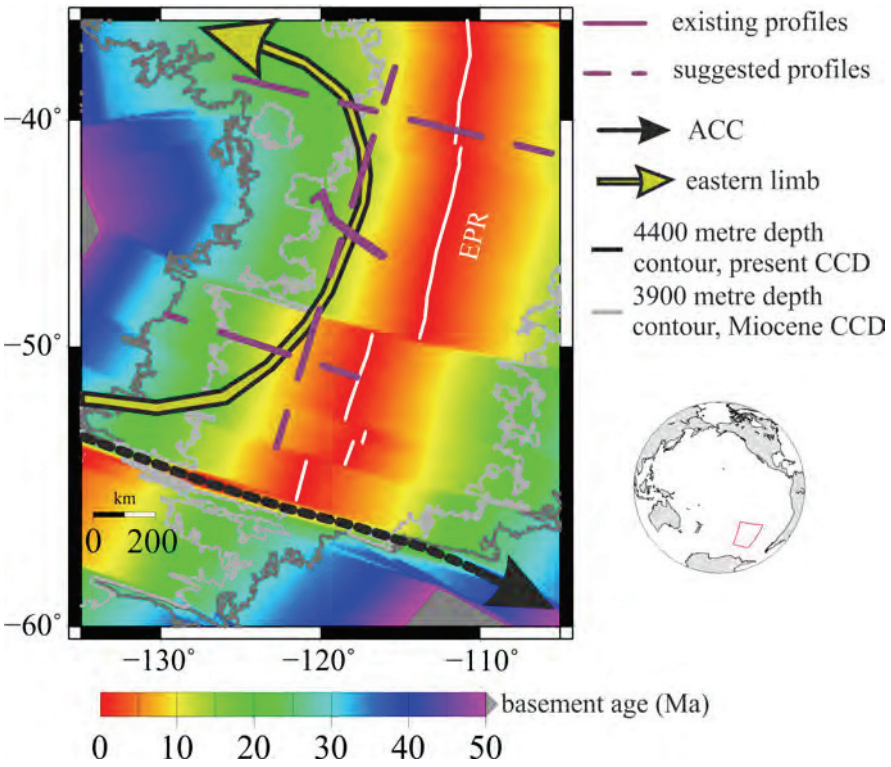

Figure 10.1: Area around the East Pacific Rise (EPR) on a map representing the age of the oceanic crust in millions of years (Mueller et al. 2008). The eastern limb of the deep Pacific inflow (black and yellow arrow) and the Antarctic Circumpolar Current (ACC, black) are marked by arrows. Additionally the depth contours (GEBCO_08 grid; Smith and Sandwell 1997) of the Miocene CCD (grey contour, 3900 m ;van Andel 1975) and the present CCD (dark grey contours, 4400 m; van Andel 1975) are shown. To survey the influence of the eastern limb, three additional seismic profiles perpendicular to the rise axis (shown in purple dashed lines) are proposed.

For the present thesis I could only rely on crustal ages to pinpoint major events but changes occurring on shorter timescales were not resolvable only on basis of the seismic reflection data. Thus a better age model based on sediment samples would be desirable.

10.2 Further research in the Outer Bounty Trough area

10.2.1 Future research on sediment drifts in the Bounty Trough area

The Outer Bounty Trough area has revealed the complete Cenozoic history of the (proto-) DWBC in the area. However, some interpretations derived in Chapter 6 would benefit from an extended dataset.

- **A narrower seismic network of profiles crossing drift bodies in the Bounty Trough area:** Besides drift bodies (DB 1 to DB 4) found on profile AWI-20110006, other single channel lines (see Plate 2d of Carter et al. 1994) hint on potential sites of sediment drifts (locations marked in purple in Figure 10.2a). A survey covering all of these drift bodies in a network centred above

ODP Site 1122 may be used to map out depositional centres and reconstruct paleocurrent pathways of this area.

- **A better age control for sediments below the Marshall Paraconformity:**

Sediments of the seismostratigraphic units C and D are extrapolated from the shelf of South Island, New Zealand, through the whole Bounty Trough to the deep sea. It is not clear whether sediments cored in the Canterbury Basin by oil exploration wells (see Figure 6.1) are comparable to the deposits found in the Outer Bounty Trough. The oil exploration wells and ODP Site 1122 are approximately 900 km apart. Thus additional deep drilling of the lower sedimentary column is desirable. Single channel seismic reflection profiles (Figure 10.2b, taken from Carter et al. 1994) show a thin sedimentary cover of seismographic unit A (sediments from the Bounty Channel, up to 1.7 Ma old, see chapter 6) and a missing unit B above units C (Eocene age) and D (Palaeocene to Cretaceous). Drilling in this area (as indicated in Figure 10.2) would allow to reach at least sediments of Eocene age, eventually also sediments of Palaeocene or even of Cretaceous age.

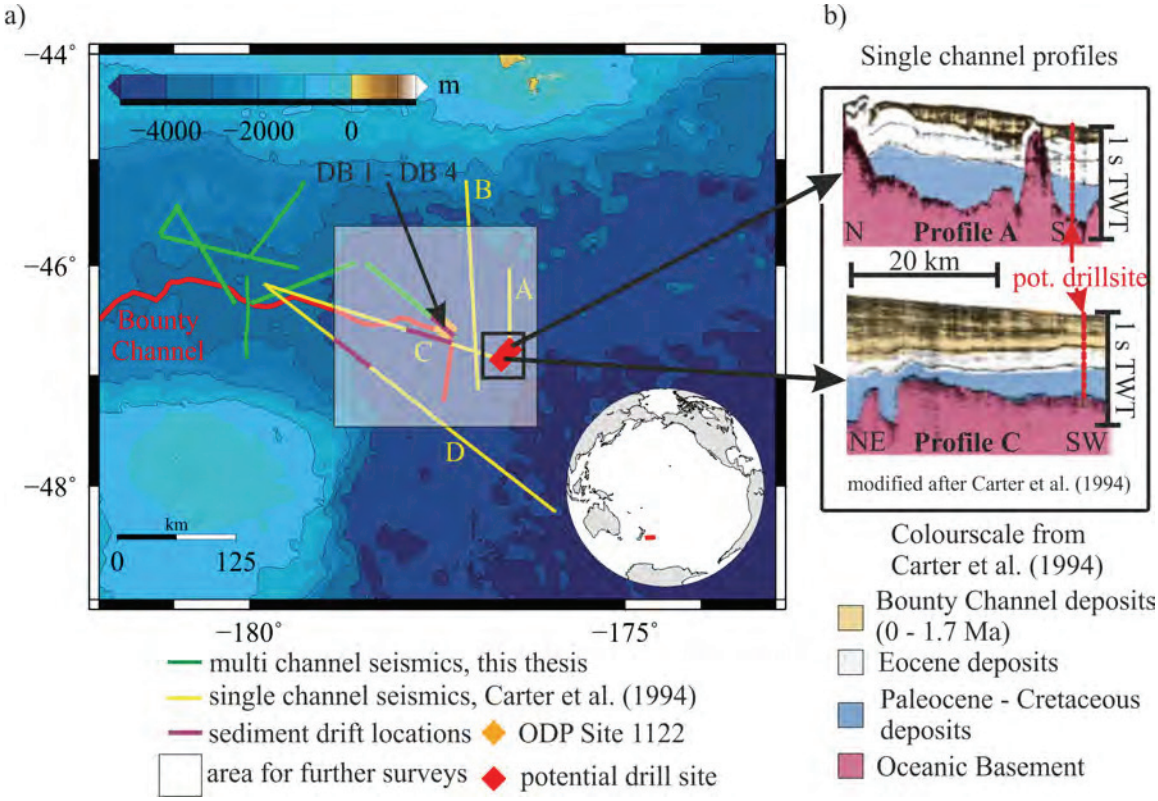

Figure 10.2: **a)** Overview over the single channel (yellow, (Carter et al. 1994)) and multichannel seismic lines (green, see chapter 6) available in the Outer Bounty Trough region. The purple marked spots represent findings of (potential on single channel lines) drift structures in this area. Further profiles crossing these locations and the surroundings (marked with white box) will help to map the depositions of the DWBC revealing further shifts of the DWBC not observable with the present dataset. **b)** Excerpts from the single channel profiles A and C of Carter et al. (1994). Note the relatively thin cover of younger sediments (yellow) above the sediments of Eocene age or older (white and blue). Here it would be possible to reach older sediments by drilling without having to penetrate more than 400 metres of sediment as at the location of ODP Site 1122.

Drilling of Eocene to Cretaceous sediments could provide a better age resolution and characterisation of the sediments below the Marshall Paraconformity (top of Eocene deposits) and is also of broad interest for climate research. Especially the transition from the relative warm climate during the late

Cretaceous to the cold climate during the Oligocene (e.g. Huber et al. 2002; Zachos et al. 2008; Friedrich et al. 2012) is not well understood. Sediments covering the Bounty Trough area have likely been deposited continuously since the formation of the oceanic crust during the Cretaceous until the Eocene/Oligocene boundary and thus have recorded the climate transition. Bottom currents do not play a major role in shaping sedimentary deposits until 33.7 Ma. Besides the observed drift bodies (DB 1 and DB 2, Figure 6.4) no large erosional events are reported south of Chatham Rise since the formation of the Marshall Paraconformity. Drilling these sediments may reveal climate changes close to an oceanic gateway. Opening of gateways allowed the establishment of the ACC that caused a major cooling of the deep oceans (McAnena et al. 2013; Sijp et al. 2014). This means the Bounty Trough area is an ideal region to study these climate changes and decipher the oceanic and climatic history during the Eocene and further back in time. Additionally, drilling sediments in the Bounty Trough area may reveal the feedback of the deep ocean to the climate change before the opening of the Tasmanian Gateway. Also, new evidence for processes preceding ocean gateway opening that may have caused Antarctic Glaciation before the Eocene/Oligocene boundary may be found (e.g. Ehrmann and Mackensen 1992; Zachos et al. 1992; Zachos et al. 2001).

10.2.2 Future use of sub-bottom profiler data for the detection of Milankovitch cycles

The orbital (Milankovitch-) cycles observed in the sediments of the left Bounty Channel Levee have been of great use to estimate the spatial extent of the DWBC into the Bounty Trough. The method may be a valuable tool for further studies in the Bounty Trough area and in other regions of the world oceans. Identifications of different Milankovitch cycles in an area can be used to map the extent on climate related processes shaping the upper sedimentary units. The only necessary precondition is that the process that is analysed has a unique frequency observable in spectral analysis in comparison to other processes shaping sedimentary deposits.

The Parasound system offers a method to map orbitally controlled sedimentation over large areas in relatively short time. The MeBo coring rig, capable of coring the upper 80 metres of sediment (Freudenthal and Wefer 2013) and possibly down to 200 m in the future (MARUM-MeBo200) can be a valuable addition for age control and ground truth of the acoustic data.

10.3 References

Carter, R. M., L. Carter, et al. (1994). "Seismic stratigraphy of the Bounty Trough, south-west Pacific Ocean." Marine and Petroleum Geology **11**(1): 79-93. doi:10.1016/0264-8172(94)90011-6

Ehrmann, W. U. and A. Mackensen (1992). "Sedimentological evidence for the formation of an East Antarctic ice sheet in Eocene/Oligocene time." Palaeogeography, Palaeoclimatology, Palaeoecology **93**(1–2): 85-112. doi:10.1016/0031-0182(92)90185-8

Ewing, J. and M. Ewing (1967). "Sediment Distribution on the Mid-Ocean Ridges with Respect to Spreading of the Sea Floor." Science **156**(3782): 1590 – 1592. doi:10.1126/science.156.3782.1590

Freudenthal, T. and G. Wefer (2013). "Drilling cores on the sea floor with the remote-controlled sea floor drilling rig MeBo." Geosci. Instrum. Method. Data Syst. **2**(2): 329-337. doi:10.5194/gi-2-329-2013

Friedrich, O., R. D. Norris, et al. (2012). "Evolution of middle to Late Cretaceous oceans—A 55 m.y. record of Earth's temperature and carbon cycle." Geology **40**(2): 107-110. doi:10.1130/g32701.1

Hauschild, J., I. Grevemeyer, et al. (2003). "Asymmetric sedimentation on young ocean floor at the East Pacific Rise, 15°S." Marine Geology **193**(1 – 2): 49 – 59. doi:10.1016/S0025-3227(02)00613-8

Huber, B. T., R. D. Norris, et al. (2002). "Deep-sea paleotemperature record of extreme warmth during the Cretaceous." Geology **30**(2): 123-126. doi:10.1130/0091-7613(2002)030<0123:dsproe>2.0.co;2

McAnena, A., S. Flogel, et al. (2013). "Atlantic cooling associated with a marine biotic crisis during the mid-Cretaceous period." Nature Geoscience **6**(7): 558-561. doi:10.1038/ngeo1850

Mueller, R. D., M. Sdrolias, et al. (2008). "Age, spreading rates, and spreading asymmetry of the world's ocean crust." Geochemistry Geophysics Geosystems **9**(4): Q04006. doi:10.1029/2007gc001743

Sijp, W. P., A. S. von der Heydt, et al. (2014). "The role of ocean gateways on cooling climate on long time scales." Global and Planetary Change **119**(0): 1-22. doi:10.1016/j.gloplacha.2014.04.004

Smith, W. H. F. and D. T. Sandwell (1997). "Global Sea Floor Topography from Satellite Altimetry and Ship Depth Soundings." Science **277**(5334): 1956 – 1962. doi:10.1126/science.277.5334.1956

van Andel, T. H. (1975). "Mesozoic/cenozoic calcite compensation depth and the global distribution of calcareous sediments." Earth and Planetary Science Letters **26**(2): 187 – 194. doi:10.1016/0012-821X(75)90086-2

Zachos, J. C., J. R. Breza, et al. (1992). "Early Oligocene ice-sheet expansion on Antarctica: Stable isotope and sedimentological evidence from Kerguelen Plateau, southern Indian Ocean." Geology **20**(6): 569-573.

Zachos, J. C., G. R. Dickens, et al. (2008). "An early Cenozoic perspective on greenhouse warming and carbon-cycle dynamics." Nature **451**(7176): 279-283. doi:doi: 10.1038/nature06588

Zachos, J. C., M. Pagani, et al. (2001). "Trends, Rhythms, and Aberrations in Global Climate 65 Ma to Present." Science **292**: 686-693. doi:10.1126/science.1059412

11. Complete Bibliography

Alves, T. M., T. Cunha, et al. (2004). "Surveying the flanks of the Mid-Atlantic Ridge: the Atlantis Basin, North Atlantic Ocean (36°N)." Marine Geology **209**(1 – 4): 199 – 222. doi:10.1016/j.margeo.2004.06.002

Antoine, D., J.-M. André, et al. (1996). "Oceanic primary production: 2. Estimation at global scale from satellite (coastal zone color scanner) chlorophyll." Global Biochemical Cycles **10**(1): 57 – 69. doi:10.1029/95GB02832

Atlas Hydrographic GmbH (2010). ATLAS PARASOUND Deep-Sea parametric sub-bottom profiler. Bremen, http://www.atlas-elektronik.com/what-we-do/hydrographic-systems/parasound/.

Beckmann, A. and D. B. Haidvogel (1993). "Numerical Simulation of Flow around a Tall Isolated Seamount. Part I: Problem Formulation and Model Accuracy." Journal of Physical Oceanography **23**(8): 1736 – 1753. doi:10.1175/1520-0485(1993)023<1736:NSOFAA>2.0.CO;2

Behrenfeld, M. J. and P. G. Falkowski (1997). "Photosynthetic rates derived from satellite-based chlorophyll concentration." Limnology and Oceanography **42**(1): 1-20. doi:10.4319/lo.1997.42.1.0001

Berger, W. H. and J. C. Herguera (1992). "Reading the sedimentary record of the oceans productivity". Published in: Primary Productivity and Biogeochemical Cycles in the Sea. P. G. Falkowski and A. D. Woodhead. New York, Plenum Press**:** 455 – 486.

Cande, S. C. and D. V. Kent (1992). "A New Geomagnetic Polarity Time Scale for the Late Cretaceous and Cenozoic." J. of Geophys. Res. **97**(B10): 13917 – 13951. doi:10.1029/92JB01202

Cande, S. C. and J. M. Stock (2004). "Cenozoic Reconstructions of the Austrailia - New Zealand - South Pacific Sector of Antarctica". Published in: The Cenozoic Southern Ocean: Tectonics, Sedimentation, and Climate Change Between Australia and Antarctica. N. F. Exon, J. P. Kennett and M. Malone. Washington, DC, AGU. **151:** 5 - 18. doi:10.1029/gm151

Carter, L., R. M. Carter, et al. (2004a). "Evolution of the sedimentary system beneath the deep Pacific inflow off eastern New Zealand." Marine Geology **205**(1-4): 9-27. doi:10.1016/s0025-3227(04)00016-7

Carter, L., R. M. Carter, et al. (1996a). "Regional sediment recycling in the abyssal Southwest Pacific Ocean." Geology **24**(8): 735-738. doi:10.1130/0091-7613(1996)024<0735:rsrita>2.3.co;2

Carter, L., R. M. Carter, et al. (1990). "Evolution of Pliocene to Recent abyssal sediment waves on Bounty Channel levees, New Zealand." Marine Geology **95**(2): 97-109. doi:10.1016/0025-3227(90)90043-J

Carter, L. and I. N. McCave (1994). "Development of sediment drifts approaching an active plate margin under the SW Pacific Deep Western Boundary Current." Paleoceanography **9**(6): 1061-1085. doi:10.1029/94pa01444

Carter, L. and I. N. McCave (1997). "The sedimentary regime beneath the Deep Western Boundary Current inflow to the Southwest Pacific Ocean." Journal of Sedimentary Research **67**(6): 1005-1017. doi:10.1306/d42686b2-2b26-11d7-8648000102c1865d

Carter, L. and J. Wilkin (1999). "Abyssal circulation around New Zealand - a comparison between observations and a global circulation model." Marine Geology **159**(1–4): 221-239. doi:10.1016/S0025-3227(98)00205-9

Carter, R. M. (1988). "Post-breakup stratigraphy of the Kaikoura Synthem (Cretaceous-Cenozoic), continental margin, southeastern New Zealand." New Zealand Journal of Geology and Geophysics **31**(4): 405-429. doi:10.1080/00288306.1988.10422141

Carter, R. M. and L. Carter (1996). "The abyssal Bounty Fan and lower Bounty Channel: evolution of a rifted-margin sedimentary system." Marine Geology **130**(3–4): 181-202. doi:10.1016/0025-3227(95)00139-5

Carter, R. M., L. Carter, et al. (1994). "Seismic stratigraphy of the Bounty Trough, south-west Pacific Ocean." Marine and Petroleum Geology **11**(1): 79-93. doi:10.1016/0264-8172(94)90011-6

Carter, R. M., L. Carter, et al. (1996b). "Current controlled sediment deposition from the shelf to the deep ocean: the Cenozoic evolution of circulation through the SW Pacific gateway." Geologische Rundschau **85**(3): 438-451. doi:10.1007/bf02369001

Carter, R. M., I. N. McCave, et al. (2004b). "1. Leg 181 Synthesis: Fronts, Flows, Drifts, Vocanoes, and the Evolution of the Southwestern Gateway to the Pacific Ocean, Eastern New Zealand". Published in: Proceedings of the Ocean Drilling Programm, Scientific Results. C. Richter. Texas, College Station (Ocean Drilling Program). **181**. doi:10.2973/odp.proc.sr.181.210.2004

Carter, R. M., I. N. McCave, et al. (1999a). "Site 1121: The Campbell "Drift"". Published in: Proceedings of the Ocean Drilling Program, Initial reports:. R. M. Carter, I. N. McCave, C. Richter and L. Carter. Texas, USA, College Station (Ocean Drilling Program). **181:** 1 - 62. doi:10.2973/odp.proc.ir.181.105.2000

Carter, R. M., I. N. McCave, et al. (1999b). "Site 1122: Turbidites with a Contourite Foundation". Published in: Proceedings of the Ocean Drilling Program, Initial reports:. R. M. Carter, I. N. McCave, C. Richter and L. Carter. Texas, USA, College Station (Ocean Drilling Program). **181:** 1 - 146. doi:10.2973/odp.proc.ir.181.106.2000

Carter, R. M., I. N. McCave, et al. (1999c). "Site 1123: North Chatham Drift—a 20-Ma Record of the Pacific Deep Western Boundary Current". Published in: Proceedings of the Ocean Drilling Program, Initial reports:. R. M. Carter, I. N. McCave, C. Richter and L. Carter. Texas, USA, College Station (Ocean Drilling Program). **181:** 1 - 184. doi:10.2973/odp.proc.ir.181.107.2000

Carter, R. M., I. N. McCave, et al. (1999d). "Site 1124: Rekohu Drift—from the K/T Boundary to the Deep Western Boundary Current". Published in: Proceedings of the Ocean Drilling Program, Initial reports:. R. M. Carter, I. N. McCave, C. Richter and L. Carter. Texas, USA, College Station (Ocean Drilling Program). **181:** 1 - 137. doi:10.2973/odp.proc.ir.181.108.2000

Chen, Y. and W. J. Morgan (1990). "Rift Valley/No Rift Valley Transition at Mid-Ocean Ridges." Journal of Geophysical Research: Solid Earth **95**(B11): 17571 – 17581. doi:10.1029/JB095iB11p17571

Clark, P. U., N. G. Pisias, et al. (2002). "The role of the thermohaline circulation in abrupt climate change." Nature **415**(6874): 863-869. doi:10.1038/415863a

Cook, R. A., R. Sutherland, et al. (1999). "Regional Synthesis". Published in: Cretaceous-Cenozoic geology and petroleum systems of the Great South Basin, New Zealand. A. Sherwood. Lower Hutt, New Zealand, Institute of Geological and Nuclear Sciences monograph**:** 98 - 104.

Cooley, J. W. and J. W. Tukey (1965). "An algorithm for the machine calculation of complex Fourier series." Mathematics of Computation **19**(90): 297-301.

Cramer, B. S., J. R. Toggweiler, et al. (2009). "Ocean overturning since the Late Cretaceous: Inferences from a new benthic foraminiferal isotope compilation." Paleoceanography **24**(4): PA4216. doi:10.1029/2008pa001683

Crundwell, M., G. Scott, et al. (2008). "Glacial–interglacial ocean climate variability from planktonic foraminifera during the Mid-Pleistocene transition in the temperate Southwest Pacific, ODP Site 1123." Palaeogeography, Palaeoclimatology, Palaeoecology **260**(1–2): 202-229. doi:10.1016/j.palaeo.2007.08.023

D'Hondt, S., F. Inagaki, et al. (2011a). "Expedition 329 summary". Published in: Proceedings of the Integrated Ocean Drilling Program. S. D'Hondt, F. Inagaki, C. A. Alvarez Zarikian and a. t. E. Scientists. Tokyo, Integrated Ocean Drilling Program Management International, Inc. **329**. doi:10.2204/iodp.proc.329.101.2011

D'Hondt, S., F. Inagaki, et al. (2011b). "Site U1369". Published in: Integrated Ocean Drilling Program Expedition 329 Preliminary Report. S. D'Hondt, F. Inagaki, C. A. Alvarez Zarikian and Expedition 329 Scientists. Tokyo, Integrated Ocean Drilling Program Management International. **329:** 58. doi:10.2204/iodp.proc.329.107.2011

Davey, F. J. (1977). "Marine seismic measurements in the New Zealand region." New Zealand Journal of Geology and Geophysics **20**(4): 719-777. doi:10.1080/00288306.1977.10430730

Davis, A. S. and A. S. Laughton (1972). "Sedimentary Processes in the North Atlantic". Published in: Initial Reports of Deep Sea Drilling Project. L. A. S., W. A. Berggren, R. N. Bensonet al. Washington, D.C., U.S. Government Printing Office. **12:** 905-934. doi:10.2973/dsdp.proc.12.111.1972

Davy, B. (1993). "The Bounty Trough—Basement Structure Influences on Sedimentary Basin Evolution". Published in: South Pacific sedimentary basins. P. F. Ballance, Elsevier**:** 69-92.

Davy, B. (2006). "Bollons Seamount and early New Zealand–Antarctic seafloor spreading." Geochemistry, Geophysics, Geosystems **7**(6): Q06021. doi:10.1029/2005gc001191

DeMets, C., R. G. Gordon, et al. (1990). "Current plate motions." Geophys. J. Int. **101**(2): 425 – 478. doi:10.1111/j.1365-246X.1990.tb06579.x

Dubois, N. and N. C. Mitchell (2012). "Large-scale sediment redistribution on the equatorial Pacific seafloor." Deep-Sea Research I: Oceanographic Research Papers **69**: 51 – 61. doi:10.1016/j.dsr.2012.07.006

Eagles, G., K. Gohl, et al. (2004). "High-resolution animated tectonic reconstruction of the South Pacific and West Antarctic Margin." Geochemistry Geophysics Geosystems **5**(7): Q07002. doi:10.1029/2003gc000657

Edwards, A. R. (1973). "20. Southwest Pacific Regional Unconformities Encountered during Leg 21". Published in: Initial Reports of the Deep Sea Drilling Project. T. A. Davies. Washington, D.C., US Governmental Printing Office. **21:** 701 - 720. doi:10.2973/dsdp.proc.21.120.1973

Ehrmann, W. U. and A. Mackensen (1992). "Sedimentological evidence for the formation of an East Antarctic ice sheet in Eocene/Oligocene time." Palaeogeography, Palaeoclimatology, Palaeoecology **93**(1–2): 85-112. doi:10.1016/0031-0182(92)90185-8

Erickson, S. N. and R. D. Jarrard (1998). "Velocity-porosity relationships for water-saturated siliciclastic sediments." Journal of Geophysical Research: Solid Earth **103**(B12): 30385-30406. doi:10.1029/98jb02128

Ewing, J. and M. Ewing (1967). "Sediment Distribution on the Mid-Ocean Ridges with Respect to Spreading of the Sea Floor." Science **156**(3782): 1590 – 1592. doi:10.1126/science.156.3782.1590

Ewing, M., R. Houtz, et al. (1969). "South Pacific Sediment Distribution." Journal of Geophysical Research **74**(10): 2477 – 2493. doi:10.1029/JB074i010p02477

Exon, N. F., J. P. Kennett, et al. (2001). "Leg 189 Summary". Published in: Proccedings of the Ocean Drilling Program, Initial Reports. J. M. Scroggs. Texas, College Station (Ocean Drilling Program). **189:** 1 - 98. doi:10.2973/odp.proc.ir.189.101.2001

Faghmous, J. H., L. Styles, et al. (2012). "EddyScan: A Physically Consistent Ocean Eddy Monitoring Application". IEEE Proc Intelligent Data Understanding (CIDU), 2012, Boulder, CO. doi:10.1109/CIDU.2012.6382189

Faugères, J. C. and D. A. V. Stow (1993). "Bottom-current-controlled sedimentation: a synthesis of the contourite problem." Sedimentary Geology **82**(1 – 4): 287 – 297. doi:10.1016/0037-0738(93)90127-Q

Faugères, J. C. and D. A. V. Stow (2008). "Chapter 14 Contourite Drifts: Nature, Evolution and Controls". Published in: Developments in Sedimentology. M. Rebesco and A. Camerlenghi. Amsterdam, Elsevier Science**:** 257 – 288. doi:10.1016/S0070-4571(08)10014-0

Faugères, J. C., D. A. V. Stow, et al. (1999). "Seismic features diagnostic of contourite drifts." Marine Geology **162**(1): 1-38. doi:10.1016/s0025-3227(99)00068-7

Freudenthal, T. and G. Wefer (2013). "Drilling cores on the sea floor with the remote-controlled sea floor drilling rig MeBo." Geosci. Instrum. Method. Data Syst. **2**(2): 329-337. doi:10.5194/gi-2-329-2013

Friedrich, O., R. D. Norris, et al. (2012). "Evolution of middle to Late Cretaceous oceans—A 55 m.y. record of Earth's temperature and carbon cycle." Geology **40**(2): 107-110. doi:10.1130/g32701.1

Fulthorpe, C. S., R. M. Carter, et al. (1996). "Marshall Paraconformity: a mid-Oligocene record of inception of the Antarctic circumpolar current and coeval glacio-eustatic lowstand?" Marine and Petroleum Geology **13**(1): 61-77. doi:10.1016/0264-8172(95)00033-X

Gohl, K. (2003). Structure and dynamics of a submarine continent: Tectonic-magmatic evolution of the Campbell Plateau (New Zealand) Report of the RV SONNE cruise SO-169, Project CAMP 17 January to 24 February 2003 Reports on Polar and Marine Research. Bremerhaven, Alfred Wegner Institut, Helmholtz Centre for Polar and Marine Reseach, Bremerhaven. **457:** 88. doi:10.2312/BzPM_0457_2003

Griggs, G. B., L. Carter, et al. (1983). "Late Quaternary marine stratigraphy southeast of New Zealand." Geological Society of America Bulletin **94**(6): 791-797. doi:10.1130/0016-7606(1983)94<791:lqmsso>2.0.co;2

Grobys, J. W. G., K. Gohl, et al. (2007). "Is the Bounty Trough off eastern New Zealand an aborted rift?" Journal of Geophysical Research: Solid Earth **112**(B3). doi:10.1029/2005JB004229

Hall, I. R., L. Carter, et al. (2002). "Major depositional events under the deep Pacific inflow." Geology **30**(6): 487-490. doi:10.1130/0091-7613(2002)030<0487:mdeutd>2.0.co;2

Hall, I. R., I. N. McCave, et al. (2001). "Intensified deep Pacific inflow and ventilation in Pleistocene glacial times." Nature **412**(6849): 809-812. doi:10.1038/35090552

Hall, I. R., I. N. McCave, et al. (2003). "Paleocurrent reconstruction of the deep Pacific inflow during the middle Miocene: Reflections of East Antarctic Ice Sheet growth." Paleoceanography **18**(2): 1040. doi:10.1029/2002pa000817

Hamilton, E. L. (1976). "Variations of density and porosity with depth in deep-sea sediments." Journal of Sedimentary Research **46**(2): 280-300. doi:10.1306/212f6f3c-2b24-11d7-8648000102c1865d

Hamilton, E. L. (1978). "Sound velocity–density relations in sea-floor sediments and rocks." The Journal of the Acoustical Society of America **63**(2): 366-377. doi:10.1121/1.381747

Hauschild, J., I. Grevemeyer, et al. (2003). "Asymmetric sedimentation on young ocean floor at the East Pacific Rise, 15°S." Marine Geology **193**(1 – 2): 49 – 59. doi:10.1016/S0025-3227(02)00613-8

Hays, J. D., H. E. I. Cook, et al. (1972). "Initial Reports of the Deep Sea Drilling Project ". Washingtion, DC, US Governmental Printing Office. doi:10.2973/dsdp.proc.9.1972

Hernández-Molina, F. J., R. D. Larter, et al. (2006). "Miocene reversal of bottom water flow along the Pacific Margin of the Antarctic Peninsula: Stratigraphic evidence from a contourite sedimentary tail." Marine Geology **228**(1 – 4): 93 – 116. doi:10.1016/j.margeo.2005.12.010

Hollis, C. J. (2002). "Biostratigraphy and paleoceanographic significance of Paleocene radiolarians from offshore eastern New Zealand." Marine Micropaleontology **46**(3–4): 265-316. doi:10.1016/S0377-8398(02)00066-X

Hollis, C. J., M. J. S. Tayler, et al. (2014). "Organic-rich sedimentation in the South Pacific Ocean associated with Late Paleocene climatic cooling." Earth-Science Reviews **134**(0): 81-97. doi:10.1016/j.earscirev.2014.03.006

Hollister, C. D. (1967). "Sediment distribution and deep circulation in the western North Atlantic". Published in: Studies in Physical Oceanography. A. L. Gordon. New York, Gorodon and Breach Science Publishers. **2:** 37 - 66.

Hollister, C. D., C. Craddock, et al. (1976). "Initial Reports of the Deep Sea Drilling Project". Washingtion, DC, US Governmental Printing Office. doi:10.2973/dsdp.proc.35.1976

Horn, M. and G. Uenzelmann-Neben (2013). "Nonlinear sediment thickness increase on the western East Pacific Rise flank, 45°S." Geo-Marine Letters **33**(5): 381 - 390. doi:10.1007/s00367-013-0335-1

Horn, M. and G. Uenzelmann-Neben (2014). "The Deep Western Boundary Current at the Bounty Trough, east of New Zealand: Indications for its activity already before the opening of the Tasmanian Gateway " submitted to Marine Geology in 2014.

Houtz, R. E., D. E. Hayes, et al. (1977). "Kerguelen Plateau bathymetry, sediment distribution and crustal structure." Marine Geology **25**(1–3): 95-130. doi:10.1016/0025-3227(77)90049-4

Huber, B. T., R. D. Norris, et al. (2002). "Deep-sea paleotemperature record of extreme warmth during the Cretaceous." Geology **30**(2): 123-126. doi:10.1130/0091-7613(2002)030<0123:dsproe>2.0.co;2

Huber, M., H. Brinkhuis, et al. (2004). "Eocene circulation of the Southern Ocean: Was Antarctica kept warm by subtropical waters?" Paleoceanography **19**(4): PA4026. doi:10.1029/2004pa001014

Joseph, L. H., D. K. Rea, et al. (2004). "Neogene history of the Deep Western Boundary Current at Rekohu sediment drift, Southwest Pacific (ODP Site 1124)." Marine Geology **205**(1-4): 185-206. doi:Doi: 10.1016/s0025-3227(04)00023-4

Kearey, P. and F. J. Vine (1996). "Global Tectonics". Oxford, Blackwell Science.

Keller, G. and J. A. Barron (1983). "Paleoceanographic implications of Miocene deep-sea hiatuses." Geological Society of America Bulletin **94**(5): 590 – 613. doi:10.1130/0016-7606(1983)94<590:PIOMDH>2.0.CO;2

Kennett, J. P., R. E. Houtz, et al. (1975). "44. Cenozoic paleoceanography in the southwest Pacific Ocean, Antarctic glaciation, and the development of the Circum-Antarctic Current". Published in: Initial Reports of the Deep Sea Drilling Project. S. M. White. Washingtion, DC, US Government Priniting Office. **29:** 1155-1169. doi:10.2973/dsdp.proc.29.144.1975

Kennett, J. P., C. C. von der Borch, et al. (1986). "Site 594: Chatham Rise". Published in: Initial Reports of the Deep Sea Drilling Project. J. P. Kennett, C. C. van der Borch and J. H. Blakeslee. Washington DC, US Governmental Printing Office. **90:** 653 - 744. doi:10.2973/dsdp.proc.90.110.1986

Kuhlbrodt, T., A. Griesel, et al. (2007). "On the driving processes of the Atlantic meridional overturning circulation." Reviews of Geophysics **45**(2): RG2001. doi:10.1029/2004rg000166

Laske, G. and G. Masters (1997). "A Global Digital Map of Sediment Thickness." Eos, Transactions American Geophysical Union **78**: F 483.

Lebrun, J.-F., G. Lamarche, et al. (2003). "Subduction initiation at a strike-slip plate boundary: The Cenozoic Pacific-Australian plate boundary, south of New Zealand." Journal of Geophysical Research: Solid Earth **108**(B9): 2453. doi:10.1029/2002jb002041

Leinen, M., D. K. Rea, et al. (1986). "Initial Reports of the Deep Sea Drilling Project". Washington, DC, US Governmental Printing Office. doi:10.2973/dsdp.proc.92.1986

Lewis, K., S. D. Nodder, et al. (2012, 13.07.2012). "Sea floor geology - Zealandia: the New Zealand continent, Te Ara - the Encyclopedia of New Zealand." from http://www.TeAra.govt.nz/en/sea-floor-geology/page-1

Lonsdale, P. (1977). "Deep-tow observations at the mounds abyssal hydrothermal field, Galapagos Rift." Earth and Planetary Science Letters **36**(1): 92 – 110. doi:10.1016/0012-821X(77)90191-1

Lu, H., C. S. Fulthorpe, et al. (2003). "Three-dimensional architecture of shelf-building sediment drifts in the offshore Canterbury Basin, New Zealand." Marine Geology **193**(1–2): 19-47. doi:10.1016/S0025-3227(02)00612-6

Lyle, M., I. Raffi, et al. (2009). "Pacific Equatorial Transect". Tokyo, Integrated Ocean Drilling Program Management International. doi:10.2204/iodp.pr.321.2009

Marks, N. S. (1981). "Sedimentation on new ocean crust: The Mid-Atlantic Ridge at 37°N." Marine Geology **43**(1 – 2): 65 – 82. doi:10.1016/0025-3227(81)90129-8

Marshall, J. and K. Speer (2012). "Closure of the meridional overturning circulation through Southern Ocean upwelling." Nature GeoScience **5**(3): 171-180. doi:10.1038/ngeo1391

Marshall, P. (1911). "New Zealand and Adjacent Islands". Published in: Handbuch der regionalen Geologie. G. Steinmann and O. Wilckens. Heidelberg, C. Winter's Universitätsbuchhandlung**:** 78.

Maus, S., U. Barckhausen, et al. (2009). "EMAG2: A 2-arc min resolution Earth Magnetic Anomaly Grid compiled from satellite, airborne, and marine magnetic measurements." Geochemistry, Geophysics, Geosystems **10**(8): Q08005. doi:10.1029/2009GC002471

Mayer, L., F. Theyer, et al. (1985). "Initial Reports of the Deep Sea Drilling Project". Washington, DC, US Governmental Printing Office. doi:10.2973/dsdp.proc.85.1985

Mayer, L. A., T. H. Shipley, et al. (1986). "Equatorial Pacific Seismic Reflectors as Indicators of Global Oceanographic Events." Science **233**(4765): 761 – 764. doi:10.1126/science.233.4765.761

McAnena, A., S. Flogel, et al. (2013). "Atlantic cooling associated with a marine biotic crisis during the mid-Cretaceous period." Nature Geoscience **6**(7): 558-561. doi:10.1038/ngeo1850

McCave, I. N., L. Carter, et al. (2008). "Glacial–interglacial changes in water mass structure and flow in the SW Pacific Ocean." Quaternary Science Reviews **27**(19–20): 1886-1908. doi:10.1016/j.quascirev.2008.07.010

Miller, K. G., M. A. Kominz, et al. (2005). "The Phanerozoic Record of Global Sea-Level Change." Science **310**(5752): 1293-1298. doi:10.1126/science.1116412

Mitchell, N. C. (1998). "Sediment accumulation rates from Deep Tow profiler records and DSDP Leg 70 cores over the Galapagos spreading centre". Published in: Geological evolution of ocean basins : results from the Ocean Drilling Program. A. Cramp, C. J. MacLeod, S. V. Lee and E.

J. W. Jones. London, The Geological Society Publishing House. **131:** 199 – 209. doi:10.1144/GSL.SP.1998.131.01.13
Mitchell, N. C., S. Allerton, et al. (1998). "Sedimentation on young ocean floor at the Mid-Atlantic Ridge, 29 °N." Marine Geology **148**(1 – 2): 1 – 8. doi:10.1016/S0025-3227(98)00018-8
Mitchell, N. C., M. W. Lyle, et al. (2003). "Lower Miocene to present stratigraphy of the equatorial Pacific sediment bulge and carbonate dissolution anomalies." Paleoceanography **18**(2): 1038. doi:10.1029/2002PA000828
Molnar, P., T. Atwater, et al. (1975). "Magnetic Anomalies, Bathymetry and the Tectonic Evolution of the South Pacific since the Late Cretaceous." Geophysical Journal International **40**(3): 383 – 420. doi:10.1111/j.1365-246X.1975.tb04139.x
Moore, T. C. J. (2008). "Chert in the Pacific: Biogenic silica and hydrothermal circulation." Palaeogeography Palaeoclimatology Palaeoecology **261**(1 – 2): 87 – 99. doi:10.1016/j.palaeo.2008.01.009
Morris, M., B. Stanton, et al. (2001). "Subantarctic oceanography around New Zealand: Preliminary results from an ongoing survey." New Zealand Journal of Marine and Freshwater Research **35**(3): 499-519. doi:10.1080/00288330.2001.9517018
Mueller, R. D., M. Sdrolias, et al. (2008). "Age, spreading rates, and spreading asymmetry of the world's ocean crust." Geochemistry Geophysics Geosystems **9**(4): Q04006. doi:10.1029/2007gc001743
Nafe, J. E. and C. L. Drake (1957). "Variation with depth in shallow and deep water marine sediments of porosity, density and velocity of compressional and shear waves." Geophysics **22**(3): 523-552. doi:10.1190/1.1438386
Neil, H. L., L. Carter, et al. (2004). "Thermal isolation of Campbell Plateau, New Zealand, by the Antarctic Circumpolar Current over the past 130 kyr." Paleoceanography **19**(4): PA4008. doi:10.1029/2003pa000975
O'Malley, R. (2014). "The Ocean Productivity Homepage." Retrieved 20.10.2014, 2014, from http://www.science.oregonstate.edu/ocean.productivity/index.php.
Orsi, A. H., T. Whitworth III, et al. (1995). "On the meridional extent and fronts of the Antarctic Circumpolar Current." Deep Sea Research Part I: Oceanographic Research Papers **42**(5): 641-673. doi:10.1016/0967-0637(95)00021-w
Osborn, N. I., P. F. Ciesielski, et al. (1983). "Disconformities and paleoceanography in the southeast Indian Ocean during the past 5.4 million years." Geological Society of America Bulletin **94**(11): 1345-1358. doi:10.1130/0016-7606(1983)94<1345:dapits>2.0.co;2
Pisias, N. G., L. A. Mayer, et al. (1992). "Scientific Results". Texas (Ocean Drilling Program), College Station. doi:10.2973/odp.proc.ir.138.1992
Rea, D. K., M. W. Lyle, et al. (2006). "Broad region of no sediment in the southwest Pacific Basin." Geology **34**(10): 873 – 876. doi:10.1130/G22864.1
Rebesco, M., A. Camerlenghi, et al. (2008). "Contourites ". Amsterdam, Elsevier Science.
Rebesco, M., F. J. Hernández-Molina, et al. (2014). "Contourites and associated sediments controlled by deep-water circulation processes: State-of-the-art and future considerations." Marine Geology **352**(0): 111-154. doi:10.1016/j.margeo.2014.03.011
Rebesco, M. and D. A. V. Stow (2001). "Seismic expression of contourites and related deposits: a preface." Marine Geophysical Researches **22**(5 – 6): 303 – 308. doi:10.1023/A:1016316913639
Reid, J. L. (1997). "On the total geostrophic circulation of the pacific ocean: flow patterns, tracers, and transports." Progress In Oceanography **39**(4): 263 – 352. doi:10.1016/S0079-6611(97)00012-8
Ricker, N. (1953). "The form and laws of Propagation of seismic wavelets." Geophysics **18**(1): 10-40. doi:doi:10.1190/1.1437843
Roberts, D. G., N. G. Hogg, et al. (1974). "Sediment distribution around moated seamounts in the Rockall Trough." Deep Sea Research and Oceanographic Abstracts **21**(3): 175 – 184. doi:10.1016/0011-7471(74)90057-6
Ronge, T. A., R. Tiedemann, et al. (2013). SO213 SOPATRA – Fahrtbericht und erste Ergebnisse SONNE Statusseminar. Kiel**:** 24. doi:10013/epic.42135
Rosendahl, B. R., R. Hekinian, et al. (1980). "Initial Reports of the Deep Sea Drilling Project". Washington, DC, US Governmental Printing Office. doi:10.2973/dsdp.proc.54.1980

Scott, R. B., J. A. Goff, et al. (2011). "Global rate and spectral characteristics of internal gravity wave generation by geostrophic flow over topography." Journal of Geophysical Research: Oceans **116**(C9): C09029. doi:10.1029/2011JC007005

Seibold, E. and W. H. Berger (1996). "The Sea Floor - An Introduction to Marine Geology". Berlin, Springer-Verlag Berlin Heidelberg.

Senske, D. A. and R. A. Stephen (1988). A Seismic-Reflection Survey of DSDP Sites 417 and 418. Proceedings of the Ocean Drilling Program, Scientific Results. M. H. Salisbury and J. H. Scott. Texas, College Station (Ocean Drilling Program). **102:** 3 - 17. doi:10.2973/odp.proc.sr.102.116.1988

Shanmugam, G. (2006). "Deep-Water Processes and Facies Models: Implications for Sandstone Petroleum Reservoirs". Amsterdam, Elsevier Science.

Sheriff, R. E. and L. P. Geldart (1982). "4.3.2 Resolution". Published in: Exploration seismology Volume I: History, theory and data acquisition. Cambridge, Cambridge University Press. **1:** 117 - 122.

Sijp, W. P., M. H. England, et al. (2011). "Effect of the deepening of the Tasman Gateway on the global ocean." Paleoceanography **26**(4): PA4207. doi:10.1029/2011pa002143

Sijp, W. P., A. S. von der Heydt, et al. (2014). "The role of ocean gateways on cooling climate on long time scales." Global and Planetary Change **119**(0): 1-22. doi:10.1016/j.gloplacha.2014.04.004

Smith, W. H. F. and D. T. Sandwell (1997). "Global Sea Floor Topography from Satellite Altimetry and Ship Depth Soundings." Science **277**(5334): 1956 – 1962. doi:10.1126/science.277.5334.1956

Sparrow, M., P. Chapman, et al. (2004 - 2006). The World Ocean Circulation Experiment (WOCE) Hydrographic Atlas Series. M. Sparrow, P. Chapman and J. Gould. Southhampton, U.K., International WOCE Project Office.

Stanton, B. R. and M. Y. Morris (2004). "Direct velocity measurements in the Subantarctic Front and over Campbell Plateau, southeast of New Zealand." Journal of Geophysical Research: Oceans **109**(C1): C01028. doi:10.1029/2002jc001339

Stickley, C. E., H. Brinkhuis, et al. (2004). "Timing and nature of the deepening of the Tasmanian Gateway." Paleoceanography **19**(4): PA4027. doi:10.1029/2004pa001022

Stocker, T. F. (2000). "Past and future reorganizations in the climate system." Quaternary Science Reviews **19**(1–5): 301-319. doi:10.1016/S0277-3791(99)00067-0

Stow, D. A. V., J.-C. Faugères, et al. (2002). "Bottom currents, contourites and deep-sea sediment drifts: current state-of-the-art". Published in: Deep-water contourite systems: Modern drifts and ancient series. D. A. V. Stow, C. J. Pudsey, J. A. Howe, J.-C. Faugères and A. R. Viana. London, Geological Society of London. **22:** 7 - 20. doi:10.1144/GSL.MEM.2002.022.01.02

Stow, D. A. V. and M. Mayall (2000). "Deep-water sedimentary systems: New models for the 21st century." Marine and Petroleum Geology **17**(2): 125-135. doi:10.1016/s0264-8172(99)00064-1

Stramski, D., R. A. Reynolds, et al. (2008). "Relationships between the surface concentration of particulate organic carbon and optical properties in the eastern South Pacific and eastern Atlantic Oceans." Biogeosciences **5**(1): 171 – 201. doi:10.5194/bg-5-171-2008

Talley, L. D. (2007). "Pacific Ocean". Southampton, U.K., International WOCE Project Office.

Tebbens, S. F. and S. C. Cande (1997). "Southeast Pacific tectonic evolution from early Oligocene to Present." Journal of Geophysical Research: Solid Earth **102**(B6): 12061 – 12084. doi:10.1029/96JB02582

Thoppil, P. G., J. G. Richman, et al. (2011). "Energetics of a global ocean circulation model compared to observations." Geophysical Research Letters **38**(15): L15607. doi:10.1029/2011GL048347

Tiedemann, R., J. O'Conner, et al. (2012). Cruise Report SO213: SOPATRA. Bremerhaven, Alfred Wegener Institute, Helmholtz Centre for Polar and Marine Research**:** 111.

Tominaga, M., M. Lyle, et al. (2011). "Seismic interpretation of pelagic sedimentation regimes in the 18-53 Ma eastern equatorial Pacific: Basin-scale sedimentation and infilling of abyssal valleys." Geochemistry Geophysics Geosystems **12**(3): Q03004. doi:10.1029/2010GC003347

Tracey, J. I. J., G. H. Sutton, et al. (1971). "Initial Reports of the Deep Sea Drilling Project ". Washingtion, DC, US Governmental Printing Office. doi:10.2973/dsdp.proc.8.1971

Tucholke, B. E. (1979). "Relationships Between Acoustic Stratigraphy and Lithostratigraphy in the Western North Atlantic Basin". Published in: Initial Reports of the Deep Sea Drilling Project. A. Kaneps. Washingtion, D.C., US Governmental Printing Office. **43:** 827 - 846. doi:10.2973/dsdp.proc.43.141.1979

Turnewitsch, R., J.-L. Reyss, et al. (2004). "Evidence for a sedimentary fingerprint of an asymmetric flow field surrounding a short seamount." Earth and Planetary Science Letters **222**(3 – 4): 1023 – 1036. doi:10.1016/j.epsl.2004.03.042

Uenzelmann-Neben, G., J. W. G. Grobys, et al. (2009). "Neogene sediment structures in Bounty Trough, eastern New Zealand: Influence of magmatic and oceanic current activity." Geological Society of America Bulletin **121**(1-2): 134-149. doi:10.1130/b26259.1

van Aken, H. M. (2007). "The Oceanic Thermohaline Circulation: An Introduction". New York, Springer Science and Business Media, LLC.

van Andel, T. H. (1975). "Mesozoic/cenozoic calcite compensation depth and the global distribution of calcareous sediments." Earth and Planetary Science Letters **26**(2): 187 – 194. doi:10.1016/0012-821X(75)90086-2

Warren, B. A. (1973). "Transpacific hydrographic sections at lats. 43°S and 28°S: the SCORPIO expedition—II. deep water." Deep Sea Research and Oceanographic Abstracts **20**(1): 9-38. doi:10.1016/0011-7471(73)90040-5

Warren, B. A. (1981). "Deep circulation of the world ocean". Published in: Evolution of physical oceanography. B. A. Warren and C. Wunsch, MIT Press, Caimbridge, Ma**:** 6-41.

Weigelt, E. and G. Uenzelmann-Neben (2007). "Orbital forced cyclicity of reflector strength in the seismic records of the Cape Basin." Geophysical Research Letters **34**(1): L01702. doi:10.1029/2006gl028376

Whitworth III, T., B. A. Warren, et al. (1999). "On the deep western-boundary current in the Southwest Pacific Basin." Progress In Oceanography **43**(1): 1-54. doi:10.1016/S0079-6611(99)00005-1

Wobbe, F., K. Gohl, et al. (2012). "Structure and breakup history of the rifted margin of West Antarctica in relation to Cretaceous separation from Zealandia and Bellingshausen plate motion." Geochemistry, Geophysics, Geosystems **13**(4): Q04W12. doi:10.1029/2011gc003742

WOCE_International_Project_Office (2003). WOCE observations 1990-1998; a summary of the WOCE global data resource. W. I. P. Office. Southampton, UK.**:** 52.

Wynn, R. B. and D. G. Masson (2008). "Chapter 15 Sediment waves and bedforms". Published in: Contourites. M. Rebesco and A. Camerlenghi. Amsterdam, Elsevier Science**:** 289 - 300. doi:10.1016/S0070-4571(08)00215-X

Yilmaz, Ö. (2001). "Seismic Data Analysis". Tulsa, Society of Exploration Geophysicists.

Zachos, J. C., J. R. Breza, et al. (1992). "Early Oligocene ice-sheet expansion on Antarctica: Stable isotope and sedimentological evidence from Kerguelen Plateau, southern Indian Ocean." Geology **20**(6): 569-573.

Zachos, J. C., G. R. Dickens, et al. (2008). "An early Cenozoic perspective on greenhouse warming and carbon-cycle dynamics." Nature **451**(7176): 279-283. doi:doi: 10.1038/nature06588

Zachos, J. C., M. Pagani, et al. (2001). "Trends, Rhythms, and Aberrations in Global Climate 65 Ma to Present." Science **292**: 686-693. doi:10.1126/science.1059412

Zenk, W. (2008). "Chapter 4 Abyssal and Contour Currents". Published in: Developments in Sedimentology. M. Rebesco and A. Camerlenghi. Amsterdam, Elsevier Science**:** 35, 37 – 57. doi:10.1016/S0070-4571(08)10004-8

12. Acknowledgements

Many people gave helpful advice, have been patient and helped me a lot by completing this PHD Thesis. I would like to thank the following people:

- My two supervisors Prof. Dr. Wilfried Jokat and Prof. Dr. Katrin Huhn who consented to supervise my PHD Thesis.
- Dr. Gabriele Uenzelmann-Nebe for her excellent supervision, many helpful comments, two spectacular cruises on Maria S. Merian and Sonne, her patience during reading the first drafts of manuscripts and for the money she raised for my project.
- My collegues Dr. Jens Gruetzner, Dr. Estella Weigelt, Tabea Altenbend, Katharina Hochmuth and Ricarda Pietsch for scientific discussions, helpful commends, design questions and may funny door pictures for our office door.
- All other colleagues not mentioned for a productive working atmosphere and regular meetings in Dome D.
- My wife Kerstin Horn who I had to leave for three month of travelling. Without her, this thesis would not have been finished.

Additionally I want to thank the Bundesministerium für Bildung und Forschung who have funded this thesis!